R-B(OH)$_2$, Ag$_2$CO$_3$

Pd$^{0/II}$

R = aryl, heteroaryl
29 examples (up to 87%)

R^1 = EDG

low — yield — high

R^1 = EWG

80%

60%

40%

20%

Cross-coupling Reactions of Monosubstituted Tetrazines

Lukas V. Hoff, Simon D. Schnell, Andrea Tomio, Anthony Linden, and Karl Gademann*

Department of Chemistry, University of Zurich, Winterthurerstrasse 190, 8057 Zurich, Switzerland

*Correspondence to karl.gademann@uzh.ch

Abstract

A fast and mild method for the Pd-catalyzed cross-coupling reaction of monosubstituted 3-bromo-1,2,4,5-tetrazine is presented. Investigation of silver-based additives revealed that Ag_2CO_3 is the optimal mediator, enabling the process without the need for strong bases or high temperatures. Electronic modification of the classical 1,1′-bis(diphenylphosphine)ferrocene (dppf) ligand proved to be a powerful strategy in tailoring the catalytic system to the requirements set by the process. Under the optimized conditions a scope comprising a variety of alkyl-, heteroatom-, and halide substituted aryl- and heteroaryl-tetrazines were prepared in good to excellent yields (29 examples, up to 87% yield). This method constitutes the first example of a direct cross-coupling reaction of monosubstituted tetrazines.

Introduction

Tetrazines have been employed in a multitude of applications, especially in the field of chemical biology.[1–6] As a consequence, the development of new ways to utilize tetrazines in various fields, and in particular in biorthogonal chemistry, has flourished over the past decades.[2,4,7–10] With their fast kinetics in inverse electron-demand *Diels–Alder* (iEDDA) cycloadditions with suitable reaction partners, such as strained alkenes and alkynes, tetrazines have become an invaluable motif in bioorthogonal applications.[2,11–13] Nonetheless, there are multiple parameters crucial for maximizing their potential. Direct incorporation into target molecules should be possible, without the necessity for bulky hydrophobic linkers, which might negatively affect physiochemical properties and the kinetics of subsequent iEDDA reactions.[6] Additionally, minimal molecular weight of the tetrazine is favorable for the same reasons and can be optimized by minimizing the substituent in the *para*-position of the tetrazine. With these requirements in mind, access to non-symmetric and preferably mono-substituted tetrazines constitutes a research goal.[14] While direct incorporation of tetrazines via nucleophilic (O, N, S) aromatic substitution of suitable leaving groups was demonstrated,[9,14] introduction of an electron-donating heteroatom onto the motif negatively impacts the kinetics of iEDDA reactions.[15] In contrast to the numerous applications, the synthesis of tetrazines mainly relied for a long time on two strategies.[4,16] Due to the challenging preparation of non-symmetric derivatives by these methods, relatively few examples have been reported in comparison to a multitude of symmetrical tetrazines.[4] Three new strategies for the preparation of easily modifiable, leaving-group bearing, non-symmetric tetrazine derivatives have been published only recently.[9,14,17]
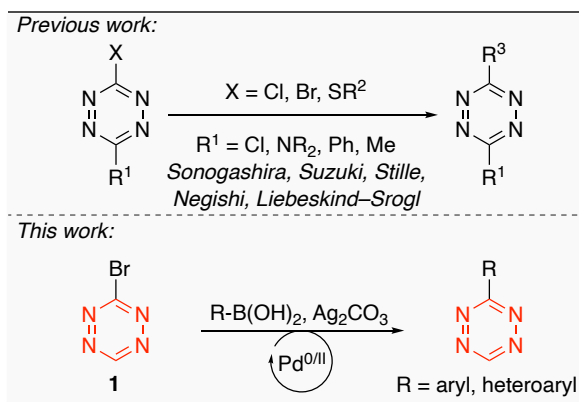

Figure 1: Overview of the previously reported cross-couplings of 3,6-disubstituted tetrazines and the method presented in this work.

The syntheses developed by the groups of Fox[17] and Riera[9] both comprise alkylation of thiocarbohydrazide and formation of the tetrazine core by reaction with an orthoester and produce the corresponding thio-tetrazin and the brominated tetrazine respectively. A third strategy developed in our group starts with the less hazardous guanidinium hydrochloride and utilizes efficient desymmetrization to furnish the monosubstituted 3-bromo-tetrazine (**1**).[14] With access to easily functionalized tetrazines, cross-coupling as a method for forming carbon-carbon bonds between tetrazines and target

molecules has recently attracted attention, since it allows the introduction of tetrazines with minimal alteration of their properties. After the first reported cross-coupling of tetrazines by Kotschy and co-workers in 2003,[18] only a few reports are found in the literature (Figure 1).[7,17–24] Among the early examples of these palladium catalyzed couplings, the requirement for an aryl moiety or a specific electron donating substituents *para* to the newly formed bond is frequently encountered. While these substituents do enable the coupling, they also considerably slow down the rates of the iEDDA reactions and hence decrease their bioorthogonal value.[4] Further progress of coupling minimal tetrazines was achieved by Wombacher and co-workers[7] and more recently by the groups of Fox[25] (Figure 2A) and Riera.[24] They reported new methods for the coupling of 6-methyl substituted tetrazines, which were to date the smallest tetrazines to be coupled. Transition metal catalyzed cross-coupling of monosubstituted tetrazines, however, remained elusive. Nonetheless, considering their improved kinetics in iEDDA reactions over 3,6-disubstituted tetrazines,[26] convenient synthetic access to those building blocks might enable the next generation of bioorthogonal applications.

In this study, we report on the first methodology for the Pd-catalyzed cross-coupling of monosubstituted *s*-tetrazines. The method utilizes 3-bromo-1,2,4,5-tetrazine (BrTet, **1**) under mild conditions and short reaction times to deliver a broad range of mono-functionalized products in good to excellent yields.

*Initial observations and optimization*
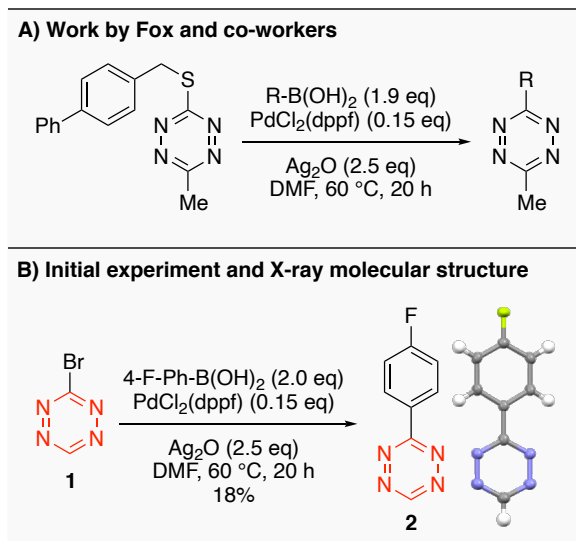
Figure 2: A) The conditions for the Liebeskind–Srogl coupling reported by Fox and co-workers. B) Initial cross-coupling conditions for **1** and the X-ray molecular structure of **2**. Dppf = 1,1′-Ferrocenediyl-bis(diphenylphosphine).

Initial experiments with 4-fluorophenylboronic acid in the presence of Pd(dppf)Cl$_2$ and Ag$_2$O afforded the desired product **2** in 18% yield. X-ray crystal structure analysis unambiguously supported the constitution of **2** (Figure 2B). Since electron deficient boronic acids, such as 4-fluorophenylboronic acid, usually undergo cross-coupling less efficiently compared to their electron-rich counterparts, we optimized the conditions by employing *tert*-butylphenylboronic acid.[27–29] The initial conditions afforded the desired product in 33% yield (Table 1, entry 1), although decomposition of the product and increased formation of side products was observed over extended reaction times. Drastically shortening the reaction time

from 20 h to 30 min resulted in a better process with fewer side products and allowed for a more efficient screening approach (Table 1, entry 2).

Additionally, we were pleased to find that even at such short reaction times, feasible amounts of product were formed, especially, since previous literature on tetrazine cross-coupling reactions reported extended reaction times of up to 20 h.[7,21,24,25] An initial investigation of classical cross-coupling solvents (DMF, toluene, THF, HFIP, 1,4-dioxane, MeOH, 1,2-DME, and MeCN) identified the superiority of acetonitrile (41%) (Table 1, entry 3). Regarding the Ag(I) source, we experienced similar trends to those noted by Fox and co-workers[25] and found that Ag_2O (41%), AgF (41%) or Ag_2CO_3 (71%) (Table 1, entries 3 – 5) to outcompete other silver salts (AgOAc, $AgNO_3$, $AgBF_4$, Ag_3PO_4, $AgPF_6$). The amounts of Ag_2CO_3 and boronic acid were minimized and 1.0 eq. and 1.5 eq. respectively provided the best results (Table 1, entries 6 – 9). When Ag_2CO_3 was omitted from the cross-coupling reactions, or when it was exchanged with Na_2CO_3, no product was formed (Table S6).

entry	boronic acid	additive	solvent (0.1 M)	temp	time	yield[a]
1	4-tBu-Ph-B(OH)₂ (2.0 eq)	Ag₂O (2.5 eq)	DMF	60 °C	20 h	33%
2	4-tBu-Ph-B(OH)₂ (2.0 eq)	Ag₂O (2.5 eq)	DMF	60 °C	30 min	23%
3	4-tBu-Ph-B(OH)₂ (2.0 eq)	Ag₂O (2.5 eq)	MeCN	60 °C	30 min	41%
4	4-tBu-Ph-B(OH)₂ (2.0 eq)	AgF (2.5 eq)	MeCN	60 °C	30 min	41%
5	4-tBu-Ph-B(OH)₂ (2.0 eq)	Ag₂CO₃ (2.5 eq)	MeCN	60 °C	30 min	71%
6	4-tBu-Ph-B(OH)₂ (2.0 eq)	Ag₂CO₃ (1.5 eq)	MeCN	60 °C	30 min	72%
7	4-tBu-Ph-B(OH)₂ (1.5 eq)	Ag₂CO₃ (1.5 eq)	MeCN	60 °C	30 min	75%
8	4-tBu-Ph-B(OH)₂ (1.5 eq)	Ag₂CO₃ (1.0 eq)	MeCN	60 °C	30 min	72%
9	4-tBu-Ph-B(OH)₂ (1.5 eq)	Ag₂CO₃ (0.5 eq)	MeCN	60 °C	30 min	41%
10	4-tBu-Ph-B(OH)₂ (1.5 eq)	Ag₂CO₃ (1.0 eq)	MeCN	25 °C	30 min	traces
11	4-tBu-Ph-B(OH)₂ (1.5 eq)	Ag₂CO₃ (1.0 eq)	MeCN	80 °C	30 min	80%
12	4-tBu-Ph-B(OH)₂ (1.5 eq)	Ag₂CO₃ (1.0 eq)	MeCN	100 °C	30 min	61%

Table 1: Representative examples of the optimization screening for solvents, silver salts, and temperature. a) Yields refer to isolated material after column chromatography.

While the electron rich *tert*-butylphenylboronic acid provided satisfying yields under these conditions, preliminary control experiments with 4-fluorophenyl- (32%) and other boronic acids identified electron poorer substrates as unsuitable coupling partners (Table S6). As a potential cause, we hypothesized that the electronic nature of these boronic acids impedes reductive elimination, as has been previously described.[30] Consequently, an imbalance between the silver mediated activation of the boronic and the palladium cycle would lead to an increase in side reactions. Similar hypotheses and observations were made by Su and co-workers for palladium and silver mediated decaboxylative C-H arylations of thiophenes, stressing the importance of a sufficiently fast palladium process compared to the generation of the silver aryl species.[31,32] We envisioned optimization of the temperature and catalytic system to be feasible handles for addressing this issue.

While at 25 °C only traces of the desired product were isolated, increasing the temperature to 80 °C resulted in 80% yield. Performing the reaction at even higher temperatures in a sealed tube resulted in lower yield (61%) (Table 1, entries 10 – 12). A similar increase in yield was observed for 4-fluorophenyl boronic acid (44%) at 80 °C (Table 2, entry 12). Next, we investigated the role of the catalyst. Adjusting its properties would allow fine tuning of the rate of the palladium cycle without

changing the silver mediated boronic acid activation. Thus, we envisioned it to be an efficient way of increasing the reactivity of those substrates still lacking reactivity. The initial three experiments clearly demonstrate the necessity for the presence of both components: the ligand and the metal center (Table 2, entries 1 – 3). Neither monodentate (Pd(PPh$_3$)$_2$Cl$_2$, 9%) nor bidentate (DPEphos, 48% and BINAP, 41%) ligands lacking the ferrocene moiety afforded the desired product in competitive yields (Table 2, entries 4 – 6). Hence, we hypothesized that electronic optimization of the ancillary ligand might be superior to drastic structural changes. For many metal complexes, electron-density and ease of oxidative addition coincide,[33,34] especially when the aryl halide has electron-deficient character.[35] Hence, oxidative addition of the extremely electron-deficient tetrazine **1** onto the relatively electron-rich Pd(dppf)Cl$_2$ is thought to proceed smoothly due to the electronics of the respective reaction partners. Contrary to oxidative addition, reductive elimination of electron-poor ligands in the presence of electron donating ancillary ligands is difficult.[27–29] Therefore, boronic acids bearing electron donating substituents posed viable substrates, while their electron-poorer alternatives resulted in diminished yield. With this in mind, we hypothesized that for a series of dppf analogs, varying electronically, a clear trend in reactivity should be observed. Thus, we investigated the di-*tert*-butylphosphino- (dtbpf), diisopropylphosphino- (dippf), and di(CF$_3$)phenylphosphino (dppf-CF$_3$) variants of dppf for both the 4-*tert*-butylphenyl-, and 4-fluorophenylboronic acid (Table 2, entries 7 – 13). For the electron-rich acid, good yields were observed generally (80 – 85%), except for the most electron-rich catalyst system (34%). Gratifyingly, the electron-poorer congener, 4-fluorophenylboronic acid, supported the postulated trend. While only resulting in low amounts of product for the di-*tert*-butyl- (15%), and diisopropylphosphino derived catalysts (31%), modification of the original dppf ligand (44%) with electron withdrawing CF$_3$ groups significantly increased the yield to 82%.

entry	boronic acid (1.5 eq)	catalyst	mol-%	yield[a]
1	4-*t*Bu-Ph-B(OH)$_2$	PdCl$_2$	15	6%
2	4-*t*Bu-Ph-B(OH)$_2$	dppf	15	<5%
3	4-*t*Bu-Ph-B(OH)$_2$	dppf,PdCl$_2$	15	72%
4	4-*t*Bu-Ph-B(OH)$_2$	Pd(PPh$_3$)$_2$Cl$_2$	15	9%
5	4-*t*Bu-Ph-B(OH)$_2$	DPEphos,PdCl$_2$	15	48%
6	4-*t*Bu-Ph-B(OH)$_2$	BINAP,PdCl$_2$	15	41%
7	4-*t*Bu-Ph-B(OH)$_2$	Pd(dtbpf)Cl$_2$	15	34%
8	4-*t*Bu-Ph-B(OH)$_2$	Pd(dippf)Cl$_2$	15	85%
9	4-*t*Bu-Ph-B(OH)$_2$	Pd(dppf-CF$_3$)Cl$_2$	15	84%
10	4-F-Ph-B(OH)$_2$	Pd(dtbpf)Cl$_2$	15	15%
11	4-F-Ph-B(OH)$_2$	Pd(dippf)Cl$_2$	15	31%
12	4-F-Ph-B(OH)$_2$	Pd(dppf)Cl$_2$	15	44%
13	4-F-Ph-B(OH)$_2$	Pd(dppf-CF$_3$)Cl$_2$	15	82%
14	4-*t*Bu-Ph-B(OH)$_2$	Pd(dppf-CF$_3$)Cl$_2$	10	83%
15	4-*t*Bu-Ph-B(OH)$_2$	Pd(dppf-CF$_3$)Cl$_2$	5	83%
16	4-*t*Bu-Ph-B(OH)$_2$	Pd(dppf-CF$_3$)Cl$_2$	3	44%
17	4-*t*Bu-Ph-B(OH)$_2$	Pd(dppf-CF$_3$)Cl$_2$	1	3%
18	4-F-Ph-B(OH)$_2$	Pd(dppf-CF$_3$)Cl$_2$	10	79%
19	4-F-Ph-B(OH)$_2$	Pd(dppf-CF$_3$)Cl$_2$	5	49%
20	4-*t*Bu-Ph-B(OH)$_2$	Pd(dppf-CF$_3$)Cl$_2$	5	83%[b]

Table 2: Investigation of the catalytic system. a) Yields refer to isolated material after column chromatography. b) This experiment was performed on a 200 mg scale. Dtbpf = 1,1′-Ferrocenediyl-bis(di-tert-butylphosphine), Dippf = 1,1′-Ferrocenediyl-bis(di-isopropylphosphine), Dppf-CF$_3$ = 1,1′-Ferrocenediyl-bis(di(trifluoromethylphenyl)phosphine).

With greatly improved performance of the catalyst, lower catalyst loading should be possible. Analogously to previous optimization iterations we expected different outcomes for electronically different boronic acids. Hence, we investigated both of our model substrates: 4-fluoro-, and 4-*tert*-butylphenylboronic acid (Table 2, entries 14 – 19). For both substrates, catalyst loading could generally be lowered. As expected, coupling of the electron-richer 4-*tert*-butylphenylboronic acid tolerated lower catalyst loading (5 mol-%, Table 2, entry 15) than coupling of the electron-poorer 4-fluorophenylboronic acid (10 mol-%, Table 2, entry 18). However, during preparation of the scope, proper estimation of the ideal catalyst loading was found to be nearly impossible. Still, 15 mol-% of Pd(dppf-CF$_3$)Cl$_2$ were found to be a viable starting point for all substrates.

Scope and limitations of the method

With optimized conditions in hand, we set out to explore the scope of the reaction (Figure 3). A typical reaction employed 1 eq. of **1**, 1.5 eq. boronic acid, 1.0 eq. Ag$_2$CO$_3$, and 0.15 eq. of Pd(dppf-CF$_3$)Cl$_2$ in MeCN at 80 °C for 30 min. Based on the observations during reaction optimization, we expected alkyl substituted phenylboronic acids to constitute a promising class of substrates. Satisfyingly, unsubstituted phenylboronic acid, as well as *para-, meta*-, and even *ortho*-alkyl substitution, was well tolerated and produced the respective phenyltetrazines **3** – **7** in good yields (61 – 81%). Due to their potential application in supramolecular and materials chemistry, we were interested in investigating the cross-coupling of bromo tetrazine (**1**) to polyaromatic systems and were pleased to find that these were also mostly feasible (**8** – **11**).[36–39] 1-Naphtyl- (**8**), 2-naphthyl- (**9**), 4-biphenyl- (**10**), and fluorenylboronic acid (**11**) afforded the desired product in moderate
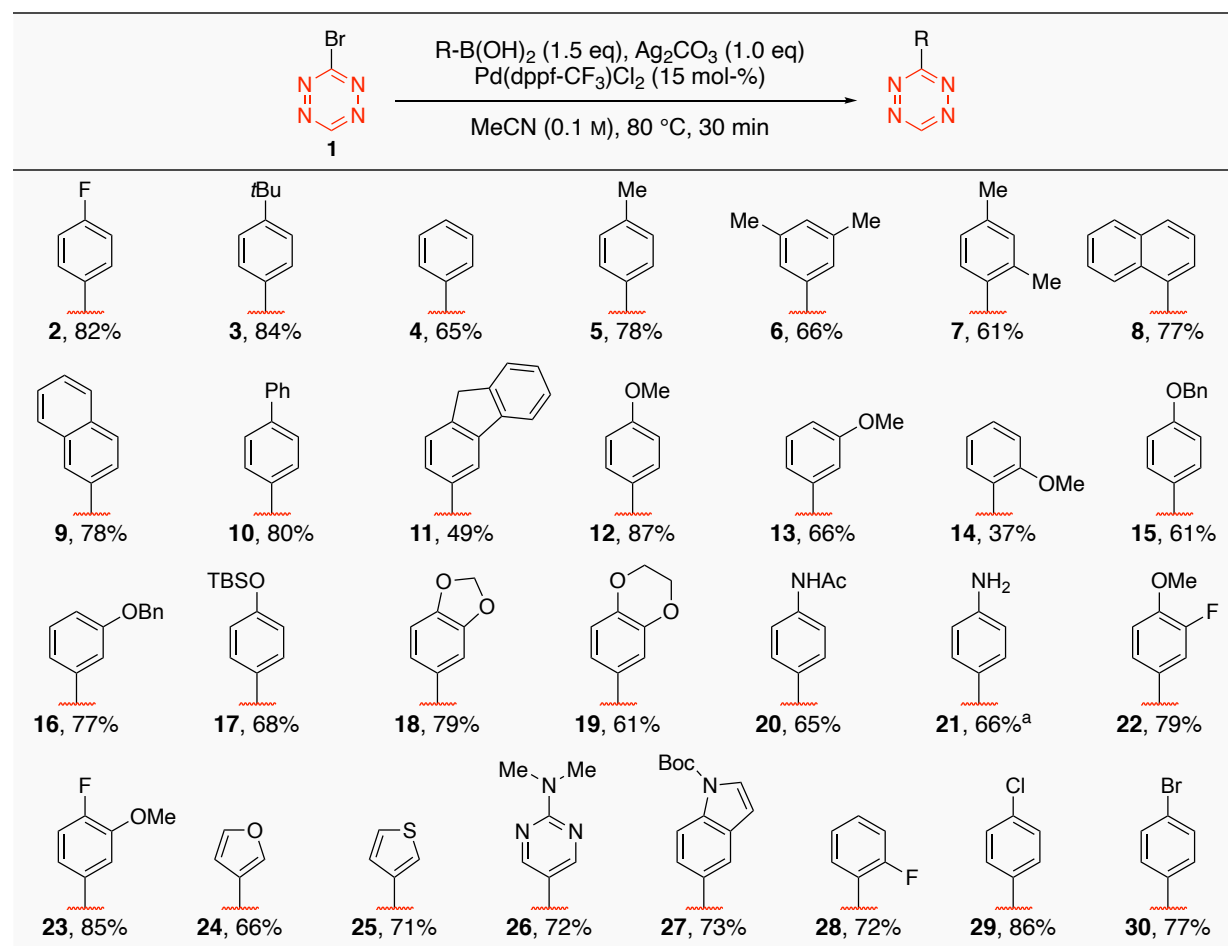
Figure 3: Scope of the reaction with optimized conditions. Alkyl substituted and polyaromatic phenyl boronic acids pose viable substrates. Various heteroatom-substitution patterns and heterocyclic boronic acids underwent conversion to the desired cross-coupling product in good to excellent yields. a) The anilinyltetrazine **21** was prepared by cross-coupling of the Boc-protected derivative, followed by deprotection with TFA (yield reported over two steps).

to very good yields (49 – 80%). In accordance with previous reports, electron rich phenylboronic acids reliably underwent cross-coupling in high yields.[25] Along these lines, *para-* and *meta-*methoxy substituted variants (**12**, **13**) produced the corresponding tetrazines in yields of 82% and 69%, respectively. The *ortho-*methoxy analog **14** however, showed greatly reduced yield (37%). However, decreased yields due to the steric impact of *ortho* substitution are not uncommon in cross-coupling reactions.[40] Benzyl (61% (**15**), 77% (**16**)) and TBS (68% (**17**)) protecting groups, as well as methylene (74% (**18**)) and ethylene bridged catechols (61% (**19**)), were also compatible with the presented method. Concerning the cross-coupling of nitrogen containing boronic acids, it was crucial to reduce the nucleophilic character at N, *i.e.* by Boc protection or acetylation (**20** (65%)). This strategy allowed, after Boc-deprotection with TFA, the preparation of free amine **21** (66%). Difunctionalized derivatives with substituents of opposite electronic nature, as in **22** or **23**, also proved to be good substrates and yielded the desired product in 79% and 85% respectively. Considering medicinal chemistry as a potential field of application and the frequent occurrence of heterocyclic moieties therein, we also investigated the cross-coupling of heterocyclic boronic acids. Clean conversion was observed when submitting 3-furanyl- (66%, (**24**)), 3-thiophenyl- (71%, (**25**)), or dimethylaminopyrimidinylboronic acid (72%, (**26**)) to our optimized conditions. As further heterocyclic coupling partners, indole- and pyridylboronic acids were investigated. While Boc-protected indole **27** was prepared in good yield (73%), all attempts to couple pyridylboronic acids failed. Further cases which produced unsatisfactory amounts of product were generally observed for electron poorer substrates, such as boronic acids of benzoates, benzaldehydes, benzonitriles and nitrobenzenes. Contrary to our initial expectation, reaction with 4-vinylphenyl- or 4-alkynylphenylboronic acid either proceeded with very low yields or not at all. Satisfyingly, however, coupling of the boronic acids of aryl halides was found to be very efficient. Fluoro- (*para*: 82% (**2**), *ortho*: 72% (**28**)), 4-chloro (86% (**29**)) and 4-bromo (77% (**30**)) analogs were obtained in very good yields. Even 4-iodophenylboronic acid produced acceptable amounts of coupling product, albeit as a mixture with the doubly-coupled iodobiphenyl tetrazine.

Conclusion

In conclusion, the formation of new carbon-carbon bonds between a monosubstituted tetrazine and an array of aryl boronic acids is reported, which proceeds in a mild and fast palladium catalyzed manner. A variety of silver salts was investigated with regard to boronic acid activation and Ag_2CO_3 was found to mediate the target reaction exceptionally well. With regard to the catalyst, screening analogs of the ferrocene based dppf scaffold proved an efficient method for fine tuning the electronic properties of the ancillary ligand and, in turn, of the palladium center. Preparation of the electron-poorer dppf-CF_3 ligand greatly improved the efficiency of the catalytic process and allowed a reduction of catalyst loading in certain cases. Coincidingly, it enabled the preparation of tetrazine coupling products in good to excellent yields, which were unattainable in useful amounts with the original dppf system, *e.g.* **2**, **29**, **28**, **33**. These results open the way for the tailored synthesis of mono-functionalized tetrazines via mild and selective cross-coupling.

Acknowledgement

Supporting information

CCDC-2080087-2080090 contain the supplementary crystallographic data for this paper. The data can be obtained free of charge from The Cambridge Crystallographic Data Center via www.ccdc.cam.ac.uk/structures.

References

[1]   H. Wu, N. K. Devaraj, *Acc. Chem. Res.* **2018**, *51*, 1249–1259.

[2]   K. Lang, J. W. Chin, *ACS Chem. Biol.* **2014**, *9*, 16–20.

[3]   D. M. Patterson, L. A. Nazarova, J. A. Prescher, *ACS Chem. Biol.* **2014**, *9*, 592–605.

[4]   B. L. Oliveira, Z. Guo, G. J. L. Bernardes, *Chemical Society Reviews* **2017**, *46*, 4895–4950.

[5]   R. Selvaraj, J. M. Fox, *Current Opinion in Chemical Biology* **2013**, *17*, 753–760.

[6]   T. Cañeque, S. Müller, R. Rodriguez, *Nature Reviews Chemistry* **2018**, *2*, 202–215.

[7]   A. Wieczorek, P. Werther, J. Euchner, R. Wombacher, *Chem. Sci.* **2017**, *8*, 1506–1510.

[8]   M. Baalmann, M. J. Ziegler, P. Werther, J. Wilhelm, R. Wombacher, *Bioconjugate Chem.* **2019**, *30*, 1405–1414.

[9]   E. Ros, M. Bellido, X. Verdaguer, L. Ribas de Pouplana, A. Riera, *Bioconjugate Chem.* **2020**, *31*, 933–938.

[10] G. B. Cserép, A. Herner, P. Kele, *Methods Appl. Fluoresc.* **2015**, *3*, 042001.

[11] M. L. Blackman, M. Royzen, J. M. Fox, *J. Am. Chem. Soc.* **2008**, *130*, 13518–13519.

[12] N. K. Devaraj, R. Weissleder, S. A. Hilderbrand, *Bioconjugate Chem.* **2008**, *19*, 2297–2299.

[13] S. D. Schnell, M. Schilling, J. Sklyaruk, A. Linden, S. Luber, K. Gademann, *Org. Lett.* **2021**, *23*, 2426–2430.

[14] S. D. Schnell, L. V. Hoff, A. Panchagnula, M. H. H. Wurzenberger, T. M. Klapötke, S. Sieber, A. Linden, K. Gademann, *Chem. Sci.* **2020**, *11*, 3042–3047.

[15] D. L. Boger, R. P. Schaum, R. M. Garbaccio, *J. Org. Chem.* **1998**, *63*, 6329–6337.

[16] A. Pinner, *Ber. Dtsch. Chem. Ges.* **1893**, *26*, 2126–2135.

[17] W. D. Lambert, Y. Fang, S. Mahapatra, Z. Huang, C. W. am Ende, J. M. Fox, *J. Am. Chem. Soc.* **2019**, *141*, 17068–17074.

[18] Z. Novák, A. Kotschy, *Org. Lett.* **2003**, *5*, 3495–3497.

[19] Y. Qu, P. Pander, O. Vybornyi, M. Vasylieva, R. Guillot, F. Miomandre, F. B. Dias, P. Skabara, P. Data, G. Clavier, P. Audebert, *J. Org. Chem.* **2020**, *85*, 3407–3416.

[20] A. Wieczorek, T. Buckup, R. Wombacher, *Org. Biomol. Chem.* **2014**, *12*, 4177–4185.

[21] F. Pop, J. Ding, L. M. L. Daku, A. Hauser, N. Avarvari, *RSC Adv.* **2013**, *3*, 3218–3221.

[22] A. M. Bender, T. C. Chopko, T. M. Bridges, C. W. Lindsley, *Org. Lett.* **2017**, *19*, 5693–5696.

[23] N. Leconte, A. Keromnes-Wuillaume, F. Suzenet, G. Guillaumet, *Synlett* **2007**, *2007*, 204–210.

[24] E. Ros, A. Prades, D. Forson, J. Smyth, X. Verdaguer, L. R. de Pouplana, A. Riera, *Chem. Commun.* **2020**, *56*, 11086–11089.

[25] W. D. Lambert, Y. Fang, S. Mahapatra, Z. Huang, C. W. am Ende, J. M. Fox, *J. Am. Chem. Soc.* **2019**, *141*, 17068–17074.

[26] J. Yang, Y. Liang, J. Šečkutė, K. N. Houk, N. K. Devaraj, *Chemistry – A European Journal* **2014**, *20*, 3365–3375.

[27] K. Tatsumi, R. Hoffmann, A. Yamamoto, J. K. Stille, *BCSJ* **1981**, *54*, 1857–1867.

[28] J. J. Low, W. A. Goddard, *J. Am. Chem. Soc.* **1986**, *108*, 6115–6128.

[29] J. J. Low, W. A. Goddard, *J. Am. Chem. Soc.* **1984**, *106*, 6928–6937.

[30] J. F. Hartwig, *Inorg. Chem.* **2007**, *46*, 1936–1947.

[31] P. Hu, M. Zhang, X. Jie, W. Su, *Angew. Chem. Int. Ed.* **2012**, *51*, 227–231.

[32] Y.-Y. Che, Y. Yue, L.-Z. Lin, B. Pei, X. Deng, C. Feng, *Angew. Chem. Int. Ed.* **2020**, *59*, 16414–16419.

[33] W. H. Thompson, C. T. Sears, *Inorg. Chem.* **1977**, *16*, 769–774.

[34] A. H. Roy, J. F. Hartwig, *J. Am. Chem. Soc.* **2001**, *123*, 1232–1233.

[35] P. Fitton, E. A. Rick, *J. Organomet. Chem.* **1971**, *28*, 287–291.

[36] Z. Li, J. Ding, N. Song, X. Du, J. Zhou, J. Lu, Y. Tao, *Chem. Mater.* **2011**, *23*, 1977–1984.

[37] J. Zhu, J. Hiltz, R. Bruce Lennox, R. Schirrmacher, *ChemComm* **2013**, *49*, 10275–10277.

[38] Z. Li, J. Ding, N. Song, J. Lu, Y. Tao, *J. Am. Chem. Soc.* **2010**, *132*, 13160–13161.

[39] D. K. Hwang, R. R. Dasari, M. Fenoll, V. Alain-Rizzo, A. Dindar, J. W. Shim, N. Deb, C. Fuentes-Hernandez, S. Barlow, D. G. Bucknall, P. Audebert, S. R. Marder, B. Kippelen, *Adv. Mater.* **2012**, *24*, 4445–4450.

[40] J. Yin, M. P. Rainka, X.-X. Zhang, S. L. Buchwald, *J. Am. Chem. Soc.* **2002**, *124*, 1162–1163.

Cross-coupling Reactions of Monosubstituted Tetrazines

Lukas V. Hoff, Simon D. Schnell, Andrea Tomio, Anthony Linden, Karl Gademann

Department of Chemistry, University of Zurich, Winterthurerstrasse 190, 8057 Zurich, Switzerland

Supporting Information

Table of Contents

Experimental Procedures

General

All chemicals were purchased from Sigma-Aldrich, Acros, Alfa Aesar, TCI, or Fluka and were used without further purification. Solvents applied for chemical transformations were either puriss. quality or HPLC grade solvents. 3-Bromo-1,2,4,5-tetrazine (BrTet, **1**) was prepared according to known procedures.[1] All synthetic transformations were monitored by either thin layer chromatography (TLC), ^{1}H-NMR spectroscopy or UHPLC/ESI-MS. TLC was performed on Merck silica gel 60 F_{254} plates (0.25 mm thickness) precoated with a fluorescent indicator. The developed plates were examined under UV light and stained with ceric ammonium molybdate or potassium permanganate followed by heating. Concentration under reduced pressure was performed by rotary evaporation *in vacuo* at the designated temperature and pressure. Flash chromatography was performed using silica gel 60 (230-400 mesh) from Sigma-Aldrich with a forced flow eluent at 0.1-0.3 bar pressure. All ^{1}H NMR, ^{13}C NMR, ^{19}F NMR, and ^{31}P NMR spectra were recorded using Bruker 400 MHz (^{1}H) & 101 MHz (^{13}C) or Bruker 500 MHz (^{1}H) & 126 MHz (^{13}C) spectrometers at 25 °C. Chemical shifts (d-values) are reported in ppm, spectra were calibrated relative to the solvents' residual proton chemical shifts (CHCl$_3$, δ = 7.26; DMSO-d_5, δ = 2.50) and residual carbon chemical shifts (CDCl$_3$, δ = 77.16; DMSO-d_6, δ = 39.52), multiplicity is reported as follows: s = singlet, d = doublet, t = triplet, q = quartet, m = multiplet or unresolved and coupling constant *J* in Hz. IR spectra were recorded on a Varian 800 FT-IR ATR spectrophotometer with intensities being reported as strong (s), medium (m), and weak (w) and given in cm^{-1}. All high-resolution mass spectra (HRMS-ESI & HRMS-APCI) were recorded by the mass spectrometry service at the University of Zürich on a *Dionex Ultimate 3000* UHPLC system (*ThermoFischer Scientifics*, Germering, Germany) connected to a *QExactive* MS with a heated ESI source (*ThermoFisher Scientific*, Bremen, Germany); on-flow injection of 1 μL sample (*c* = ca. 50 μg mL^{-1} in the indicated solvent) with an *XRS* auto-sampler (*CTC*, Zwingen, Switzerland); flow rate 120 μL min^{-1}; ESI: spray voltage 3.0 kV, capillary temperature 280 °C, sheath gas 30 L min^{-1}, aux gas 8 L min^{-1}, s-lens RF level 55.0, aux gas temperature 250 °C (N$_2$); full scan MS in the alternating (+)/(−)-ESI mode; mass ranges 80–1'200 *m/z*, 133–2'000 *m/z*, or 200–3'000 *m/z* at 70'000 resolution (full width half-maximum); automatic gain control (AGC) target of 3.00·10^6; maximum allowed ion transfer time (IT) 30 ms; mass calibrationto <2 ppm accuracy with *Pierce*® ESI calibration solutions (*ThermoFisher Scientific*, Rockford, USA); lock masses: ubiquitous erucamide (*m/z* 338.34174, (+)-ESI) and palmitic acid (*m/z* 255.23295, (−)-ESI) or (for EI) on a *DFS* double-focusing (BE geometry) magnetic sector mass spectrometer (*ThermoFisher Scientific*, Bremen, Germany). Mass spectra were measured with electron ionization (EI) at 70 eV, solid probe inlet, a source temperature of 200°C, an acceleration voltage of 5 kV, and a resolution of 10'000. The instrument was scanned between e.g. *m/z* 300 and 350 at a scan rate of 100-200 s / decade in the electric scan mode. Perfluorokerosene (*PFK, Fluorochem*, Derbyshire, UK) served for calibration. Melting points (M.p.) were determined using a *Büchi B-545* apparatus in open capillaries and are uncorrected. X-ray diffraction data were recorded using a *Rigaku Oxford Diffraction SuperNova* area-detector diffractometer.

Optimization Studies

Solvent Screening

A Schlenk tube (10 mL) equipped with a stirring bar was charged consecutively with Pd(dppf)Cl$_2$ (17 mg, 23.3 μmol, 15 mol-%), 4-*tert*-butylphenyl boronic acid (55.2 mg, 0.310 mmol, 2.0 eq.), Ag$_2$O (89.8 mg, 0.387 mmol, 2.5 eq.) and bromo tetrazine (25.0 mg, 0.155 mmol, 1.0 eq.). The tube was sealed with a septum and dry solvent (1.55 mL, 0.1 M) was added *via* syringe. Subsequently, the tube was placed in a preheated oil bath (60 °C) and the mixture was stirred (825 rpm) for the designated time (**Table S1**). Yields were determined after purification by flash column chromatography (SiO$_2$, 2x15 cm, CH$_2$Cl$_2$), removal of the solvent *in vacuo* (40 °C, 700 to 10 mbar) and subsequent drying at high vacuum.
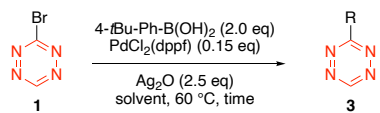
entry	solvent (0.1 M)	time	yield[a]
1	DMF	20 h	33%
2	DMF	30 min	23%
3	Toluene	30 min	3%
4	THF	30 min	2%
5	MeCN	30 min	41%
6	HFIP	30 min	0%
7	1,4-Dioxane	30 min	0%
8	MeOH	30 min	0%
9	1,2-DME	30 min	7%

Table S1: Solvent screening. [a]All reported yields were determined after purification by column chromatography.

## Screening of Silver(I) Salts and Reagent Amounts

A Schlenk tube (10 mL) equipped with a stirring bar was charged consecutively with Pd(dppf)Cl$_2$ (17 mg, 23.3 μmol, 15 mol-%), 4-*tert*-butylphenyl boronic acid (**Table S2**), a silver salt (**Table S2**) and bromo tetrazine (25.0 mg, 0.155 mmol, 1.0 eq.). The tube was sealed with a septum and dry MeCN (1.55 mL, 0.1 M) was added *via* syringe. Subsequently, the tube was placed in a preheated oil bath (60 °C) and the mixture was stirred (825 rpm) for 30 min. Yields were determined after purification by flash column chromatography (SiO$_2$, 2x15 cm, CH$_2$Cl$_2$), removal of the solvent *in vacuo* (40 °C, 700 to 10 mbar) and subsequent drying at high vacuum.
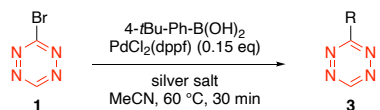
entry	boronic acid	silver salt	yield[a]
1	2.0 eq.	Ag$_2$O (2.5 eq.)	41%
2	2.0 eq.	AgOAc (2.5 eq.)	0%
3	2.0 eq.	AgNO$_3$ (2.5 eq.)	0%
4	2.0 eq.	AgF (2.5 eq.)	41%
5	2.0 eq.	Ag$_2$CO$_3$ (2.5 eq.)	71%
6	2.0 eq.	AgBF$_4$ (2.5 eq.)	0%
7	2.0 eq.	Ag$_3$PO$_4$ (2.5 eq.)	0%
8	2.0 eq.	AgPF$_6$ (2.5 eq.)	4%
9	2.0 eq.	Ag$_2$CO$_3$ (1.5 eq.)	72%
10	1.5 eq.	Ag$_2$CO$_3$ (1.5 eq.)	75%
11	1.5 eq.	Ag$_2$CO$_3$ (1.0 eq.)	72%
12	1.5 eq.	Ag$_2$CO$_3$ (0.5 eq.)	41%

Table S2: Screening of silver(I) salts and optimization of the employed equivalents of the boronic acid and silver(I) source. [a]All reported yields were determined after purification by column chromatography.

Temperature Screening

A Schlenk tube (10 mL) equipped with a stirring bar was charged consecutively with Pd(dppf)Cl$_2$ (17 mg, 23.3 μmol, 15 mol-%), 4-*tert*-butylphenyl boronic acid (41.4 mg, 0.233 mmol, 1.5 eq.), Ag$_2$CO$_3$ (42.7 mg, 0.155 mmol, 1.0 eq.) and bromo tetrazine (25.0 mg, 0.155 mmol, 1.0 eq.). The tube was sealed with a septum and dry MeCN (1.55 mL, 0.1 M) was added *via* syringe. Subsequently, the tube was placed in an oil bath of designated temperature (**Table S3**) and the mixture was stirred (825 rpm) for 30 min. Yields were determined after purification by flash column chromatography (SiO$_2$, 2x15 cm, CH$_2$Cl$_2$), removal of the solvent *in vacuo* (40 °C, 700 to 10 mbar) and subsequent drying at high vacuum.
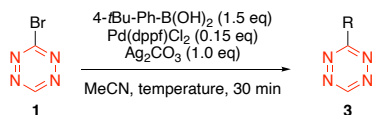
entry	temp	yield[a]
1	25 °C	traces
2	60 °C	72%
3	80 °C	80%
4	100 °C	61%

Table S3: Temperature screening. [a]All reported yields were determined after purification by column chromatography.

Catalyst Screening

A Schlenk tube (10 mL) equipped with a stirring bar was charged consecutively with catalyst (**Table S4**), boronic acid (0.233 mmol, 1.5 eq.) (**Table S4**), Ag$_2$CO$_3$ (42.7 mg, 0.155 mmol, 1.0 eq.) and bromo tetrazine (25.0 mg, 0.155 mmol, 1.0 eq.). The tube was sealed with a septum and dry MeCN (1.55 mL, 0.1 M) was added *via* syringe. Subsequently, the tube was placed in an oil bath (80 °C) and the mixture was stirred (825 rpm) for 30 min. Yields were determined after purification by flash column chromatography (SiO$_2$, 2x15 cm, CH$_2$Cl$_2$), removal of the solvent *in vacuo* (40 °C, 700 to 10 mbar) and subsequent drying at high vacuum.
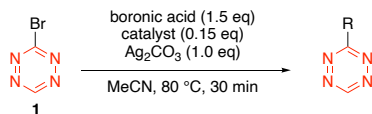
entry	catalyst	boronic acid	yield[a]
1	PdCl$_2$	*t*Bu-Ph-BOH$_2$	6%
2	dppf	*t*Bu-Ph-BOH$_2$	<5%
3	dppf, PdCl$_2$	*t*Bu-Ph-BOH$_2$	72%
4	Pd(PPh$_3$)$_2$Cl$_2$	*t*Bu-Ph-BOH$_2$	9%
5	DPEphos, PdCl$_2$	*t*Bu-Ph-BOH$_2$	48%
6	BINAP, PdCl$_2$	*t*Bu-Ph-BOH$_2$	41%
7	Pd(dtbpf)Cl$_2$	*t*Bu-Ph-BOH$_2$	34%
8	Pd(dippf)Cl$_2$	*t*Bu-Ph-BOH$_2$	85%
9	Pd(dtfpf)Cl$_2$	*t*Bu-Ph-BOH$_2$	84%
10	Pd(dppf-CF$_3$)Cl$_2$	F-Ph-BOH$_2$	15%
11	Pd(dippf)Cl$_2$	F-Ph-BOH$_2$	31%
12	Pd(dppf)Cl$_2$	F-Ph-BOH$_2$	44%

	13	Pd(dppf-CF$_3$)Cl$_2$	F-Ph-BOH$_2$	82%

Table S4: Catalyst screening. [a]All reported yields were determined after purification by column chromatography.

Screening of Catalyst Loading and Scale

A Schlenk tube (10 mL) equipped with a stirring bar was charged consecutively with Pd(dppf-CF$_3$)Cl$_2$ (**Table S5**), boronic acid (0.233 mmol, 1.5 eq.) (**Table S5**), Ag$_2$CO$_3$ (42.7 mg, 0.155 mmol, 1.0 eq.) and bromo tetrazine (25.0 mg, 0.155 mmol, 1.0 eq.). The tube was sealed with a septum and dry MeCN (1.55 mL, 0.1 M) was added *via* syringe. Subsequently, the tube was placed in an oil bath (80 °C) and the mixture was stirred (825 rpm) for 30 min. Yields were determined after purification by flash column chromatography (SiO$_2$, 2x15 cm, CH$_2$Cl$_2$), removal of the solvent *in vacuo* (40 °C, 700 to 10 mbar) and subsequent drying at high vacuum.
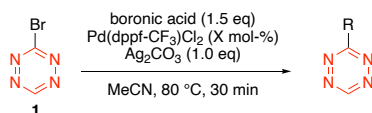
entry	catalyst mol-%	boronic acid	yield[a]	scale
1	10%	*t*Bu-Ph-B(OH)$_2$	83%	25 mg
2	5%	*t*Bu-Ph-B(OH)$_2$	83%	25 mg
3	3%	*t*Bu-Ph-B(OH)$_2$	44%	25 mg
4	1%	*t*Bu-Ph-B(OH)$_2$	3%	25 mg
5	10%	F-Ph-B(OH)$_2$	79%	25 mg
6	5%	F-Ph-B(OH)$_2$	49%	25 mg
7	5%	*t*Bu-Ph-B(OH)$_2$	83%	200 mg

Table S5: Screening of catalyst loading and increased scale of reaction. [a]All reported yields were determined after purification by column chromatography.

Additional experiments

A Schlenk tube (10 mL) equipped with a stirring bar was charged consecutively with Pd(dppf)Cl$_2$ (17.0 mg, 23.3 μmol, 15 mol-%), boronic acid (**Table S6**), Ag$_2$CO$_3$ (**Table S6**) and bromo tetrazine (25.0 mg, 0.155 mmol, 1.0 eq.). The solid additives presented in **Table S6** were added at this point. In the case of H$_2$O, it was added after the solvent. The tube was sealed with a septum and dry MeCN (1.55 mL, 0.1 M) was added *via* syringe. Subsequently, the tube was placed in an oil bath (80 °C) and the mixture was stirred (825 rpm) for 30 min. Yields were determined after purification by flash column chromatography (SiO$_2$, 2x15 cm, CH$_2$Cl$_2$), removal of the solvent *in vacuo* (40 °C, 700 to 10 mbar) and subsequent drying at high vacuum.
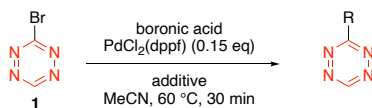
entry	boronic acid	silver salt	additive	yield[a]
1	*t*Bu-Ph-B(OH)$_2$ (1.5 eq)	–	Na$_2$CO$_3$ (1.5 eq)	0
2	*p*-tolyl-B(OH)$_2$ (1 eq)	AgCO$_3$ (2.5 eq)	5% H$_2$O	5
3	*p*-tolyl-B(OH)$_2$ (1 eq)	AgCO$_3$ (2.5 eq)	10% H$_2$O	1
4	*t*Bu-Ph-B(OH)$_2$ (1.5 eq)	Ag$_2$CO$_3$ (1.0 eq.)	PPh$_3$ (0.3 eq)	12%
5	4-F-Ph-B(OH)$_2$ (1.5 eq)	Ag$_2$CO$_3$ (1.5 eq.)	–	32%
6	4-Cl-Ph-B(OH)$_2$ (1.5 eq)	Ag$_2$CO$_3$ (1.5 eq.)	–	20%

8	4-Br-Ph-B(OH)$_2$ (1.5 eq)	Ag$_2$CO$_3$ (1.5 eq.)	–	12%
9	4-I-Ph-B(OH)$_2$ (1.5 eq)	Ag$_2$CO$_3$ (1.5 eq.)	–	0%
10	4-MeO$_2$C-Ph-B(OH)$_2$ (1.5 eq)	Ag$_2$CO$_3$ (2.5 eq.)	–	0%

Table S6: Additional experiments. [a]All reported yields were determined after purification by column chromatography.

Synthetic Procedures

General Procedure for BrTet Cross-Coupling
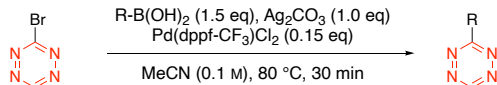
A Schlenk tube (10 mL) equipped with a stirring bar was charged consecutively with Pd(dppf-CF$_3$)Cl$_2$ (23.3 μmol, 15 mol-%), boronic acid (0.223 mmol, 1.5 eq.), Ag$_2$CO$_3$ (0.155 mmol, 1.0 eq.) and bromo tetrazine (0.155 mmol, 1.0 eq.). The tube was sealed with a septum and dry MeCN (1.55 mL, 0.1 M) was added *via* syringe. Subsequently, the tube was placed in a preheated oil bath (80 °C) and the mixture was stirred (825 rpm) for 30 min. The reaction mixture was filtered through a pad of SiO$_2$ (4 cm), concentrated *in vacuo* (40 °C, 600 to 50 mbar) and purified by flash column chromatography (SiO$_2$, 2x15 cm, CH$_2$Cl$_2$), which, after removal of the solvent *in vacuo* (40 °C, 700 to 10 mbar) and subsequent drying at high vacuum, afforded the desired product.

3-(4-Fluorophenyl)-1,2,4,5-tetrazine (2)

2
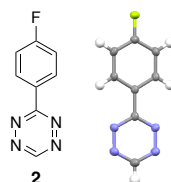
Yield: 82%. **TLC**: Rf = 0.58 (CH$_2$Cl$_2$). **M.p.** (CDCl3): 143.8 – 145.5 °C. **^{1}H NMR** (400 MHz, CDCl$_3$): δ 10.22 (s, 1H), 8.71 – 8.61 (m, 2H), 7.34 – 7.26 (m, 2H). **^{13}C NMR** (101 MHz, CDCl$_3$): d 166.2 (d, *J* = 255.0 Hz), 165.8, 157.9, 130.8 (d, *J* = 9.3 Hz), 127.9 (d, *J* = 3.0 Hz), 116.8 (d, *J* = 22.0 Hz). **IR** (neat): 3112w, 3083m, 3075m, 1933w, 1850w, 1688w, 1598m, 1510m, 1438m, 1363m, 1350m, 1294m, 1238m, 1165m, 1142m, 1101m, 1007w, 911m, 895m, 854s, 804m, 718m, 593w, 562s, 473w. **HR-EI-MS**: 176.04919 (100, C$_8$H$_5$N$_4$F$^{+\bullet}$; [*M*]$^{+\bullet}$; calc. 176.04928; Δ = −0.47 ppm).

3-(4-(tert-Butyl)phenyl)-1,2,4,5-tetrazine (3)

3
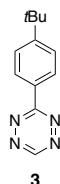
Yield: 84%. **TLC:** *R*$_f$ = 0.31 (CH$_2$Cl$_2$/*n*-pentane = 1:1). **M.p.** (CDCl$_3$): 80.1 – 80.9 °C. **^{1}H NMR** (400 MHz, CDCl$_3$): δ 10.17 (s, 1H), 8.56 – 8.51 (m, 2H), 7.64 – 7.59 (m, 2H), 1.39 (s, 9H). **^{13}C NMR** (101 MHz, CDCl$_3$): δ 166.4, 157.7, 157.0, 128.8, 128.1, 126.4, 35.2, 31.1. **IR** (neat): 3095w, 2958m, 2863w, 1743w, 1607m, 1466w, 1434s, 1417m, 1371m, 1347s, 1268m, 1195m, 1168w, 1145m, 1123w, 1110w, 1068w, 1028w, 1007w, 900m, 855m, 805m, 581s, 509w. **HR-ESI-MS** (MeOH + NaI): 215.12928 (100, C$_{12}$H$_{15}$N$_4$$^+$; [*M* + H]$^+$; calc. 215.12912; Δ = 0.73 ppm).

3-Phenyl-1,2,4,5-tetrazine (4)

4

Yield: 65%. **TLC:** R_f = 0.50 (Et$_2$O/n-pentane = 1:9). **M.p.** (CDCl$_3$): 125.2 − 126.7 °C. **^{1}H NMR** (400 MHz, CDCl$_3$): δ 10.22 (s, 1H), 8.66 − 8.60 (m, 2H), 7.69 − 7.58 (m, 3H). **^{13}C NMR** (101 MHz, CDCl$_3$): δ 166.5, 157.8, 133.2, 131.6, 129.4, 128.3. **IR** (neat): 3085m, 2926w, 1982w, 1923w, 1848w, 1597m, 1499w, 1455m, 1437m, 1380m, 1349m, 1310m, 1180w, 1153w, 1142m, 1103w, 1073m, 1031w, 1012w, 1000w, 927w, 913m, 896m, 790w, 761s, 733m, 688s, 566s. **HR-EI-MS**: 158.05868 (100, C$_8$H$_6$N$_4$$^{+\cdot}$; [$M$]$^{+\cdot}$; calc. 158.05870; Δ = −0.12 ppm).
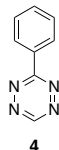
3-(p-Tolyl)-1,2,4,5-tetrazine (5)

5

Yield: 78%. **TLC:** R_f = 0.64 (CH$_2$Cl$_2$). **M.p.** (CDCl$_3$): 86.2 − 86.8 °C. **^{1}H NMR** (400 MHz, CDCl$_3$): δ 10.18 (s, 1H), 8.54 − 8.49 (m, 2H), 7.43 − 7.39 (m, 2H), 2.48 (s, 3H). **^{13}C NMR** (101 MHz, CDCl$_3$): δ 166.6, 157.8, 144.1, 130.3, 129.0, 128.4, 21.9. **IR** (neat): 3087w, 3076w, 2922w, 1606m, 1434s, 1347s, 1310w, 1215w, 1188m, 1162w, 1141m, 1025w, 911m, 896m, 839m, 824w, 799m, 715w, 565m. **HR-EI-MS**: 172.07470 (100, C$_9$H$_8$N$_4$$^{+\cdot}$; [$M$]$^{+\cdot}$; calc. 172.07435; Δ = 2.05 ppm).

3-(3,5-Dimethylphenyl)-1,2,4,5-tetrazine (6)

6

Yield: 66%. **TLC:** R_f = 0.36 (CH$_2$Cl$_2$/n-pentane = 1:1). **M.p.** (CDCl$_3$): 106.7 − 107.8 °C. **^{1}H NMR** (400 MHz, CDCl$_3$): δ 10.19 (s, 1H), 8.26 − 8.22 (m, 2H), 7.29 − 7.27 (m, 1H), 2.45 (s, 6H). **^{13}C NMR** (101 MHz, CDCl$_3$): δ 166.7, 157.8, 139.2, 134.9, 131.4, 126.1, 21.4. **IR** (neat): 2921w, 1605m, 1495w, 1429m, 1380m, 1354s, 1244m, 1133w, 1077w, 1040w, 995w, 955w, 904m, 864m, 806w, 691m, 602w. **HR-EI-MS**: 186.08933 (100, C$_{10}$H$_{10}$N$_4$$^{+\cdot}$; [$M$]$^{+\cdot}$; calc. 186.09000; Δ = −3.61 ppm).
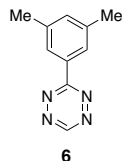
3-(2,4-Dimethylphenyl)-1,2,4,5-tetrazine (7)

7
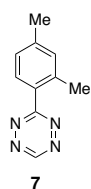
Yield: 61%. **TLC:** R_f = 0.45 (Et$_2$O/*n*-pentane = 15:85). **^{1}H NMR** (400 MHz, CDCl$_3$): δ 10.19 (s, 1H), 8.09 – 8.02 (m, 1H), 7.26 – 7.22 (m, 3H), 2.64 (s, 3H), 2.44 (s, 3H). **^{13}C NMR** (101 MHz, CDCl$_3$): δ 169.6, 156.6, 142.4, 138.8, 132.9, 131.2, 128.7, 127.4, 21.6, 21.4. **IR** (neat): 2925w, 1613m, 1430m, 1381w, 1340s, 1283w, 1236w, 1153m, 1117m, 1036w, 894m, 832m, 807m, 722w, 580m, 513w, 480w. **HR-ESI-MS** (MeOH/CHCl$_3$ 3:2): 187.09797 (100, C$_{10}$H$_{11}$N$_4^+$; [M + H]$^+$; calc. 187.09782; Δ = 0.77 ppm).

3-(Naphthalen-1-yl)-1,2,4,5-tetrazine (8)

8
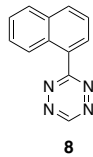
Yield: 77%. **TLC:** R_f = 0.61 (CH$_2$Cl$_2$). **M.p.** (CDCl$_3$): 123.2 – 124.0 °C. **^{1}H NMR** (400 MHz, CDCl$_3$): δ 10.32 (s, 1H), 8.71 – 8.67 (m, 1H), 8.36 (dd, J = 7.3, 1.3 Hz, 1H), 8.14 (dt, J = 8.3, 1.2 Hz, 1H), 8.02 – 7.97 (m, 1H), 7.70 (dd, J = 8.2, 7.3 Hz, 1H), 7.67 – 7.59 (m, 2H). **^{13}C NMR** (101 MHz, CDCl$_3$): δ 169.7, 157.0, 134.1, 133.2, 131.3, 130.6, 129.2, 128.9, 128.2, 126.7, 125.3, 124.8. **IR** (neat): 3051w, 1575w, 1514m, 1465m, 1427m, 1374w, 1327m, 1259m, 1204w, 1152m, 1100w, 970w, 893m, 799m, 773s, 647w, 557w, 481m. **HR-ESI-MS** (MeOH/CHCl$_3$ 3:2): 209.08223 (100, C$_{12}$H$_9$N$_4^+$; [M + H]$^+$; calc. 209.08217; Δ = 0.30 ppm).

3-(Naphthalen-2-yl)-1,2,4,5-tetrazine (9)

9
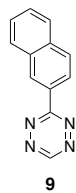
Yield: 78%. **TLC:** R_f = 0.58 (CH$_2$Cl$_2$). **M.p.** (CDCl$_3$): 159.7 – 160.6 °C. **^{1}H NMR** (400 MHz, CDCl$_3$): δ 10.22 (s, 1H), 9.23 – 9.16 (m, 1H), 8.65 – 8.59 (m, 1H), 8.05 – 8.00 (m, 2H), 7.94 – 7.88 (m, 1H), 7.65 – 7.55 (m, 2H). **^{13}C NMR** (101 MHz, CDCl$_3$): δ 166.6, 157.7, 135.7, 133.1, 129.8, 129.6, 129.3, 128.8, 128.6, 128.0, 127.1, 123.8, 110.0. **IR** (neat): 1626w, 1598w, 1475m, 1430m, 1385w, 1367w, 1339m, 1325m, 1271w, 1238w, 1199w, 1140m, 946w, 906m, 868m, 826m, 805m, 747s, 652m, 628w, 556m, 474s. **HR-APCI-MS** (MeOH/CHCl$_3$ 3:2, MeOH + 0.1% FA): 209.08223 (100, C$_{12}$H$_9$N$_4^+$; [M + H]$^+$; calc. 209.08217; Δ = 0.30 ppm).

3-([1,1'-Biphenyl]-4-yl)-1,2,4,5-tetrazine (10)

10
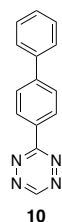
Yield: 80%. **TLC:** R_f = 0.36 (CH$_2$Cl$_2$/*n*-pentane = 1:1). **M.p.** (CDCl$_3$): 189.5 – 190.4 °C. **^{1}H NMR** (400 MHz, CDCl$_3$): δ 10.22 (s, 1H), 8.73 – 8.67 (m, 2H), 7.87 – 7.82 (m, 2H), 7.73 – 7.67 (m, 2H), 7.54 – 7.47 (m, 2H), 7.46 – 7.40 (m, 1H). **^{13}C NMR** (101 MHz, CDCl$_3$): δ 166.4, 157.7, 145.9, 139.8, 130.4, 129.0, 128.8, 128.8, 128.4, 128.0, 127.2. **IR** (neat): 3034w, 1606w, 1488w, 1440m, 1352m, 1182w,

1146m, 1116w, 1006w, 902m, 851s, 825w, 805w, 763s, 725m, 696m, 576s, 529m. **HR-ESI-MS** (MeOH + NaI): 235.09784 (100, $C_{14}H_{11}N_4^+$; $[M + H]^+$; calc. 235.09782; Δ = 0.09 ppm).

3-(9H-Fluoren-3-yl)-1,2,4,5-tetrazine (11)
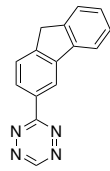
11

Yield: 49%. **TLC:** R_f = 0.57 (CH_2Cl_2). **M.p.** ($CDCl_3$): 213.8 − 214.9 °C. **¹H NMR** (400 MHz, $CDCl_3$) δ 10.18 (s, 1H), 8.82 − 8.77 (m, 1H), 8.68 (dd, J = 8.2, 1.5 Hz, 1H), 8.02 − 7.96 (m, 1H), 7.92 − 7.87 (m, 1H), 7.66 − 7.59 (m, 1H), 7.48 − 7.37 (m, 2H), 4.05 (s, 2H). **¹³C NMR** (101 MHz, $CDCl_3$) δ 166.9, 157.6, 146.8, 144.4, 144.2, 140.5, 129.8, 128.2, 127.5, 127.2, 125.4, 124.9, 121.0, 120.7, 37.1. **IR** (neat): 1614w, 1494w, 1461w, 1436m, 1420m, 1396w, 1342s, 1231w, 1188w, 1156w, 1137w, 1062w, 957w, 909m, 853w, 842w, 803w, 771m, 736s, 608m, 529m, 455m. **HR-APCI-MS** (MeOH/CHCl₃ 3:2, MeOH + 0.1% FA): 247.09806 (100, $C_{15}H_{11}N_4^+$; $[M + H]^+$; calc. 247.09782; Δ = 0.97 ppm).

3-(4-Methoxyphenyl)-1,2,4,5-tetrazine (12)
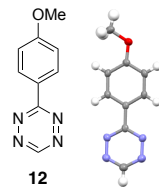
12

Yield: 87%. **TLC:** R_f = 0.35 (Et₂O/n-pentane = 1:4). **M.p.** ($CDCl_3$): 153.4 − 154.8 °C. **¹H NMR** (400 MHz, $CDCl_3$): δ 10.13 (s, 1H), 8.63 − 8.55 (m, 2H), 7.15 − 7.07 (m, 2H), 3.93 (s, 3H). **¹³C NMR** (101 MHz, $CDCl_3$): δ 166.2, 163.8, 157.4, 130.2, 124.0, 114.9, 55.6. **IR** (neat): 2963w, 2919w, 2840w, 1601s, 1580m, 1516m, 1436s, 1353s, 1306m, 1255s, 1181m, 1142w, 1116m, 1030m, 1015w, 1002w, 915m, 901m, 845m, 801m, 762w, 724w, 601w, 562s, 476w. **HR-ESI-MS** (MeOH/CHCl₃ 3:2): 189.07716 (100, $C_9H_9N_4O^+$; $[M + H]^+$; calc. 189.07709; Δ = 0.38 ppm).

3-(3-Methoxyphenyl)-1,2,4,5-tetrazine (13)
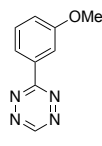
13

Yield: 66%. **TLC:** R_f = 0.47 (CH_2Cl_2). **M.p.** ($CDCl_3$): 124.3 − 125.1 °C. **¹H NMR** (400 MHz, $CDCl_3$): δ 10.21 (s, 1H), 8.22 (ddd, J = 7.8, 1.6, 1.0 Hz, 1H), 8.14 (dd, J = 2.7, 1.6 Hz, 1H), 7.54 − 7.47 (m, 1H), 7.18 (ddd, J = 8.3, 2.7, 1.0 Hz, 1H). **¹³C NMR** (101 MHz, $CDCl_3$): δ 166.4, 160.4, 157.9, 132.8, 130.5, 120.9, 120.0, 112.4, 55.6. **IR** (neat): 3099w, 3025w, 2957w, 2936w, 2836w, 1596m, 1500m, 1488w, 1466s, 1455m, 1434m, 1373m, 1345s, 1317m, 1280m, 1240s, 1175w, 1156w, 1133m, 1079m, 1047w, 1033m, 1020m, 993w, 910m, 871m, 810w, 795m, 690m, 626w, 566w, 484m. **HR-APCI-MS** (MeOH/CHCl₃ 3:2, MeOH + 0.1% FA): 189.07702 (100, $C_9H_9N_4O^+$; $[M + H]^+$; calc. 189.07709; Δ = − 0.37 ppm).

3-(2-Methoxyphenyl)-1,2,4,5-tetrazine (14)

14
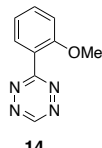
Yield: 37%. **TLC**: Rf = 0.33 (CH$_2$Cl$_2$). **M.p.** (CDCl3): 70.0 – 71.3 °C. **^{1}H NMR** (400 MHz, CDCl$_3$): δ 10.21 (s, 1H), 7.99 – 7.92 (m, 1H), 7.64 – 7.55 (m, 1H), 7.23 – 7.10 (m, 2H), 3.92 (s, 3H). **^{13}C NMR** (101 MHz, CDCl$_3$): δ 168.6, 158.6, 156.9, 133.7, 132.2, 122.1, 121.3, 112.4, 56.2. **IR** (neat): 3082w, 2941w, 2840w, 1602s, 1582m, 1499s, 1465m, 1438m, 1423m, 1369w, 1346s, 1278s, 1255s, 1165m, 1146m, 1115m, 1051w, 1022m, 891m, 812w, 756m, 650w, 585w, 504w. **HR-EI-MS**: 188.06959 (100, C$_8$H$_5$N$_4$O$^{+\bullet}$; [M]$^{+\bullet}$; calc. 188.06926; Δ = 1.76 ppm).

3-(4-(Benzyloxy)phenyl)-1,2,4,5-tetrazine (15)

15
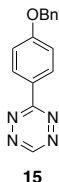
Yield: 61%. **TLC:** R_f = 0.62 (CH$_2$Cl$_2$). **M.p.** (CDCl$_3$): 145.8 – 148.0 °C. **^{1}H NMR** (400 MHz, CDCl$_3$): δ 10.12 (s, 1H), 8.62 – 8.55 (m, 2H), 7.49 – 7.32 (m, 5H), 7.21 – 7.14 (m, 2H), 5.19 (s, 2H). **^{13}C NMR** (101 MHz, CDCl$_3$): δ 166.1, 163.0, 157.4, 136.2, 130.2, 128.8, 128.3, 127.5, 124.2, 115.7, 70.3. **IR** (neat): 3099w, 3036w, 2924w, 2874w, 1603s, 1579w, 1513w, 1496w, 1454w, 1437s, 1427m, 1386w, 1368w, 1351s, 1306m, 1256s, 1238m, 1172s, 1146w, 1113w, 1066w, 1025w, 1010m, 1000m, 915m, 901m, 850m, 806w, 741m, 700m, 648w, 570m. **HR-APCI-MS** (CH$_2$Cl$_2$, MeOH + 0.1% FA): 265.10786 (100, C$_{15}$H$_{13}$N$_4$O$^+$; [M + H]$^+$; calc. 265.10839; Δ = −1.99 ppm).

3-(3-(Benzyloxy)phenyl)-1,2,4,5-tetrazine (16)

16
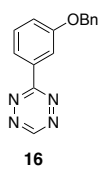
Yield: 77%. **TLC:** R_f = 0.34 (Et$_2$O/n-pentane = 1:9). **M.p.** (CDCl$_3$): 122.8 – 123.7 °C. **^{1}H NMR** (400 MHz, CDCl$_3$): δ 10.21 (s, 1H), 8.28 – 8.22 (m, 2H), 7.54 – 7.46 (m, 4H), 7.44 – 7.38 (m, 2H), 7.37 – 7.32 (m, 1H), 7.28 – 7.25 (m, 1H), 5.20 (s, 2H). **^{13}C NMR** (101 MHz, CDCl$_3$): δ 166.3, 159.5, 157.8, 136.5, 132.9, 130.5, 128.7, 128.2, 127.6, 121.1, 120.7, 113.5, 70.2. **IR** (neat): 3086w, 3032w, 2938w, 2877w, 1954w, 1588m, 1497m, 1448m, 1426m, 1387m, 1374m, 1342s, 1287m, 1233s, 1176w, 1136m, 1080m, 1046m, 1006s, 990m, 923m, 911m, 893m, 875m, 841w, 814w, 790m, 776w, 745s, 696s, 687s, 624m, 522w, 486m. **HR-ESI-MS** (MeOH + NaI): 265.10835 (100, C$_{15}$H$_{13}$N$_4$O$^+$; [M + H]$^+$; calc. 265.10839; Δ = −0.14 ppm).

3-(4-((tert-Butyldimethylsilyl)oxy)phenyl)-1,2,4,5-tetrazine (17)
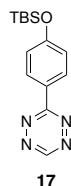
17

Yield: 68%. **TLC:** R_f = 0.71 (CH$_2$Cl$_2$). **M.p.** (CDCl$_3$): 73.5 – 74.6 °C. **^{1}H NMR** (400 MHz, CDCl$_3$): δ 10.13 (s, 1H), 8.55 – 8.50 (m, 2H), 7.06 – 7.00 (m, 2H), 1.02 (s, 9H), 0.28 (s, 6H). **^{13}C NMR** (101 MHz, CDCl$_3$): δ 166.2, 160.6, 157.3, 130.2, 124.5, 121.0, 25.7, 18.3, -4.3. **IR** (neat): 2958m, 2928m, 2887w, 2857m, 1599m, 1511m, 1472m, 1436m, 1353m, 1253s, 1181m, 1112m, 1004w, 906s, 854m, 826s, 805m, 778s, 722w, 667w, 632w, 571m, 555m, 462w. **HR-HR-ESI-MS** (MeOH + NaI): 289.14781 (100, C$_{14}$H$_{21}$N$_4$OSi$^+$; [M + H]$^+$; calc. 289.14791; Δ = –0.36 ppm).

3-(Benzo[d][1,3]dioxol-5-yl)-1,2,4,5-tetrazine (18)
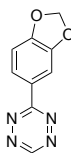
18

Yield: 79%. **TLC:** R_f = 0.50 (CH$_2$Cl$_2$). **M.p.** (CDCl$_3$): 124.6 – 125.5 °C. **^{1}H NMR** (400 MHz, CDCl$_3$): δ 10.12 (s, 1H), 8.25 (dd, J = 8.3, 1.7 Hz, 1H), 8.04 (d, J = 1.7 Hz, 1H), 7.00 (d, J = 8.3 Hz, 1H), 6.10 (s, 2H). **^{13}C NMR** (101 MHz, CDCl$_3$): δ 166.0, 157.4, 152.1, 148.8, 125.6, 124.2, 109.2, 107.9, 102.0. **IR** (neat): 3103w, 3088w, 3078w, 3017w, 2915w, 1627w, 1606w, 1506m, 1500m, 1489w, 1449s, 1431s, 1394m, 1338s, 1301w, 1267m, 1242m, 1196w, 1168m, 1131m, 1105m, 1038s, 936m, 917m, 901m, 875m, 834w, 824w, 796m, 775w, 726w, 625m, 577w, 490m. **HR-APCI-MS** (MeOH/CHCl$_3$ 3:2, MeOH + 0.1% FA): 203.05627 (100, C$_9$H$_7$N$_4$O$_2$$^+$; [$M$ + H]$^+$; calc. 203.05635; Δ = –0.39 ppm).

3-(2,3-Dihydrobenzo[b][1,4]dioxin-6-yl)-1,2,4,5-tetrazine (19)

19

Yield: 61%. **TLC**: Rf = 0.35 (CH$_2$Cl$_2$). **M.p.** (CDCl3): 169.0 – 170.1 °C. **^{1}H NMR** (400 MHz, CDCl$_3$): δ 10.12 (s, 1H), 8.18 – 8.10 (m, 2H), 7.08 – 7.01 (m, 1H), 4.40 – 4.30 (m, 4H). **^{13}C NMR** (101 MHz, CDCl$_3$): δ 166.1, 157.5, 148.4, 144.4, 124.9, 122.3, 118.4, 117.6, 64.9, 64.3. **IR** (neat): 2994w, 1609m, 1583m, 1513m, 1488w, 1464w, 1437m, 1365m, 1338s, 1314m, 1286m, 1266m, 1253m, 1200m, 1138m, 1120w, 1065m, 935w, 908m, 899m, 877m, 832w, 805w, 772w, 745w, 726w, 672w, 630m, 597w, 498w, 481w. **HR-EI-MS**: 216.06423 (100, C$_{10}$H$_8$N$_4$O$_2$$^{+\bullet}$; [$M$]$^{+\bullet}$; calc. 216.06418; Δ = 0.24 ppm).
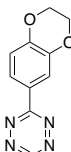
N-(4-(1,2,4,5-Tetrazin-3-yl)phenyl)acetamide (20)

20
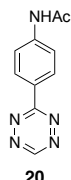
Yield: 65%. **TLC:** R_f = 0.11 (CH$_2$Cl$_2$). **¹H NMR** (400 MHz, DMSO-d_6): δ 10.56 (s, 1H), 10.41 (s, 1H), 8.51 (d, J = 8.8 Hz, 2H), 7.93 (d, J = 8.8 Hz, 2H), 3.41 (s, 6H), 2.17 (s, 3H). **¹³C NMR** (101 MHz, DMSO): δ 169.5, 165.5, 158.2, 144.0, 129.2, 126.3, 119.6, 24.7. **IR** (neat): 3316w, 3076w, 2921w, 2851w, 1688m, 1593m, 1529m, 1494m, 1431m, 1416m, 1347s, 1314s, 1256s, 1229m, 1172m, 1142m, 1114m, 1067w, 1004m, 917m, 901m, 852m, 832m, 803m, 704m, 599w, 562s, 452w. **HR-ESI-MS** (MeOH): 216.08810 (100, C$_{10}$H$_{10}$N$_5$O$^+$; [M + H]$^+$; calc. 216.08799; Δ = 0.50 ppm).

4-(1,2,4,5-Tetrazin-3-yl)aniline (21)

21
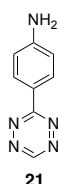
For the preparation of **21**, Boc-aminophenylboronic acid was used in the general procedure. Deprotection of the amine was facilitated by stirring at room temperature for 10 min in TFA (1.55 mL, 95%), followed by purification by column chromatography (SiO$_2$, CH$_2$Cl$_2$ + 2% MeOH).

Yield: 66%. **TLC**: Rf = 0.36 (CH$_2$Cl$_2$ + 2% MeOH). **M.p.** (CDCl3): 146.5 – 149.9 °C. **¹H NMR** (400 MHz, CDCl$_3$): δ 10.04 (s, 1H), 8.48 – 8.39 (m, 2H), 6.85 – 6.77 (m, 2H), 4.10 (s, 2H). **¹³C NMR** (101 MHz, CDCl$_3$): δ 166.4, 157.1, 151.3, 130.4, 121.2, 115.1. **IR** (neat): 3450w, 3344m, 3223m, 1638m, 1598s, 1526w, 1426s, 1356s, 1323m, 1175m, 1062w, 923w, 836m, 799w, 780w, 599w, 554m, 460w. **HR-EI-MS**: 173.06945 (100, C$_8$H$_7$N$_5$$^{+\cdot}$; [$M$]$^{+\cdot}$; calc. 173.06960; Δ = –0.86 ppm).

3-(3-Fluoro-4-methoxyphenyl)-1,2,4,5-tetrazine (22)

22

Yield: 79%. **TLC:** R_f = 0.51 (CH$_2$Cl$_2$). **M.p.** (CDCl$_3$): 154.1 – 155.2 °C. **¹H NMR** (400 MHz, CDCl$_3$): δ 10.15 (s, 1H), 8.41 (ddd, J = 8.7, 2.2, 1.3 Hz, 1H), 8.33 (dd, J = 12.1, 2.1 Hz, 1H), 7.15 (t, J = 8.5 Hz, 1H), 4.01 (s, 3H). **¹³C NMR** (101 MHz, CDCl$_3$): δ 165.6 (d, J = 3.0 Hz), 157.6, 152.8 (d, J = 247.5 Hz), 152.2 (d, J = 10.7 Hz), 125.4 (d, J = 3.4 Hz), 124.4 (d, J = 7.1 Hz), 115.9 (d, J = 20.9 Hz), 113.6 (d, J = 2.2 Hz), 56.5. **IR** (neat): 3080w, 1609m, 1580w, 1519m, 1442m, 1423m, 1375m, 1341s, 1315m, 1279s, 1214m, 1181m, 1146m, 1118m, 1062m, 1030m, 1011m, 910m, 889s, 832m, 805m, 763m, 723w, 629m, 616m, 494m. **HR-APCI-MS** (MeOH/CHCl$_3$ 3:2, MeOH + 0.1% FA): 207.06767 (100, C$_9$H$_8$FN$_4$O$^+$; [M + H]$^+$; calc. 207.06767; Δ = 0.04 ppm).

3-(4-Fluoro-3-methoxyphenyl)-1,2,4,5-tetrazine (23)

23

Yield: 85%. **TLC:** R_f = 0.60 (CH$_2$Cl$_2$). **M.p.** (CDCl$_3$): 139.6 – 142.3 °C. **¹H NMR** (400 MHz, CDCl$_3$): δ 10.21 (s, 1H), 8.31 – 8.20 (m, 2H), 7.33 – 7.24 (m, 1H), 4.03 (s, 3H). **¹³C NMR** (101 MHz, CDCl$_3$): δ 165.7, 157.9, 156.0 (d, J = 255.2 Hz), 148.8 (d, J = 11.0 Hz), 128.1 (d, J = 3.7 Hz), 122.0 (d, J = 7.8 Hz), 117.2 (d, J = 19.1 Hz), 112.9 (d, J = 2.9 Hz), 56.5. **IR** (neat): 3088w, 2923w, 2853w, 1609w, 1595w, 1519m, 1465m, 1429m, 1422m, 1374s, 1341s, 1317m, 1266s, 1255m, 1213s, 1180m, 1122s, 1065m, 1033m, 1016m, 914m, 883w, 871m, 833w, 807m, 784m, 762w, 718w, 638m, 622w, 566w, 491m. **HR-APCI-MS** (CH$_2$Cl$_2$, MeOH + 0.1% FA): 207.06752 (100, C$_9$H$_8$FN$_4$O$^+$; [M + H]$^+$; calc. 207.06767; Δ = – 0.72 ppm).

3-(Furan-3-yl)-1,2,4,5-tetrazine (24)

24

Yield: 66%. **TLC:** R_f = 0.14 (Et$_2$O/n-pentane = 1:9). **M.p.** (CDCl$_3$): 114.7 – 115.5 °C. **¹H NMR** (400 MHz, CDCl$_3$): δ 10.12 (s, 1H), 8.54 (dd, J = 1.6, 0.8 Hz, 1H), 7.63 (t, J = 1.7 Hz, 1H), 7.24 (dd, J = 1.9, 0.8 Hz, 1H). **¹³C NMR** (101 MHz, CDCl$_3$): δ 164.2, 157.5, 146.5, 145.1, 121.1, 108.6. **IR** (neat): 3149w, 3126m, 3087w, 2922w, 2851w, 1693w, 1637w, 1584m, 1512m, 1498w, 1446m, 1366w, 1344m, 1174s, 1156m, 1091m, 1009m, 932m, 904m, 870s, 845m, 807m, 758m, 704w, 652s, 600m, 500m, 456w. **HR-EI-MS**: 148.03854 (100, C$_6$H$_4$N$_4$O$^{+\bullet}$; [M]$^{+\bullet}$; calc. 148.03796; Δ = 3.90 ppm).

3-(Thiophen-3-yl)-1,2,4,5-tetrazine (25)

25

Yield: 71%. **TLC:** R_f = 0.14 (Et$_2$O/n-pentane = 1:9). **M.p.** (CDCl$_3$): 137.3 – 138.5 °C. **¹H NMR** (400 MHz, CDCl$_3$): δ 10.13 (s, 1H), 8.65 (dd, J = 3.0, 1.2 Hz, 1H), 8.06 (dd, J = 5.2, 1.2 Hz, 1H), 7.53 (dd, J = 5.1, 3.0 Hz, 1H). **¹³C NMR** (101 MHz, CDCl$_3$): δ 164.0, 157.3, 134.7, 131.1, 127.7, 126.6. **IR** (neat): 3099m, 2972w, 1847w, 1531s, 1497w, 1451s, 1312s, 1215m, 1131m, 1080w, 1033w, 910s, 871m, 831m, 796m, 712m, 643s, 493m. **HR-EI-MS**: 164.01528 (100, C$_6$H$_4$N$_4$S$^{+\bullet}$; [M]$^{+\bullet}$; calc. 164.01512; Δ = 0.97 ppm).

N,N-Dimethyl-5-(1,2,4,5-tetrazin-3-yl)pyrimidin-2-amine (26)

26

Yield: 72%. **TLC**: Rf = 0.19 (CH$_2$Cl$_2$ + 1% MeOH). **M.p.** (CDCl3): 224.7 – 225.4 °C. **^{1}H NMR** (400 MHz, CDCl$_3$): δ 10.12 (s, 1H), 9.44 (s, 2H), 3.34 (s, 6H). **^{13}C NMR** (101 MHz, CDCl$_3$): δ 165.1, 163.2, 158.1, 157.7, 113.2, 37.6. **IR** (neat): 3094w, 2924w, 1609s, 1573m, 1532m, 1457m, 1412m, 1351s, 1314m, 1249w, 1208w, 1151m, 1071w, 969m, 894m, 795m, 661w, 644w, 565m, 538m, 490w. **HR-EI-MS**: 203.09125 (100, C$_8$H$_9$N$_7$$^{+•}$; [$M$]$^{+•}$; calc. 203.09139; Δ = –0.72 ppm).
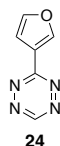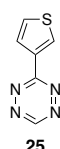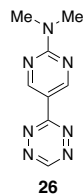
tert-Butyl 5-(1,2,4,5-tetrazin-3-yl)-1H-indole-1-carboxylate (27)

27
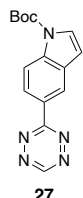
Yield: 73%. **TLC**: Rf = 0.61 (CH$_2$Cl$_2$). **M.p.** (CDCl3): 135.9 – 138.7 °C. **^{1}H NMR** (400 MHz, CDCl$_3$): δ 10.16 (s, 1H), 8.86 (dd, J = 1.8, 0.7 Hz, 1H), 8.57 (dd, J = 8.8, 1.8 Hz, 1H), 8.34 (d, J = 8.8 Hz, 1H), 7.68 (d, J = 3.7 Hz, 1H), 6.71 (dd, J = 3.8, 0.8 Hz, 1H), 1.71 (s, 9H). **^{13}C NMR** (101 MHz, CDCl$_3$): δ 167.0, 157.7, 149.5, 138.3, 131.4, 127.7, 126.1, 124.3, 122.0, 116.2, 108.0, 84.7, 28.3. **IR** (neat): 2980w, 1734m, 1612w, 1538w, 1479w, 1427m, 1394m, 1359s, 1344m, 1317m, 1294m, 1283m, 1244s, 1201m, 1157s, 1123m, 1086m, 1063w, 1042w, 1023m, 903m, 837m, 800m, 766m, 729m, 679w, 639m, 608w, 579w, 525w, 503w, 461w. **HR-EI-MS**: 297.12250 (100, C$_{15}$H$_{15}$N$_5$O$_2$$^{+•}$; [$M$]$^{+•}$; calc. 297.12203; Δ = 1.60 ppm).

3-(2-Fluorophenyl)-1,2,4,5-tetrazine (28)

28
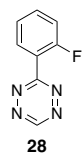
Yield: 72%. **TLC**: Rf = 0.43 (CH$_2$Cl$_2$). **M.p.** (CDCl3): 67.2 – 69.2 °C. **^{1}H NMR** (400 MHz, CDCl$_3$): δ 10.27 (s, 1H), 8.34 – 8.24 (m, 1H), 7.69 – 7.59 (m, 1H), 7.44 – 7.36 (m, 1H), 7.37 – 7.28 (m, 1H). **^{13}C NMR** (101 MHz, CDCl$_3$): δ 166.7 (d, J = 5.8 Hz), 161.6 (d, J = 259.9 Hz), 157.3, 134.6 (d, J = 8.5 Hz), 131.7, 125.0 (d, J = 4.1 Hz), 120.6 (d, J = 9.7 Hz), 117.6 (d, J = 21.5 Hz). **^{19}F NMR** (376 MHz, CDCl$_3$) δ – 112.2. **IR** (neat): 3091w, 3052w, 1609s, 1581w, 1496m, 1459s, 1430m, 1371w, 1342s, 1296m, 1268m, 1236m, 1223m, 1168m, 1145m, 1108m, 1066w, 1044w, 1012w, 964w, 932w, 898m, 832m, 769m, 727w, 640m, 573m, 553w, 505m. **HR-EI-MS**: 176.04929 (100, C$_8$H$_5$N$_4$F$^{+•}$; [M]$^{+•}$; calc. 176.04928; Δ = 0.09 ppm).

3-(4-Chlorophenyl)-1,2,4,5-tetrazine (29)

29
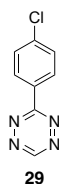
Yield: 86%. **TLC**: Rf = 0.61 (CH$_2$Cl$_2$). **M.p.** (CDCl3): 162.8 − 164.2 °C. **^{1}H NMR** (400 MHz, CDCl$_3$): δ 10.23 (s, 1H), 8.63 − 8.55 (m, 2H), 7.63 − 7.55 (m, 2H). **^{13}C NMR** (101 MHz, CDCl$_3$): δ 166.0, 158.0, 140.0, 130.2, 129.9, 129.7. **IR** (neat): 3090m, 3051w, 1955w, 1842w, 1700w, 1594m, 1492m, 1437m, 1417m, 1357s, 1349m, 1277m, 1167w, 1142m, 1108m, 1093m, 1005m, 912m, 896m, 854m, 802m, 731m, 715m, 562s, 500w. **HR-EI-MS**: 192.01966 (100, C$_8$H$_5$N$_4$Cl$^{+\cdot}$; [M]$^{+\cdot}$; calc. 192.01973; Δ = − 0.36 ppm).

3-(4-Bromophenyl)-1,2,4,5-tetrazine (30)

30
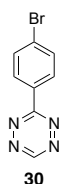
Yield: 77%. **TLC**: Rf = 0.66 (CH$_2$Cl$_2$). **M.p.** (CDCl3): 177.3 − 179.1 °C. **^{1}H NMR** (400 MHz, CDCl$_3$): δ 10.24 (s, 1H), 8.53 − 8.45 (m, 2H), 7.79 − 7.71 (m, 2H). **^{13}C NMR** (101 MHz, CDCl$_3$): δ 166.1, 158.0, 132.9, 130.6, 129.8, 128.6. **IR** (neat): 3088m, 1954w, 1588m, 1487w, 1438m, 1414m, 1357s, 1348m, 1274w, 1167w, 1141m, 1106m, 1071m, 1005m, 911s, 896m, 851s, 801m, 733w, 712m, 560s. **HR-EI-MS**: 235.96893 (100, C$_8$H$_5$N$_4$Br$^{+\cdot}$; [M]$^{+\cdot}$; calc. 235.96921; Δ = −1.20 ppm).

1,1'-Bis(di-para-(trifluoromethyl)phenylphosphino)ferrocene (dppf-CF$_3$)[2,3]
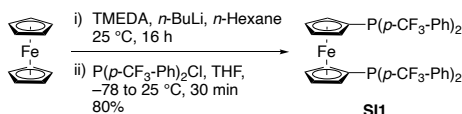
A flame-dried one-necked flask (25 mL) equipped with a stirring bar was charged under N$_2$ with ferrocene (569 mg, 3.06 mmol, 1.0 eq.) and dry hexane (6.0 mL). TMEDA (1.11 mL, 7.34 mmol, 2.4 eq.) and *n*-BuLi (4.2 mL, 1.6 M in hexane, 6.73 mmol, 2.2 eq.) were added consecutively and dropwise resulting in complete dissolution of the ferrocene. The solution was stirred for 16 h at room temperature, during which an orange solid precipitated. Stirring was stopped and after the precipitate had settled the hexane was removed by syringe. The solid was washed once with hexane (3 mL) and was subsequently dissolved in dry THF (6.0 mL). The red solution was cooled to –78 °C with acetone/dry ice and P(*p*-CF$_3$-Ph)$_2$Cl (2.89 g, 8.10 mmol, 2.65 eq.) was added dropwise by syringe. After stirring for 15 min at the previous temperature, cooling was removed, and the mixture was allowed to warm to room temperature. After 30 min, the reaction was quenched with H$_2$O (6 mL), then H$_2$O (6 mL) and CH$_2$Cl$_2$ (15 mL) were added to achieve proper separation of the phases. Extraction of the aqueous phase with CH$_2$Cl$_2$ (4 x 10 mL) and subsequent drying of the combined organic phases over anhydrous Na$_2$SO$_4$ afforded, after removal of solvent *in vacuo* (40 °C, 600 to 50 mbar), a brownish yellow oil. After purification of the residue by flash column chromatography (SiO2, 15 x 5 cm, CH$_2$Cl$_2$) and drying under high vacuum the desired ferrocene **SI1** (2.02 g, 2.45 mmol, 80%) was obtained as an orange foam.

Yield: 80%. **TLC:** R_f = 0.91 (CH$_2$Cl$_2$). **M.p.** (CH$_2$Cl$_2$): 68.2 − 70.4 °C. **^{1}H NMR** (400 MHz, CDCl$_3$): δ 7.57 − 7.53 (m, 8H), 7.40 − 7.35 (m, 8H), 4.35 − 4.30 (m, 4H), 4.02 − 3.96 (m, 4H). **^{13}C NMR** (101 MHz,

CDCl₃): δ 143.1 (d, *J* = 13.6 Hz), 133.8 (d, *J* = 19.9 Hz), 131.1 (q, *J* = 32.6 Hz), 125.2 (dq, *J* = 7.4, 3.7 Hz), 124.1 (q, *J* = 272.4 Hz), 75.0 (d, *J* = 7.5 Hz), 74.0 (d, *J* = 15.2 Hz), 72.9 (d, *J* = 3.8 Hz). **¹⁹F NMR** (376 MHz, CDCl₃): δ –62.8. **³¹P NMR** (162 MHz, CDCl₃): δ –17.2. **IR** (neat): 1607w, 1396m, 1322s, 1164m, 1124m, 1105m, 1060m, 1031w, 1016m, 957w, 830m, 737w, 696m, 635w, 599w, 499w. **HR-ESI-MS** (MeOH/CHCl₃): 827.05844 (100, $C_{38}H_{25}F_{12}FeP_2^+$; [*M* + H]⁺; calc. 827.05838; *Δ* = 0.08 ppm).

[1,1'-Bis(di-para-(trifluoromethyl)phenyl)phosphino)ferrocene]dichloropalladium(II) (Pd(dppf-CF₃)Cl₂)[4]
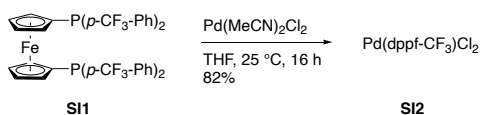
A flame-dried two-necked flask (250 mL) equipped with a stirring bar was charged under N₂ with dppf-CF₃ (**SI1**, 402 mg, 0.486 mmol, 1.0 eq.), PdCl₂(MeCN)₂ (126 mg, 0.486 mmol, 1.0 eq.) and dry THF (75 mL) and the mixture was stirred for 16 h at room temperature. The solvent was removed by evaporation under a N₂ stream and the reddish-brown residue was dissolved in CH₂Cl₂ and filtered through celite. The celite was rinsed with CH₂Cl₂ (25 mL and 20 mL) and the filtrate was concentrated to approx. 20 mL by a N₂ stream. Et2O (40 mL) was added and the mixture was placed at –20 °C for 4 h. The resulting precipitate was collected by filtration and dried at high vacuum to afford the palladium complex **SI2** (400 mg, 0.399 mmol, 82%) as a reddish solid.

Yield: 82%. **TLC:** R_f = 0.14 (CH₂Cl₂). **M.p.** (Et₂O/CH₂Cl₂ 2:1): 276.2 – 278.6 °C (decomposition). **¹H NMR** (400 MHz, CDCl3): δ 8.02 (s, 1H), 7.71 (d, J = 7.3 Hz, 1H), 4.54 (s, 1H), 4.26 (s, 1H). **¹³C NMR** (101 MHz, CDCl₃): δ 135.9 – 135.1 (m), 133.8 (q, *J* = 33.0 Hz), 125.8 – 125.2 (m), 123.5 (q, *J* = 272.9 Hz), 76.4 – 76.1 (m), 75.2 – 74.8 (m), 73.2 (d, *J* = 61.7 Hz). **¹⁹F NMR** (376 MHz, CDCl₃) δ –63.1. **³¹P NMR** (162 MHz, CDCl₃) δ 32.9. **IR** (neat): 1609w, 1397m, 1323s, 1168m, 1126m, 1062m, 1016m, 827m, 706m, 699m, 640w, 600w, 550w, 535w, 500w, 476w. **HR-ESI-MS** (MeOH/CHCl₃): 1036.86269 (100, $C_{38}H_{24}Cl_3F_{12}FeP_2Pd^-$; [*M* + Cl]⁻; calc. 1036.86169; *Δ* = 0.96 ppm).

Annex

References

[1] S. D. Schnell, L. V. Hoff, A. Panchagnula, M. H. H. Wurzenberger, T. M. Klapötke, S. Sieber, A. Linden, K. Gademann, *Chem. Sci.* **2020**, *11*, 3042–3047.

[2] D. A. Khobragade, S. G. Mahamulkar, L. Pospíšil, I. Císařová, L. Rulíšek, U. Jahn, *Chem. – Eur. J.* **2012**, *18*, 12267–12277.

[3] J. J. Bishop, A. Davidson, M. L. Katcher, D. W. Lichtenberg, R. E. Merrill, J. C. Smart, *J. Organomet. Chem.* **1971**, *27*, 241–249.

[4] J. J. Adams, O. J. Curnow, G. M. Fern, *Inorganica Chim. Acta* **2006**, *359*, 3596–3604.

[5] a) for **2**, **5** and **12**: Rigaku Oxford Diffraction, *CrysAlisPro* Software System, Version 1.171.40.81a, Rigaku Corporation, Wroclaw, Poland, 2020.

b) for **23**: Rigaku Oxford Diffraction, *CrysAlisPro* Software System, Version 1.171.40.84a, Rigaku Corporation, Wroclaw, Poland, 2020.

[6] P. Coppens, L. Leiserowitz, D. Rabinovich, *Acta Crystallogr.* **1965**, *18*, 1035–1038.

[7] G. M. Sheldrick, *Acta Crystallogr. Sect. A*, **2015**, *71*, 3–8.

[8] G. M. Sheldrick, *Acta Crystallogr. Sect. C*, **2015**, *71*, 3–8.

Crystallographic Data

Crystals of compounds **2** and **5** were grown by slow evaporation of a solution of the compound in CH_2Cl_2. Crystals of **12** were grown by slow vapour diffusion of *n*-pentane into a solution of the compound in CH_2Cl_2. Crystals of **23** were grown by slow vapour diffusion of CH_2Cl_2 into a solution of the compound in $CHCl_3$.

For the crystal structure determinations, each selected crystal was mounted on a cryo-loop. All measurements were then made at 160 K on a *Rigaku Oxford Diffraction SuperNova* area-detector diffractometer[10] using Cu *K*a radiation (λ = 1.54184 Å) from a micro-focus X-ray source and an *Oxford Instruments Cryojet XL* cooler.

Data reduction was performed with *CrysAlisPro*.[5] The intensities were corrected for Lorentz and polarization effects, and an empirical absorption correction using spherical harmonics[5] was applied for **5**, **12** and **23**, while a numerical absorption correction[6] was applied for **2**. The chosen crystal of **23** was a non-merohedral twin resulting from a rotation of 180° about the direct lattice vector [100] with a twin matrix of [1 0 0 / 0.911 -1 0 / 0.321 0 -1] and a major twin fraction of 0.591(2). All reflections from both twin components were integrated; a total of 8440 and 8380 non-overlapping reflections from twin components 1 and 2, respectively, plus 774 reflections from both twin components that were overlapping.

Each structure was solved by dual space methods using *SHELXT-2018*,[7] which revealed the positions of all non-hydrogen atoms. The non-hydrogen atoms were refined anisotropically. All H-atoms were placed in geometrically calculated positions and refined by using a riding model where each H-atom was assigned a fixed isotropic displacement parameter with a value equal to $1.2U_{eq}$ of its parent atom ($1.5U_{eq}$ for the methyl groups). The refinement of each structure was carried out on F^2 by using the full-matrix least-squares procedures of *SHELXL-2018*,[8] which minimised the function $\Sigma w(F_o^2 - F_c^2)^2$. For **12**, two reflections, whose intensities were considered to be extreme outliers, were omitted from the final refinement.

The molecule in the structure of **2** sits across a crystallographic C_2-axis which passes longitudinally through the molecule from the F-atom to the para C-atom of the heterocyclic ring. In **5**, there are two molecules with similar conformations in the asymmetric unit; no additional symmetry could be found.

All other data collection and refinement parameters and additional details are given in *Tables S7–S10* and in the CIFs deposited with the Cambridge Crystallographic Data Centre (deposition numbers CCDC-2080087-2080090). The data can be obtained free of charge from The Cambridge Crystallographic Data Center via www.ccdc.cam.ac.uk/structures.

Table S7. Crystallographic data for compound **2**.

Crystallised from	CH_2Cl_2
Empirical formula	$C_8H_5FN_4$
Formula weight [g mol^{-1}]	176.16
Crystal colour, habit	red, plate
Crystal dimensions [mm]	$0.05 \times 0.19 \times 0.28$
Temperature [K]	160(1)
Crystal system	monoclinic
Space group	*I2/a* (#15)
Z	4
Reflections for cell determination	3388
2θ range for cell determination [°]	9−157
Unit cell parameters *a* [Å]	5.58292(10)
b [Å]	19.3177(3)
c [Å]	7.05278(11)
β [°]	102.5765(16)
V [Å^3]	742.39(2)
F(000)	360
D_X [g cm^{-3}]	1.576
μ(Cu $K\alpha$) [mm^{-1}]	1.030
Scan type	ω
2θ(max) [°]	157.5
Transmission factors (min; max)	0.440; 1.000
Total reflections measured	3970
Symmetry independent reflections	788
R_{int}	0.014
Reflections with $I > 2\sigma(I)$	758
Reflections used in refinement	788
Parameters refined	63
Final *R*(*F*) [$I > 2\sigma(I)$ reflections]	0.0359
$wR(F^2)$ (all data)	0.1083
Weights:	$w = [\sigma^2 (F_o^2) + (0.0624P)^2 + 0.2528P]^{-1}$ where $P = (F_o^2 + 2F_c^2)/3$
Goodness of fit	1.103
Secondary extinction coefficient	0.0038(9)
Final Δ_{max}/σ	0.001
$\Delta\rho$ (max; min) [e Å^{-3}]	0.25; -0.17
$\sigma(d_{(C-C)})$ [Å]	0.0011 − 0.0018

Figure S1. View of the molecular structure of **2** showing the atom-labelling scheme. Displacement ellipsoids are drawn at the 50% probability level. H atoms are represented by circles of arbitrary size. Symmetry code (i): ½–*x*, *y*, 1–*z*.

Table S8. Crystallographic data for compound **5**.

Crystallised from	CH_2Cl_2
Empirical formula	$C_9H_8N_4$
Formula weight [g mol^{-1}]	172.19
Crystal colour, habit	pink, plate
Crystal dimensions [mm]	$0.02 \times 0.10 \times 0.20$
Temperature [K]	160(1)
Crystal system	monoclinic
Space group	$P2_1/n$ (#14)
Z	8
Reflections for cell determination	8516
2θ range for cell determination [°]	6−153
Unit cell parameters a [Å]	9.1661(2)
b [Å]	14.6209(3)
c [Å]	13.0151(4)
β [°]	102.332(3)
V [Å^3]	1703.99(8)
$F(000)$	720
D_X [g cm^{-3}]	1.342
μ(Cu $K\alpha$) [mm^{-1}]	0.707
Scan type	ω
2θ(max) [°]	152.7
Transmission factors (min; max)	0.652; 1.000
Total reflections measured	19681
Symmetry independent reflections	3575
R_{int}	0.028
Reflections with $I > 2\sigma(I)$	3079
Reflections used in refinement	3575
Parameters refined	237
Final $R(F)$ [$I > 2\sigma(I)$ reflections]	0.0441
$wR(F^2)$ (all data)	0.1384
Weights:	$w = [\sigma^2 (F_o^2) + (0.0851P)^2 + 0.3060P]^{-1}$ where $P = (F_o^2 + 2F_c^2)/3$
Goodness of fit	1.058
Final Δ_{max}/σ	0.000
$\Delta\rho$ (max; min) [e Å^{-3}]	0.28; -0.20
$\sigma(d_{(C–C)})$ [Å]	0.0016 – 0.0018
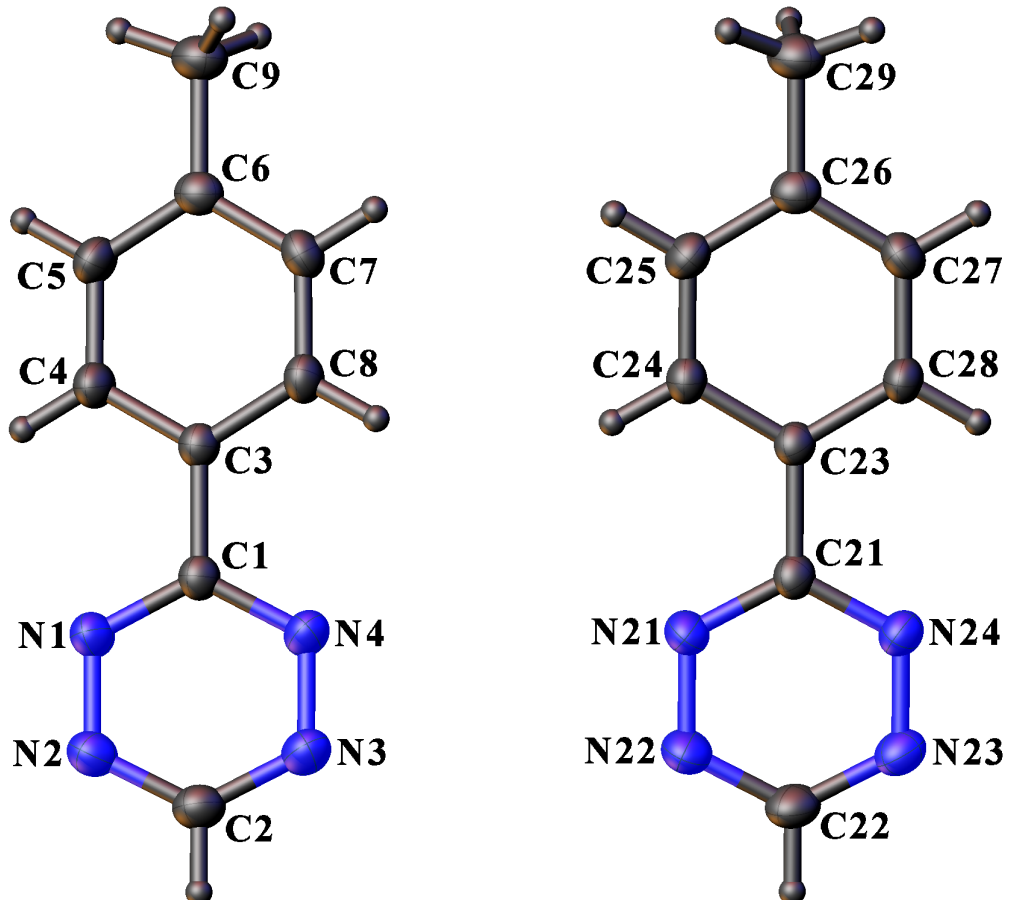
Figure S2. Views of the molecular structure the two symmetry-independent molecules of **5** showing the atom-labelling scheme. Displacement ellipsoids are drawn at the 50% probability level. H atoms are represented by circles of arbitrary size.

Table S9. Crystallographic data for compound **12**.
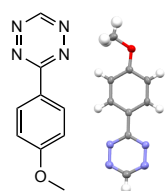
Crystallised from	CH$_2$Cl$_2$ / *n*-pentane
Empirical formula	C$_9$H$_8$N$_4$O
Formula weight [g mol^{-1}]	188.19
Crystal colour, habit	red, plate
Crystal dimensions [mm]	0.08 × 0.20 × 0.22
Temperature [K]	160(1)
Crystal system	triclinic
Space group	$P\bar{1}$ (#2)
Z	2
Reflections for cell determination	4245
2θ range for cell determination [°]	8−146
Unit cell parameters a [Å]	5.8828(3)
b [Å]	6.9620(3)
c [Å]	10.9328(5)
α [°]	78.038(4)
β [°]	87.617(4)
γ [°]	75.133(5)
V [Å^3]	423.35(4)
F(000)	196
D_X [g cm^{-3}]	1.476
μ(Cu $K\alpha$) [mm^{-1}]	0.855
Scan type	ω
2θ(max) [°]	145.9
Transmission factors (min; max)	0.918; 1.000
Total reflections measured	7478
Symmetry independent reflections	1655
R_{int}	0.015
Reflections with $I > 2\sigma(I)$	1492
Reflections used in refinement	1653
Parameters refined	128
Final $R(F)$ [$I > 2\sigma(I)$ reflections]	0.0377
$wR(F^2)$ (all data)	0.1155
Weights:	$w = [\sigma^2 (F_o^2) + (0.0595P)^2 + 0.0975P]^{-1}$ where $P = (F_o^2 + 2F_c^2)/3$
Goodness of fit	1.116
Final Δ_{max}/σ	0.000
$\Delta\rho$ (max; min) [e Å^{-3}]	0.21; -0.16
$\sigma(d_{(C-C)})$ [Å]	0.0015 − 0.0017
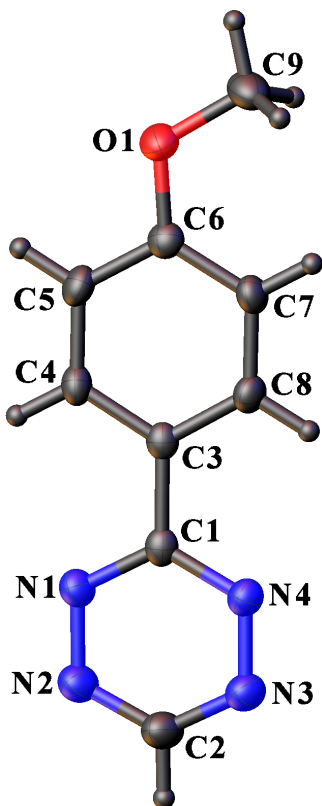
Figure S3. View of the molecular structure of **12** showing the atom-labelling scheme. Displacement ellipsoids are drawn at the 50% probability level. H atoms are represented by circles of arbitrary size.

Table S10. Crystallographic data for compound **23**.

Crystallised from	CH_2Cl_2 / $CHCl_3$
Empirical formula	$C_9H_7FN_4O$
Formula weight [g mol^{-1}]	206.19
Crystal colour, habit	red, plate
Crystal dimensions [mm]	$0.03 \times 0.15 \times 0.15$
Temperature [K]	160(1)
Crystal system	triclinic
Space group	$P\bar{1}$ (#2)
Z	2
Reflections for cell determination	4452
2θ range for cell determination [°]	14−152
Unit cell parameters a [Å]	6.6567(5)
b [Å]	7.6221(6)
c [Å]	10.0748(8)
α [°]	70.879(7)
β [°]	83.769(6)
γ [°]	66.541(7)
V [Å^3]	442.91(7)
$F(000)$	212
D_X [g cm^{-3}]	1.546
μ(Cu $K\alpha$) [mm^{-1}]	1.042
Scan type	ω
2θ(max) [°]	152.9
Transmission factors (min; max)	0.833; 1.000
Total reflections measured	17594
Symmetry independent reflections	3522
R_{int}	0.039
Reflections with $I > 2\sigma(I)$	3133
Reflections used in refinement	3522
Parameters refined	138
Final $R(F)$ [$I > 2\sigma(I)$ reflections]	0.0463
$wR(F^2)$ (all data)	0.1497
Weights:	$w = [\sigma^2 (F_o^2) + (0.0604P)^2 + 0.1975P]^{-1}$ where $P = (F_o^2 + 2F_c^2)/3$
Goodness of fit	1.126
Final Δ_{max}/σ	0.000
$\Delta\rho$ (max; min) [e Å^{-3}]	0.25; -0.26
$\sigma(d_{(C-C)})$ [Å]	0.002 − 0.003
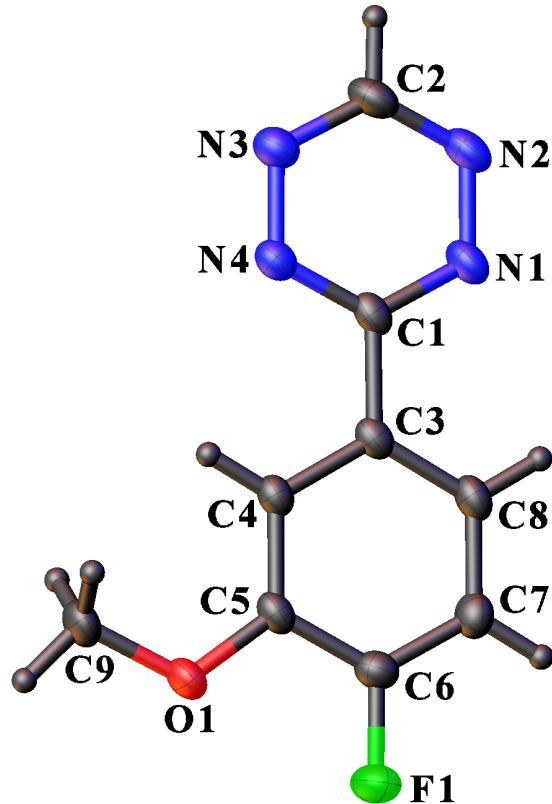
Figure S4. View of the molecular structure of **23** showing the atom-labelling scheme. Displacement ellipsoids are drawn at the 50% probability level. H atoms are represented by circles of arbitrary size.

NMR Spectra

¹H NMR of **2**
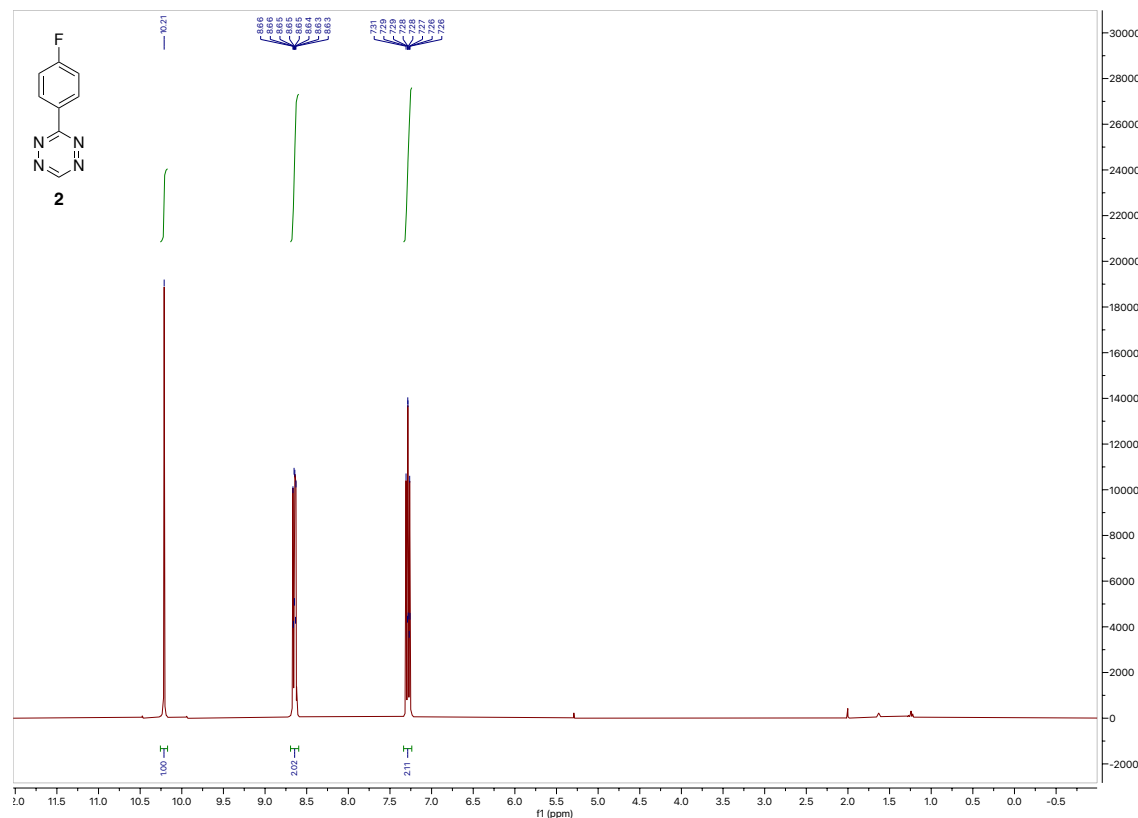
¹³C NMR of **2**
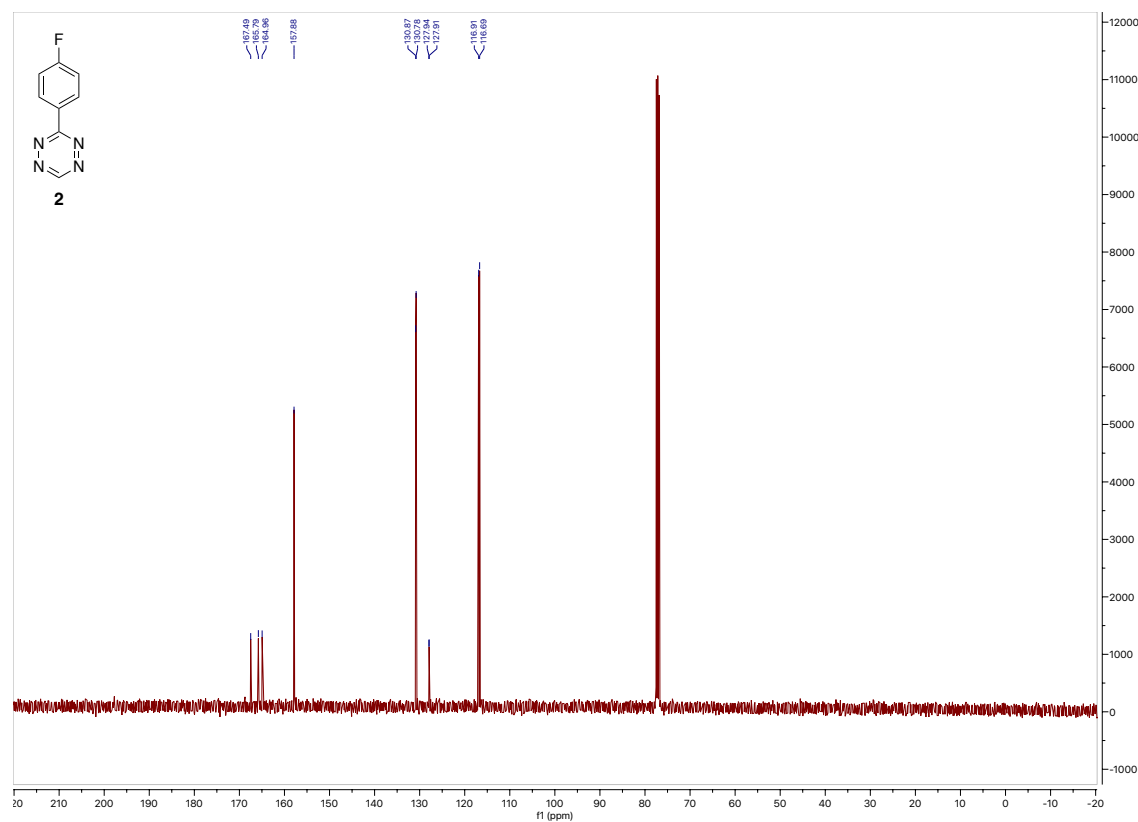
¹⁹F NMR of **2**
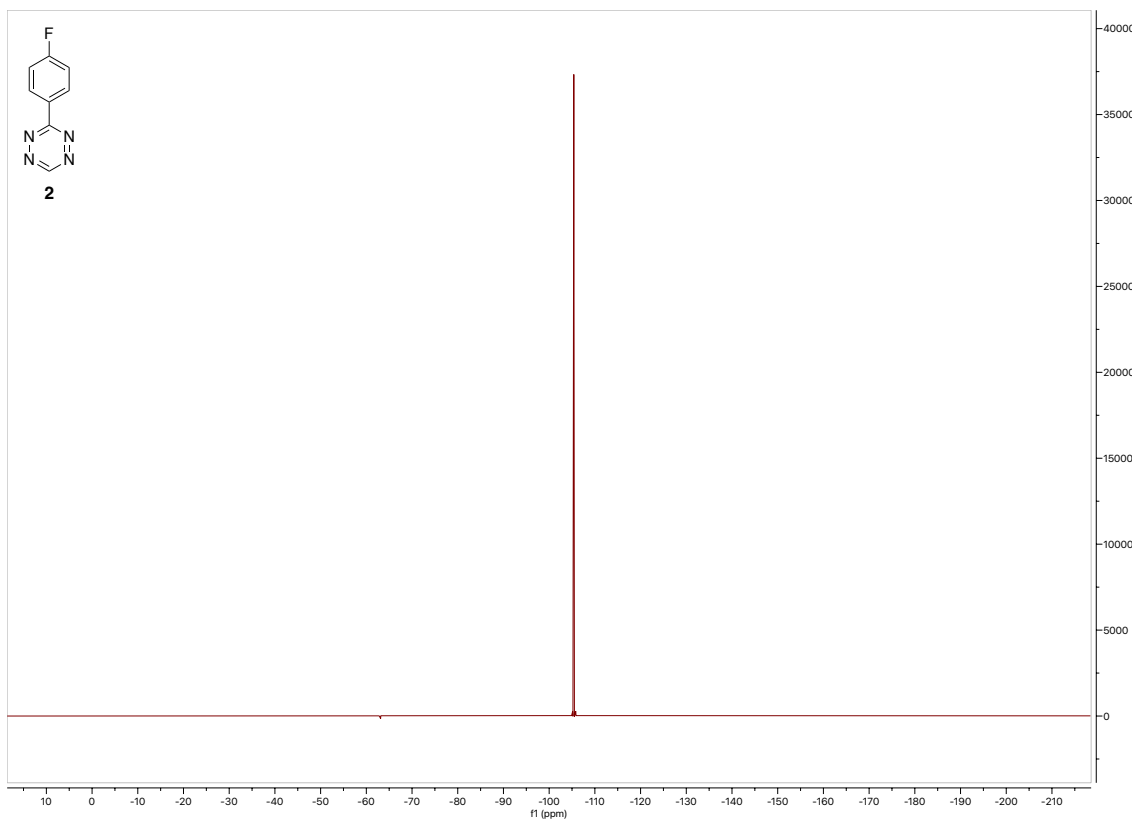
¹H NMR of **3**
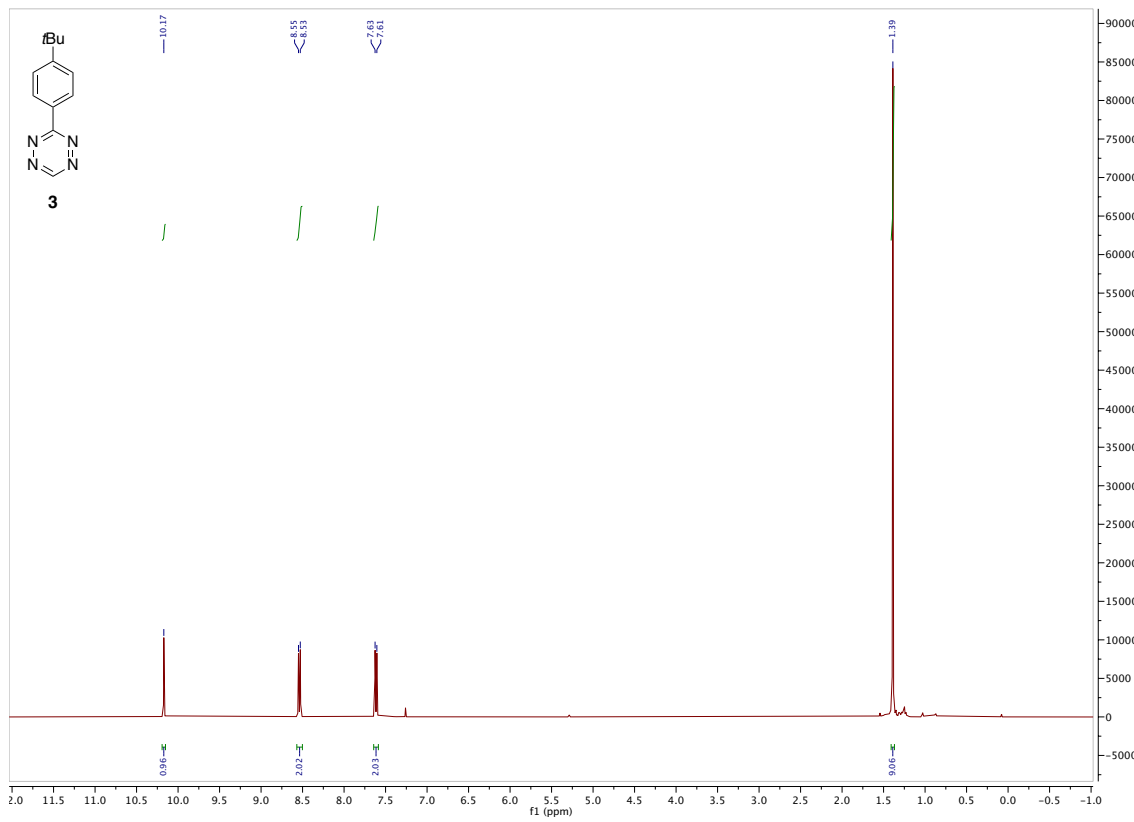
^{13}C NMR of **3**
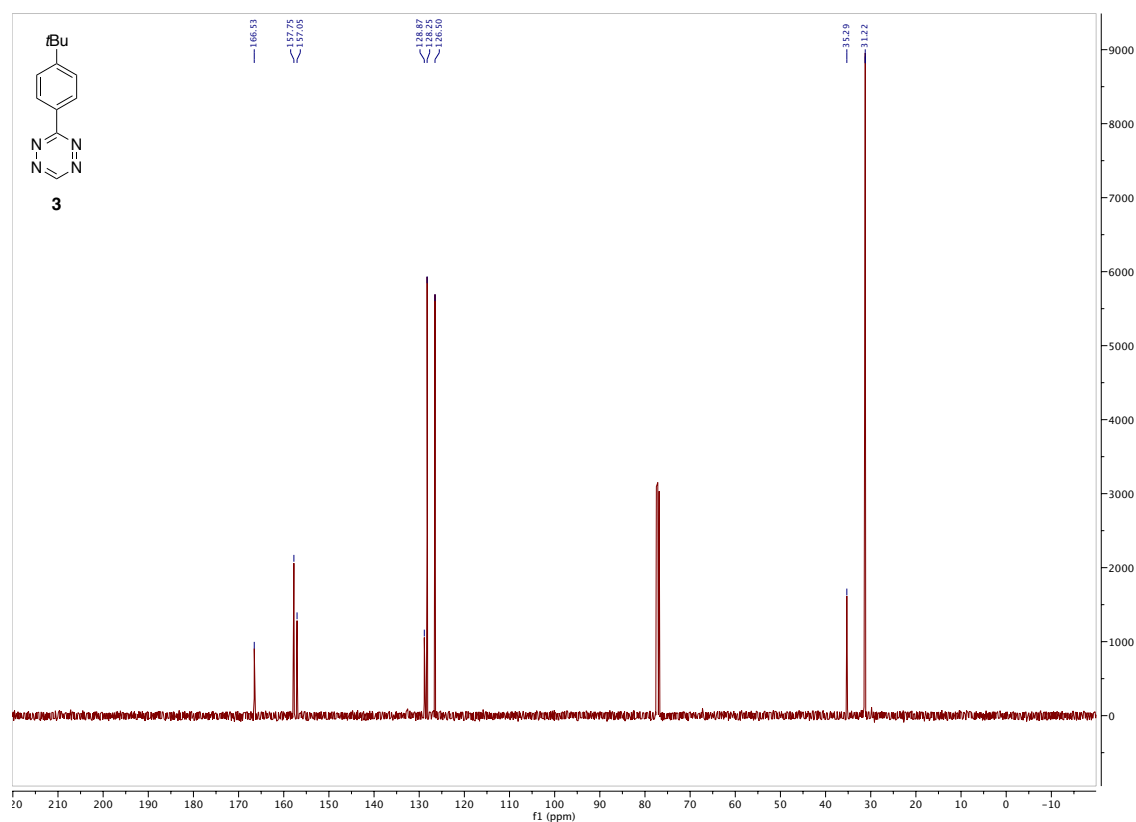
## ^{1}H NMR of **4**
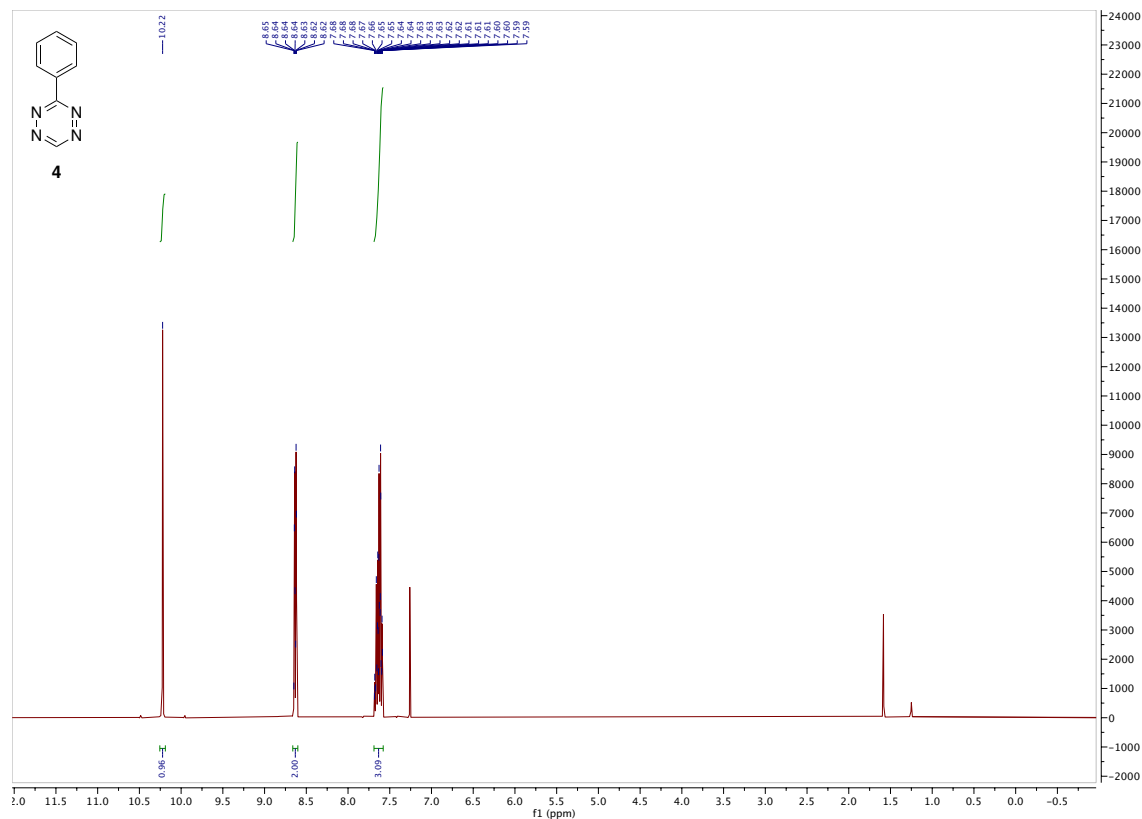
## 13C NMR of **4**
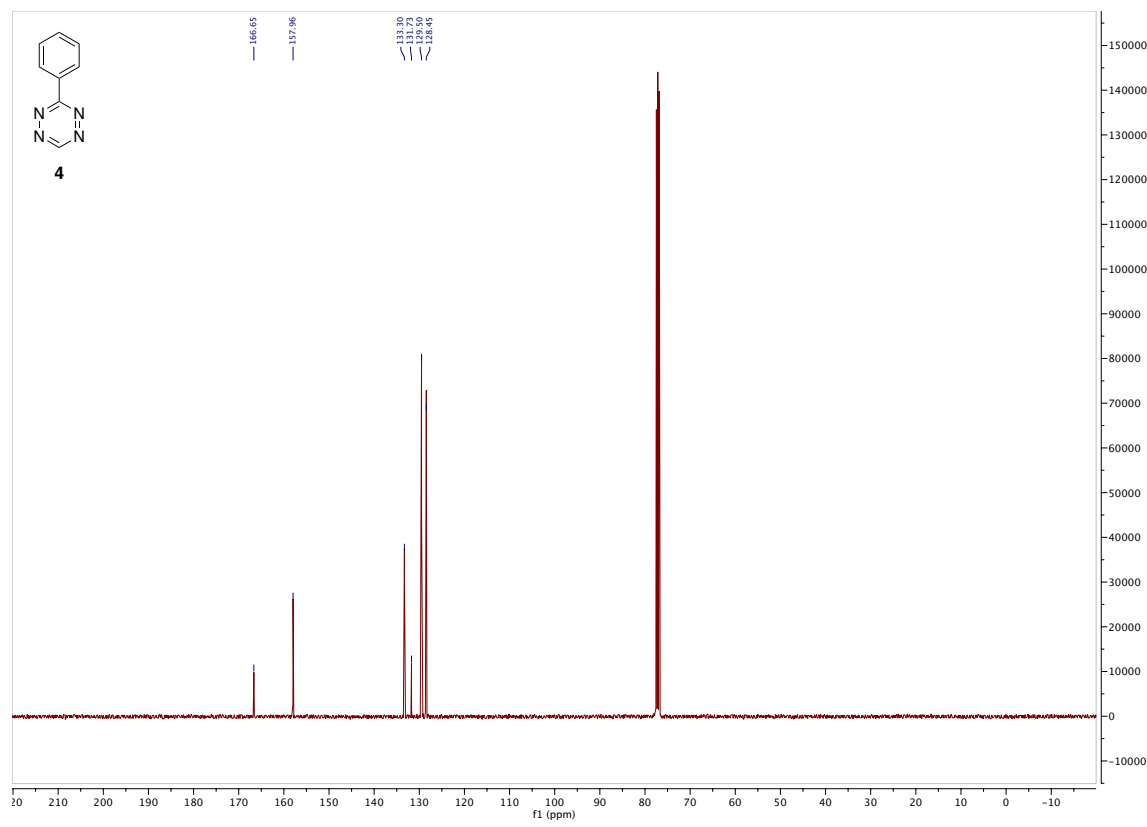
1H NMR of **5**
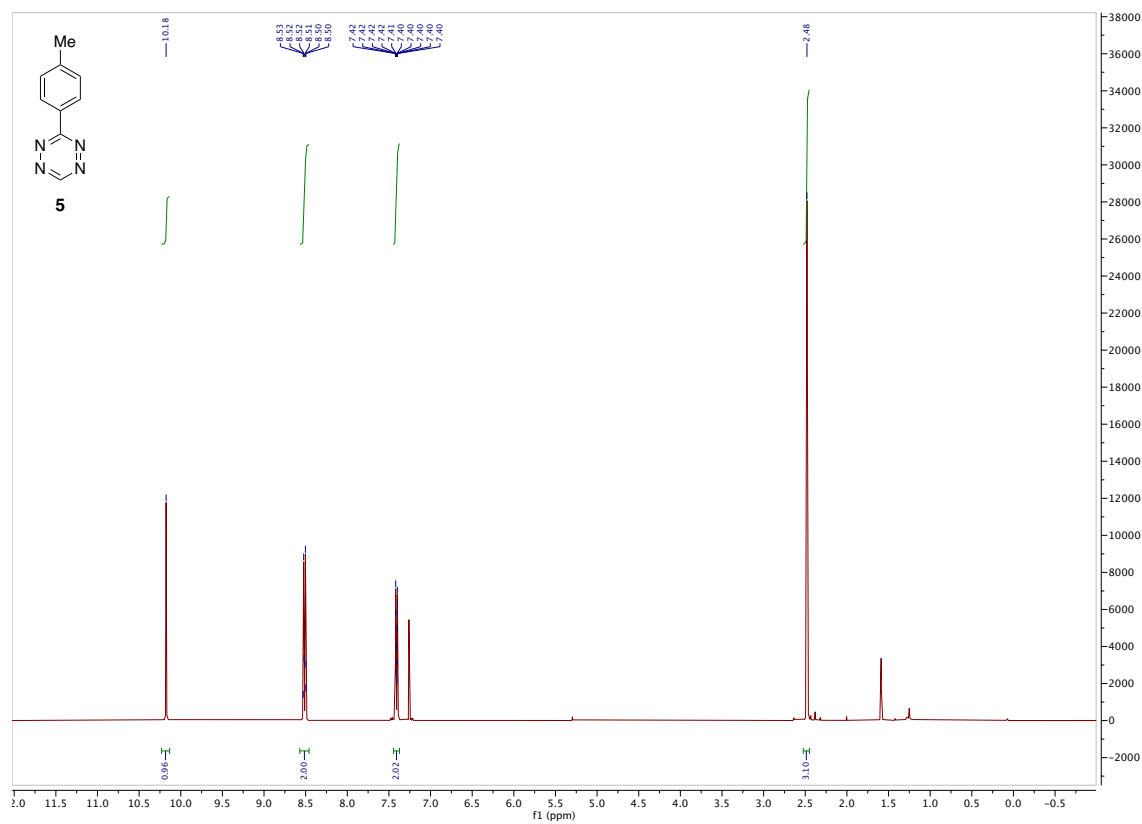
^{13}C NMR of **5**
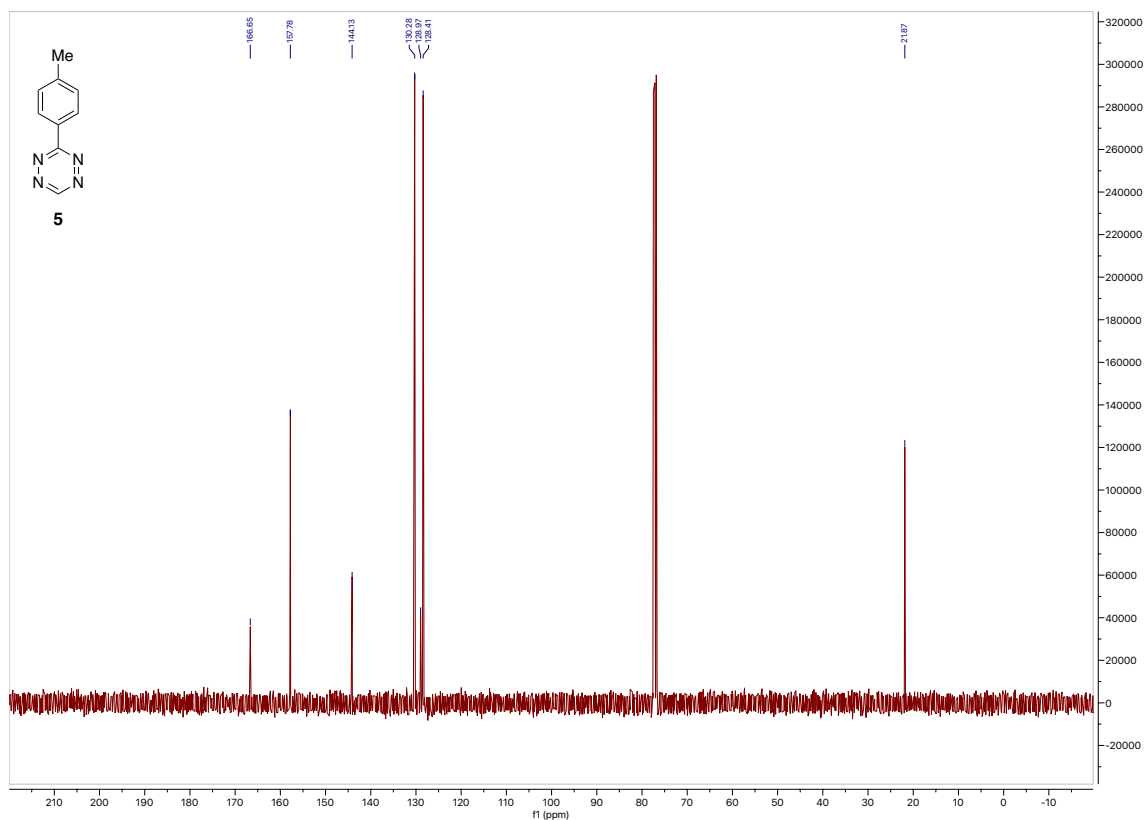
^{1}H NMR of **6**
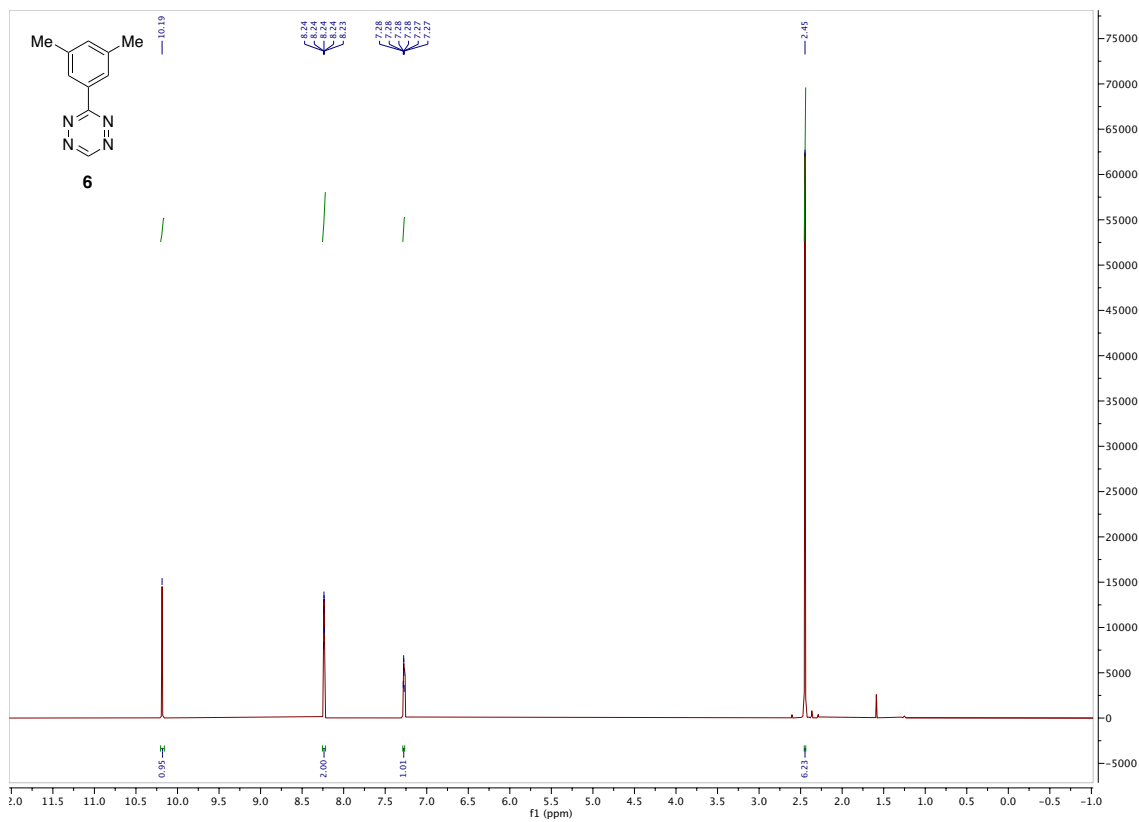
^{13}C NMR of **6**
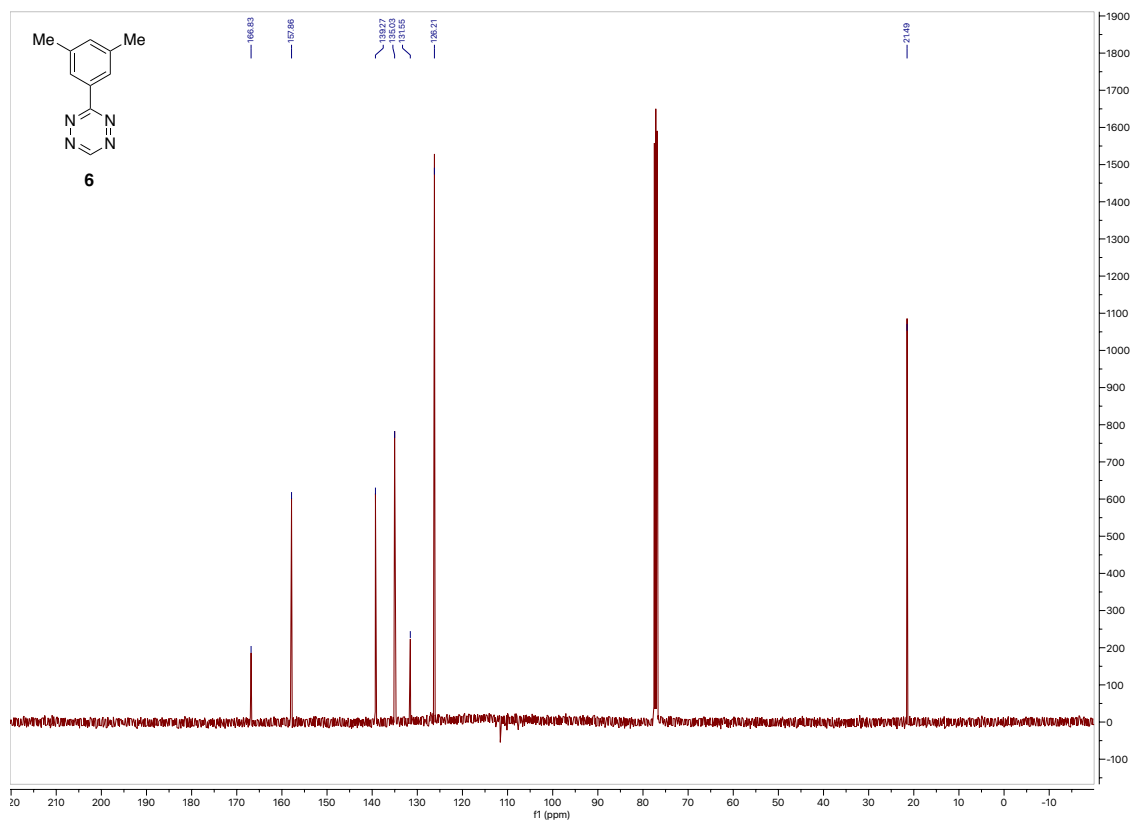
^{1}H NMR of **7**
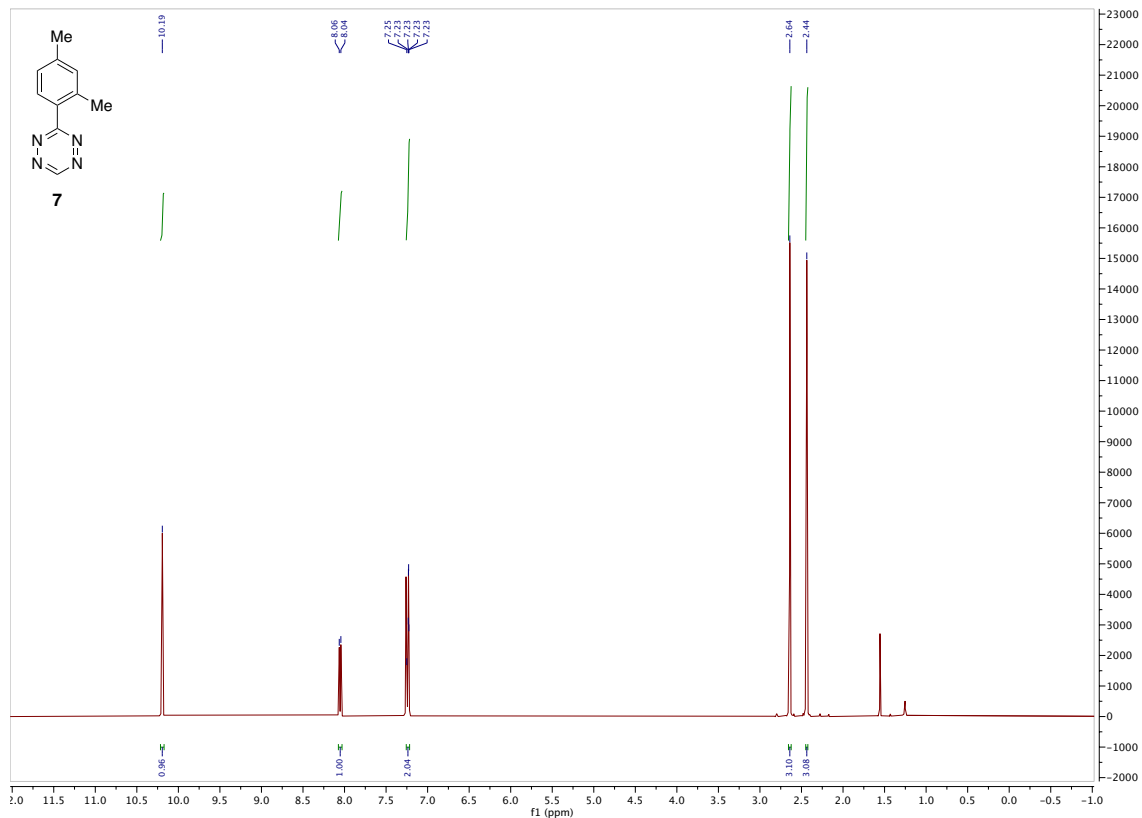
^{13}C NMR of 7
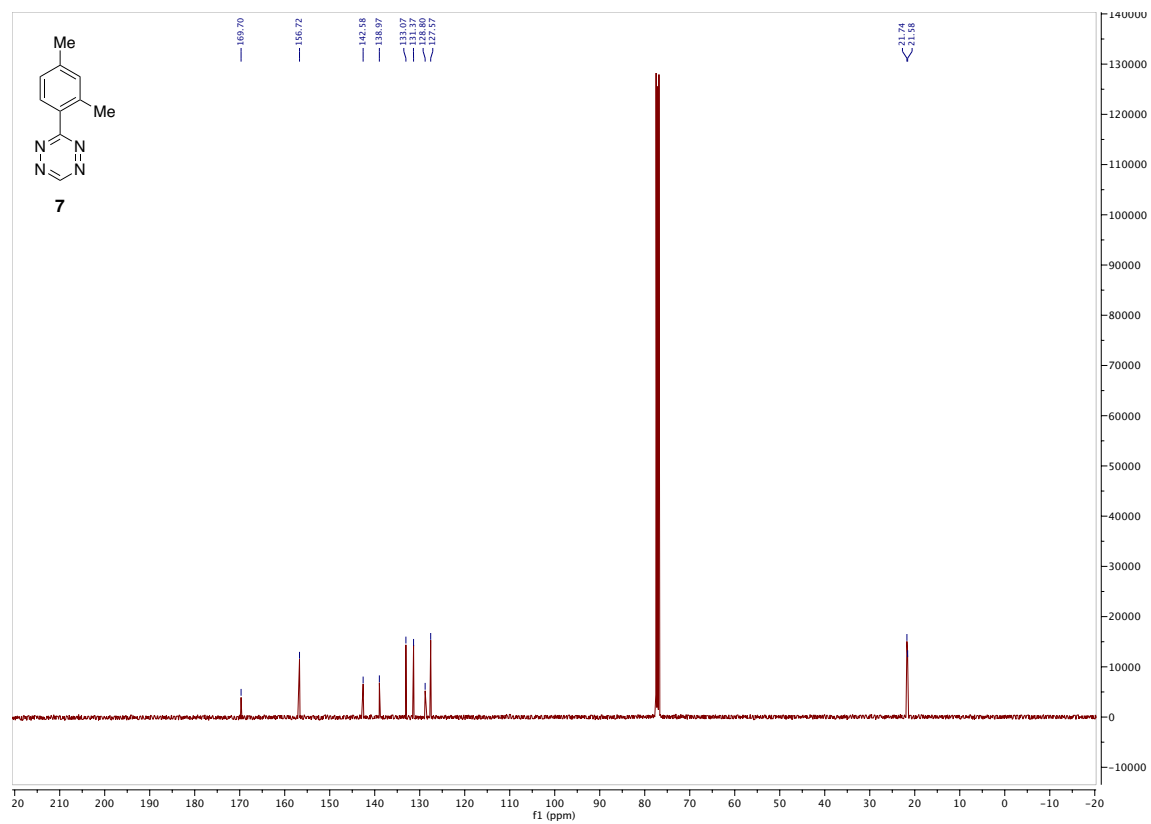
^{1}H NMR of 8
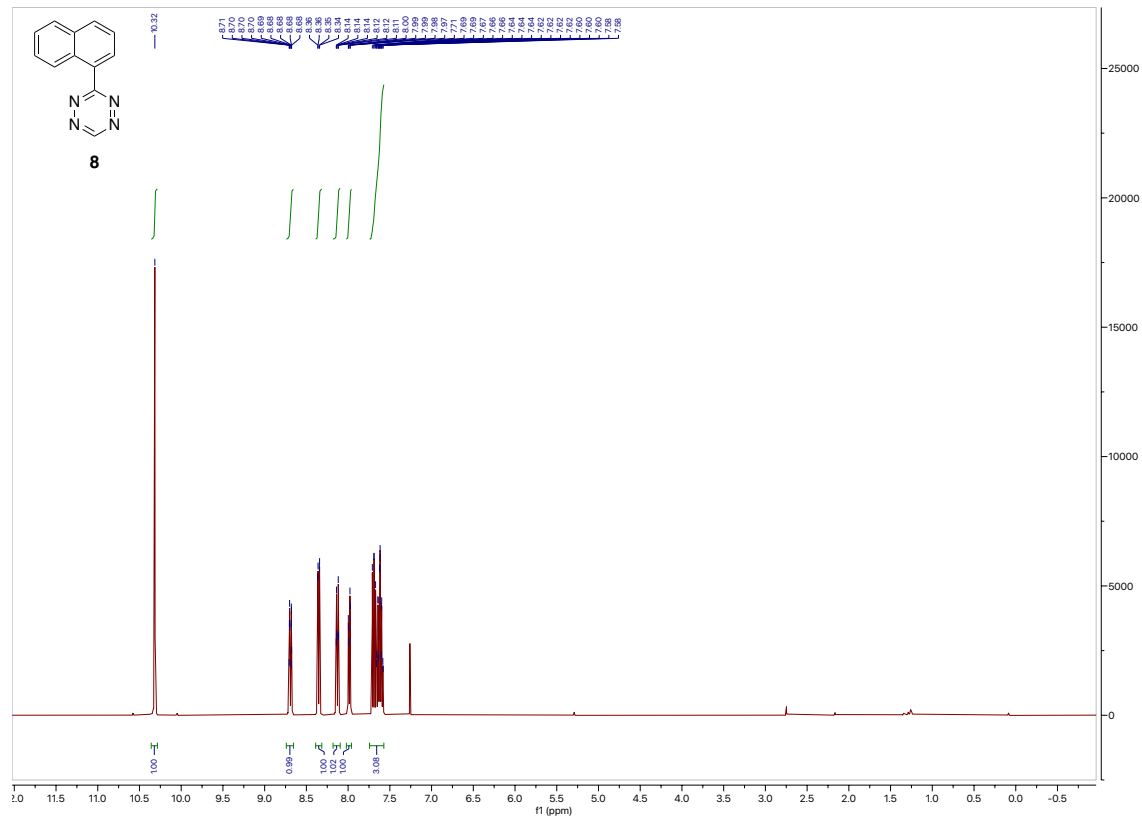
^{13}C NMR of **8**
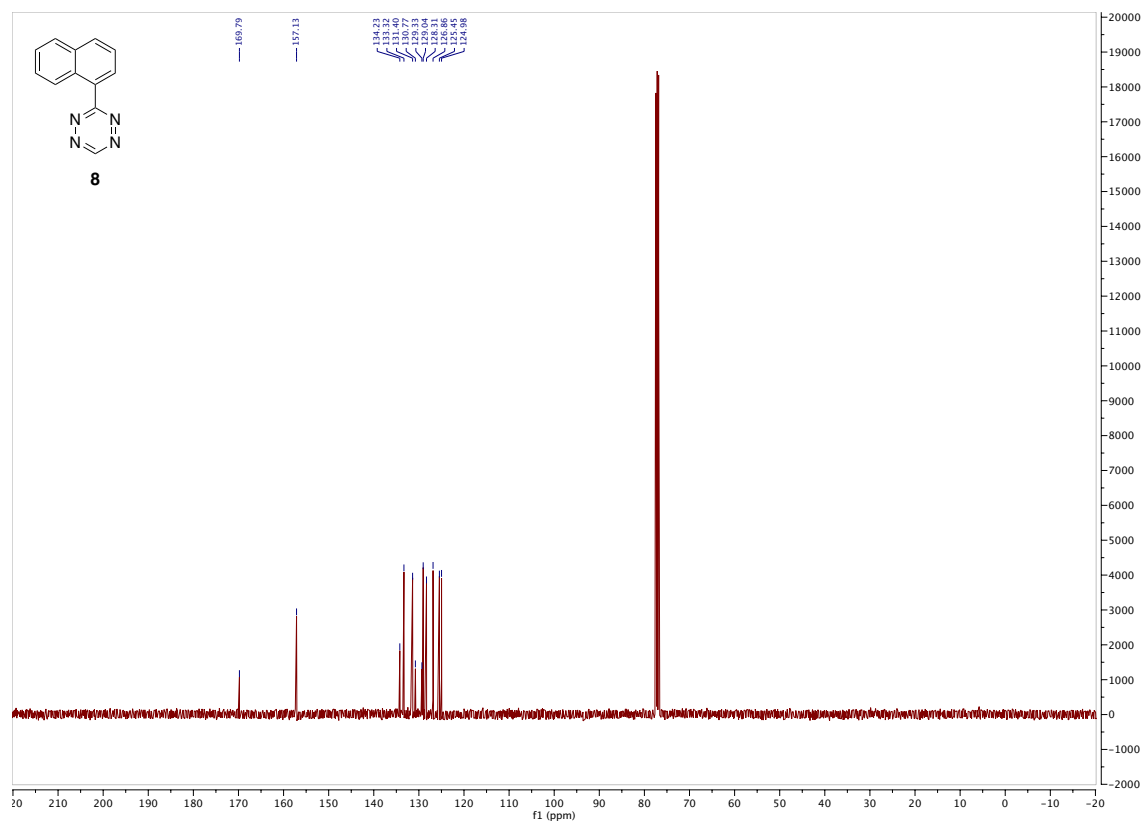
^{1}H NMR of **9**
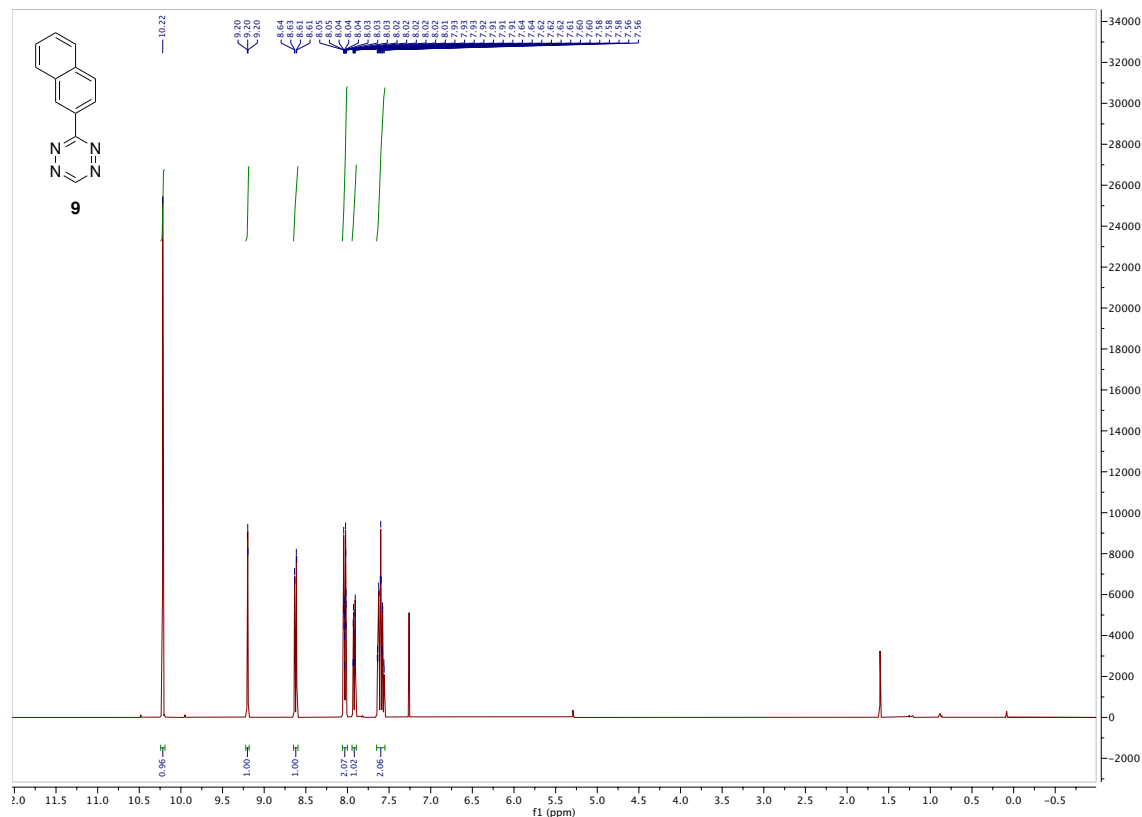
^{13}C NMR of **9**
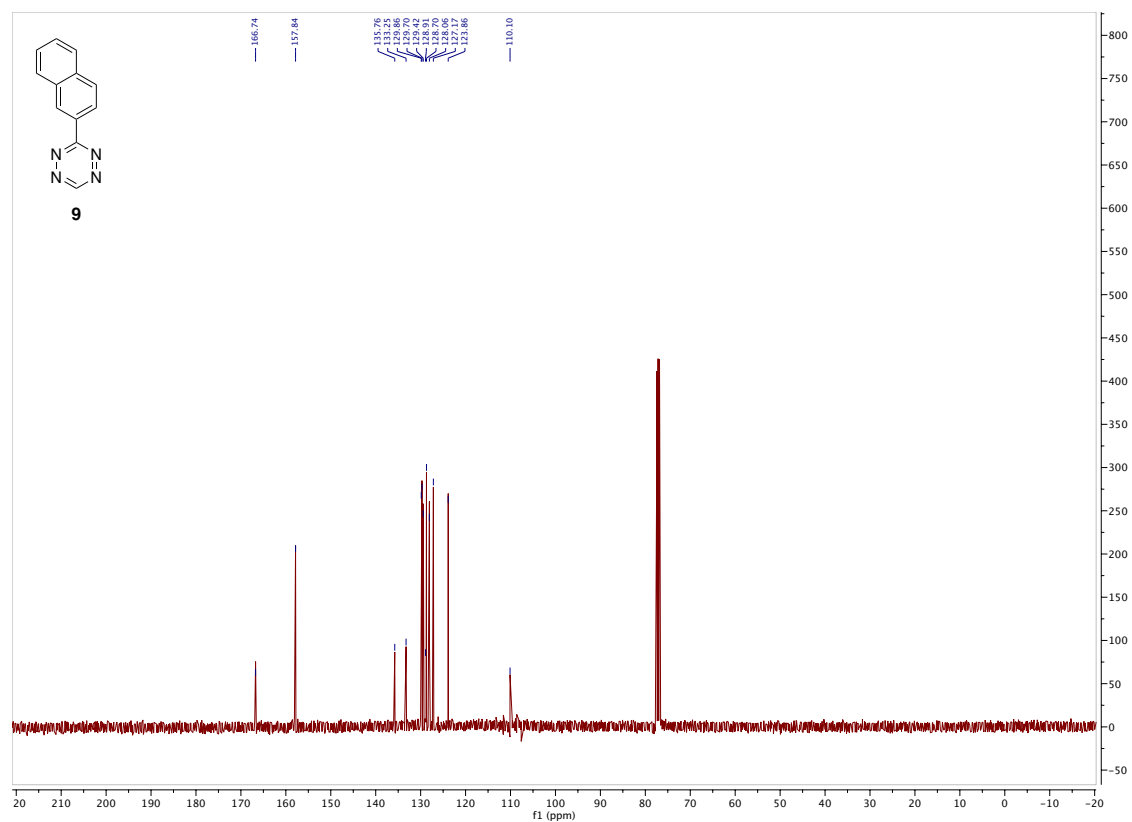
^{1}H NMR of **10**
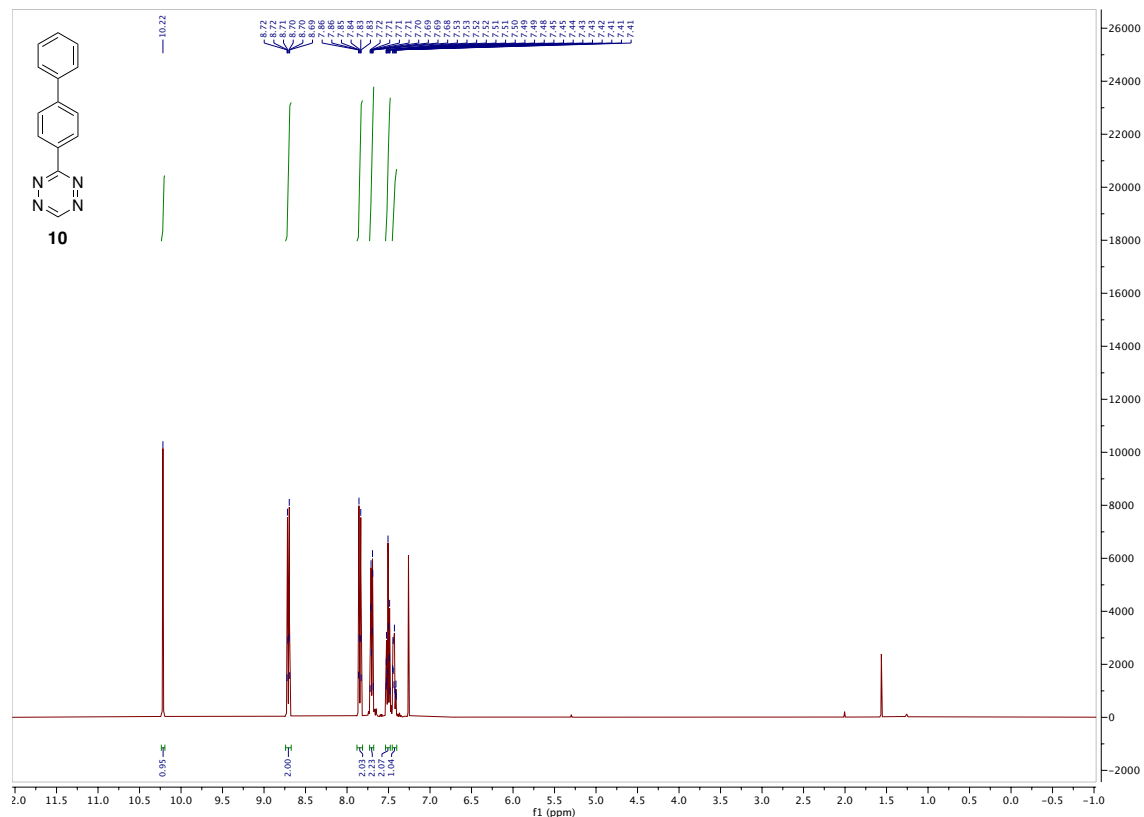
^{13}C NMR of **10**
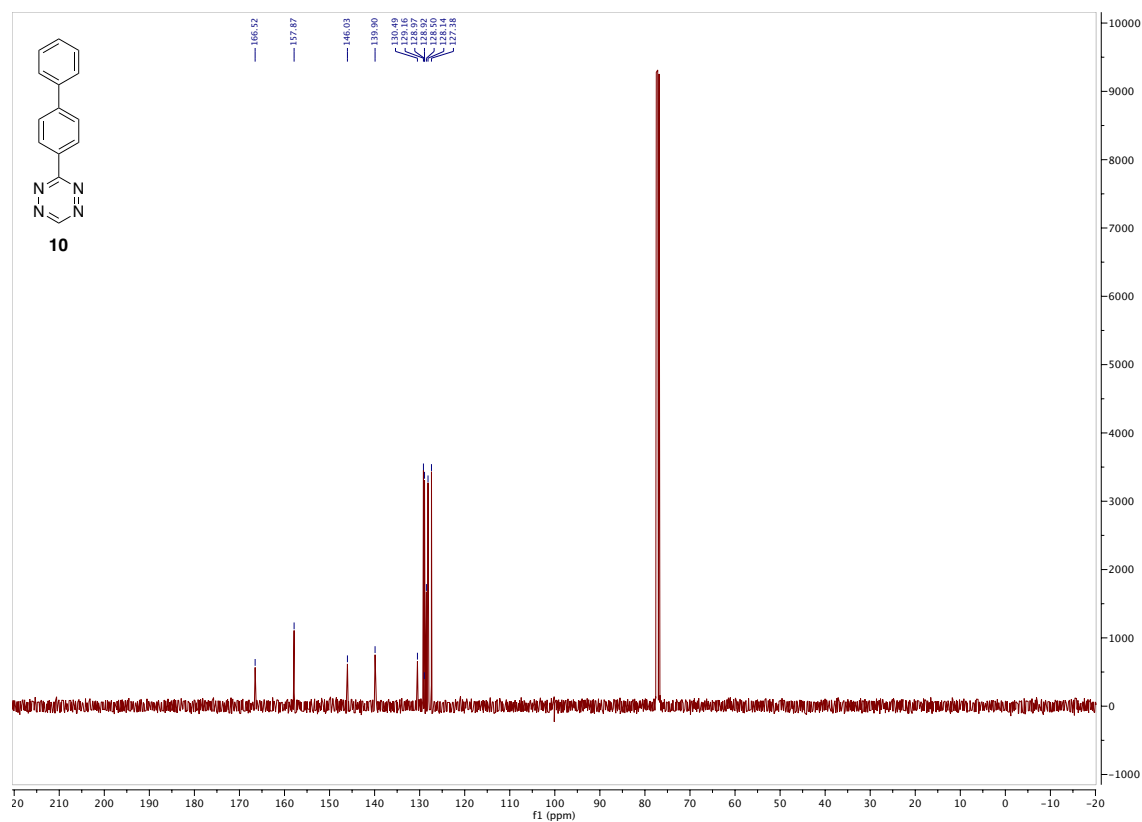
^{1}H NMR of **11**
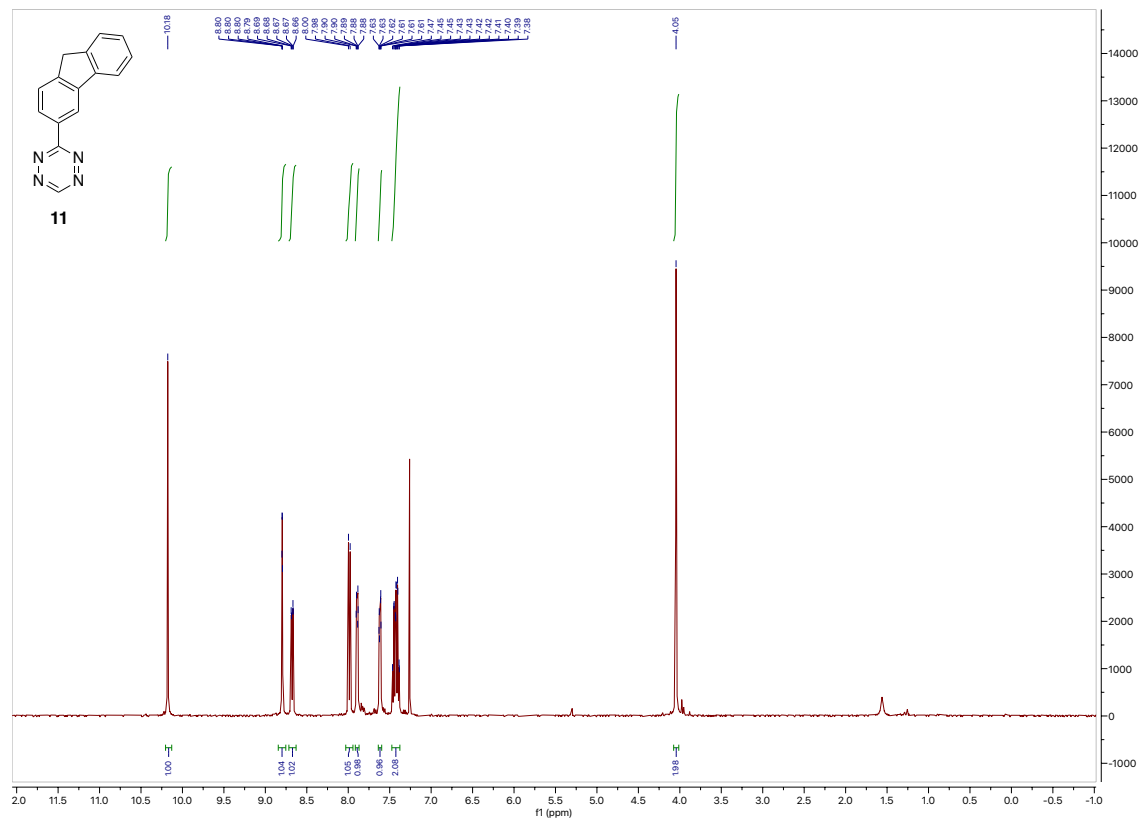
13C NMR of 11
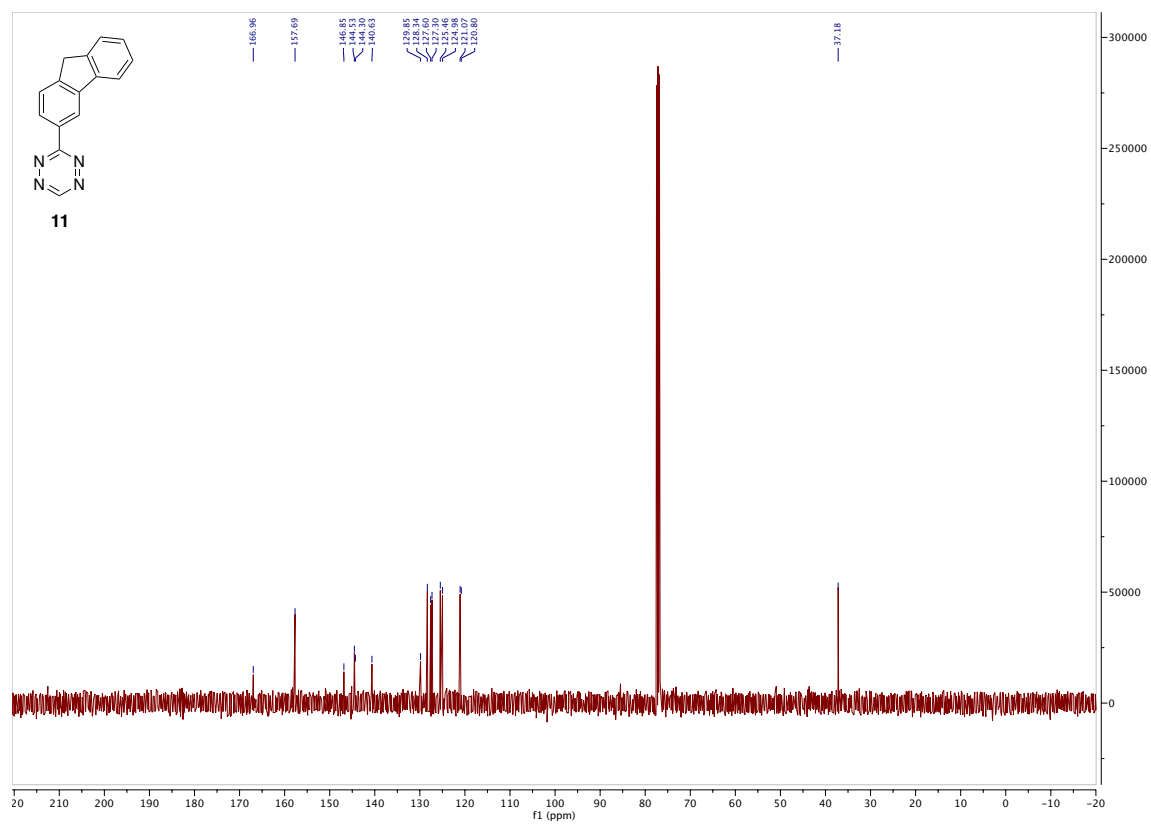
1H NMR of 12
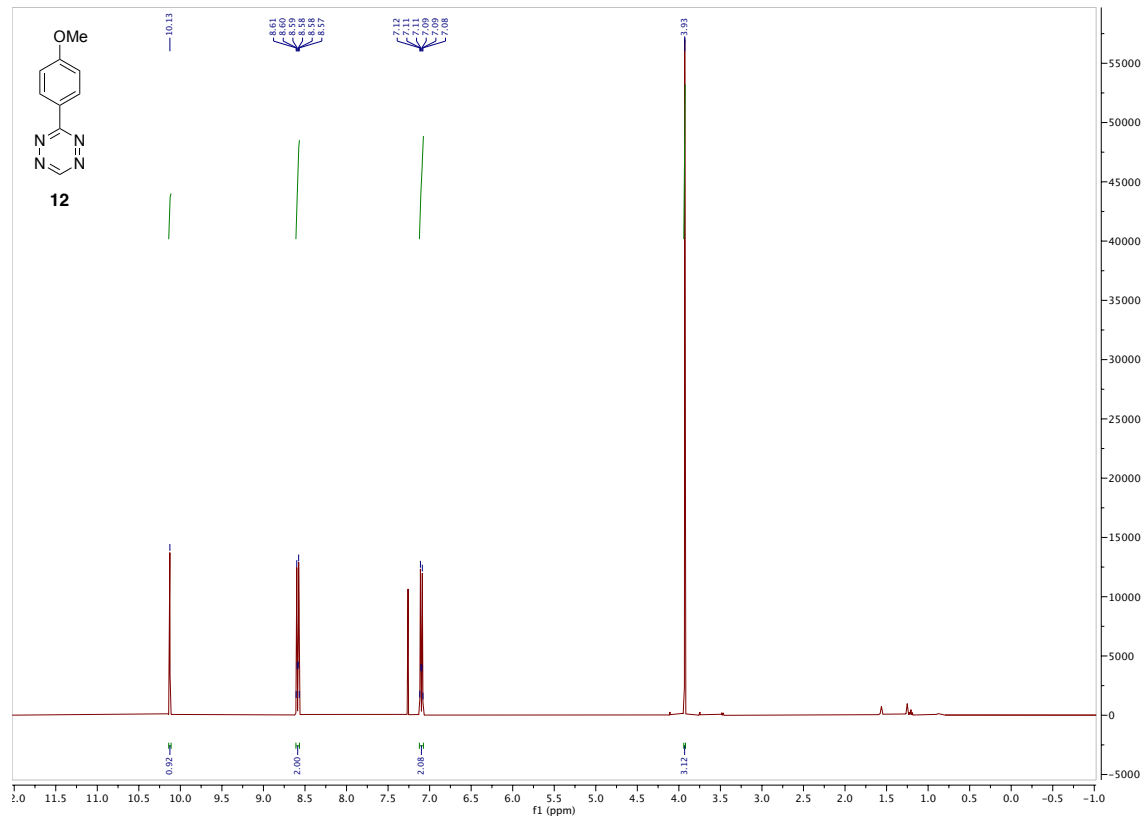
^{13}C NMR of **12**
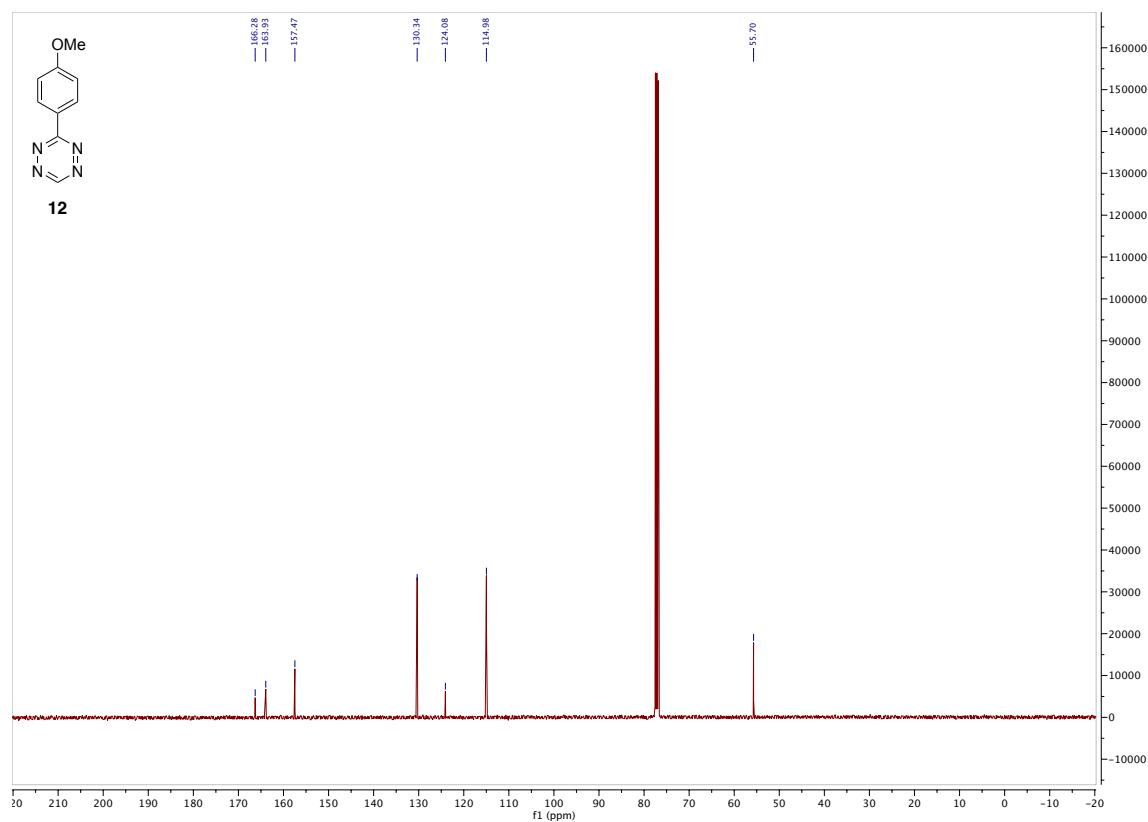
^{1}H NMR of **13**
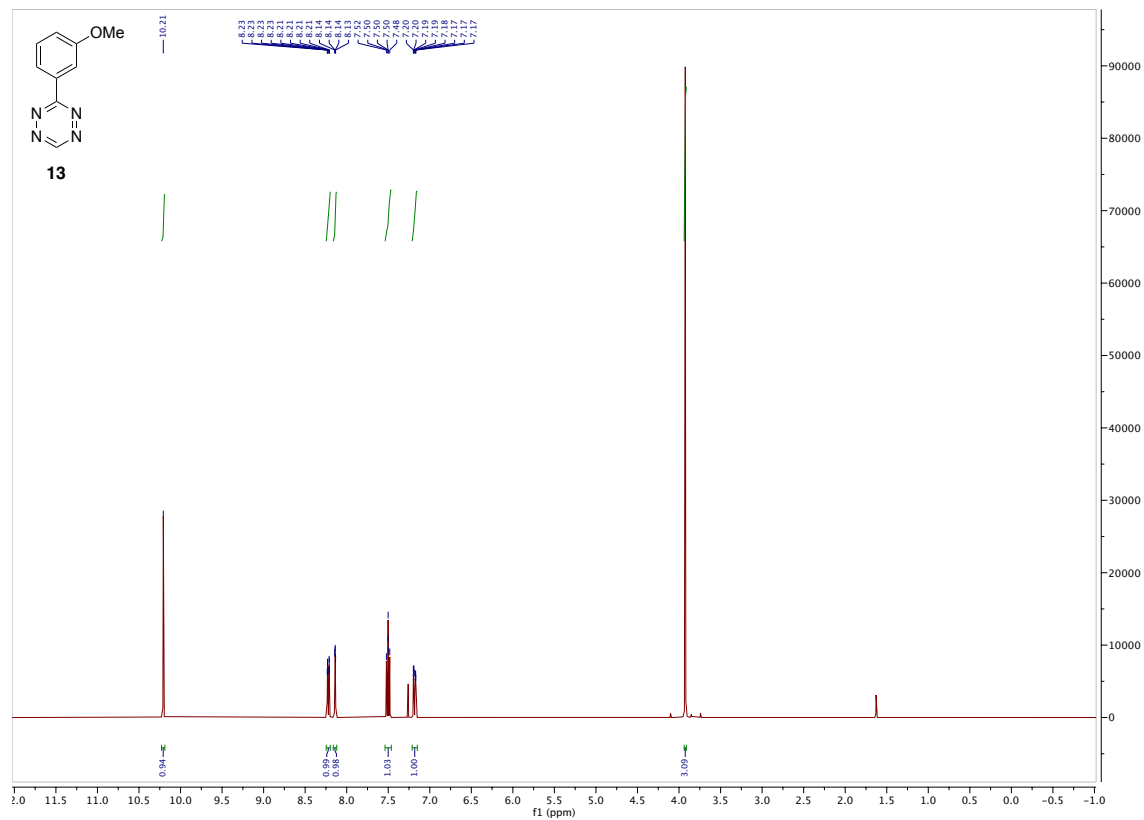
^{13}C NMR of 13
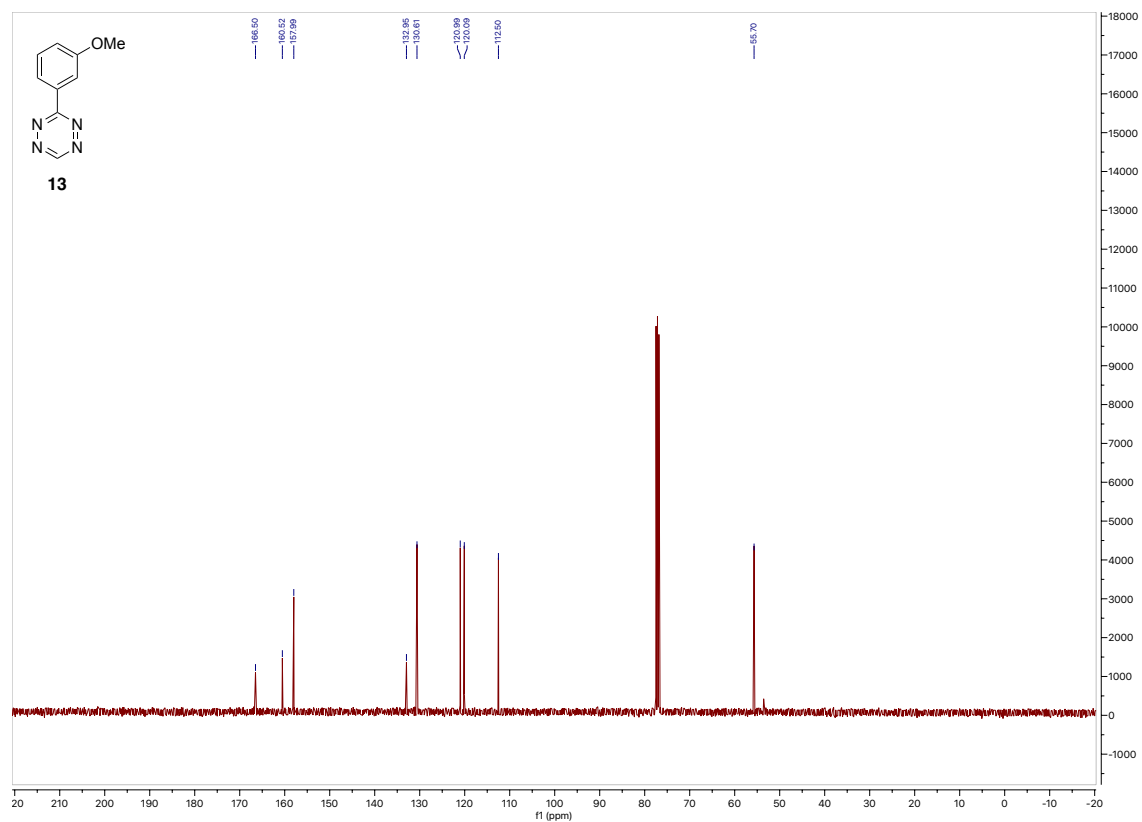
^{1}H NMR of 14
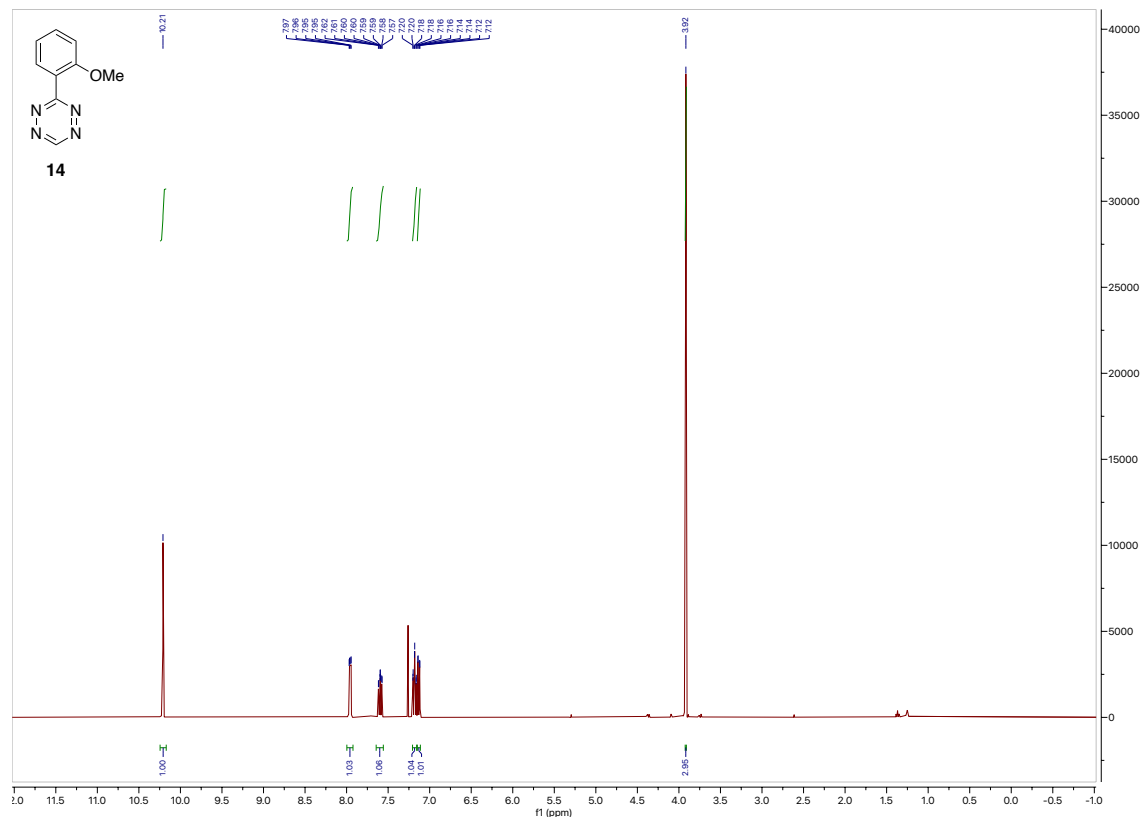
^{13}C NMR of **14**
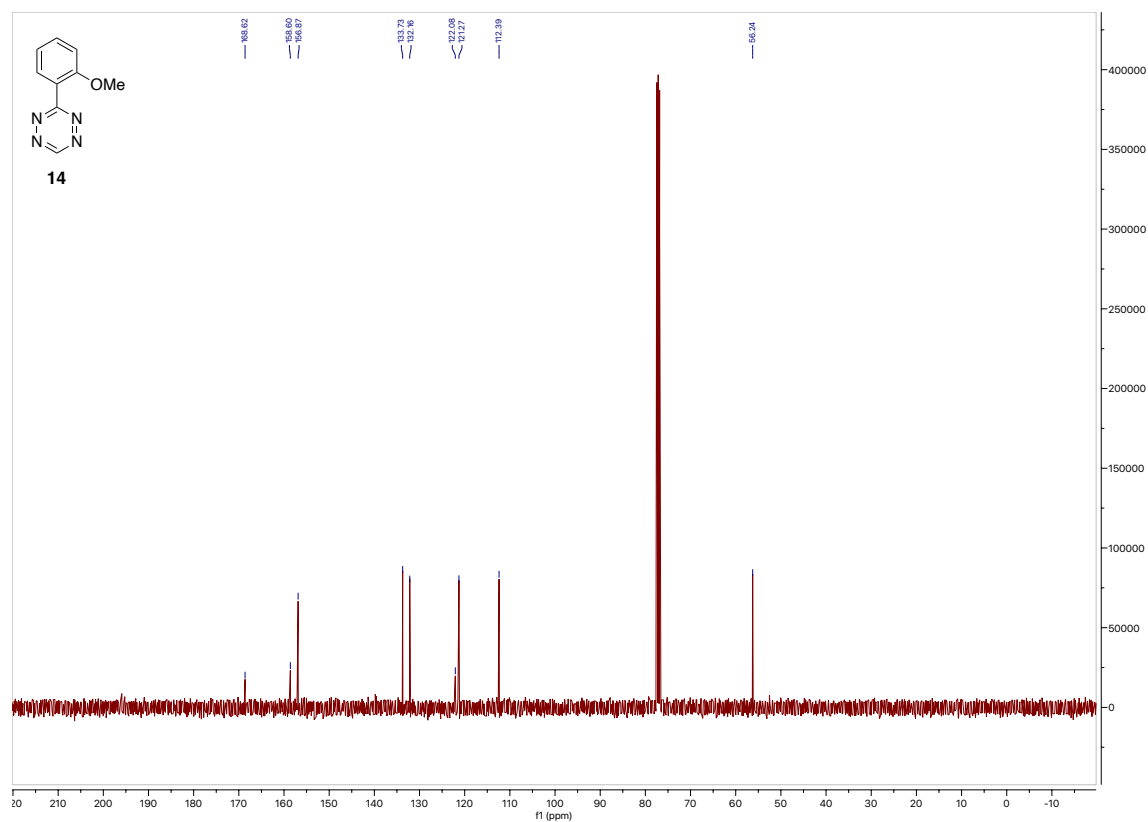
^{1}H NMR of **15**
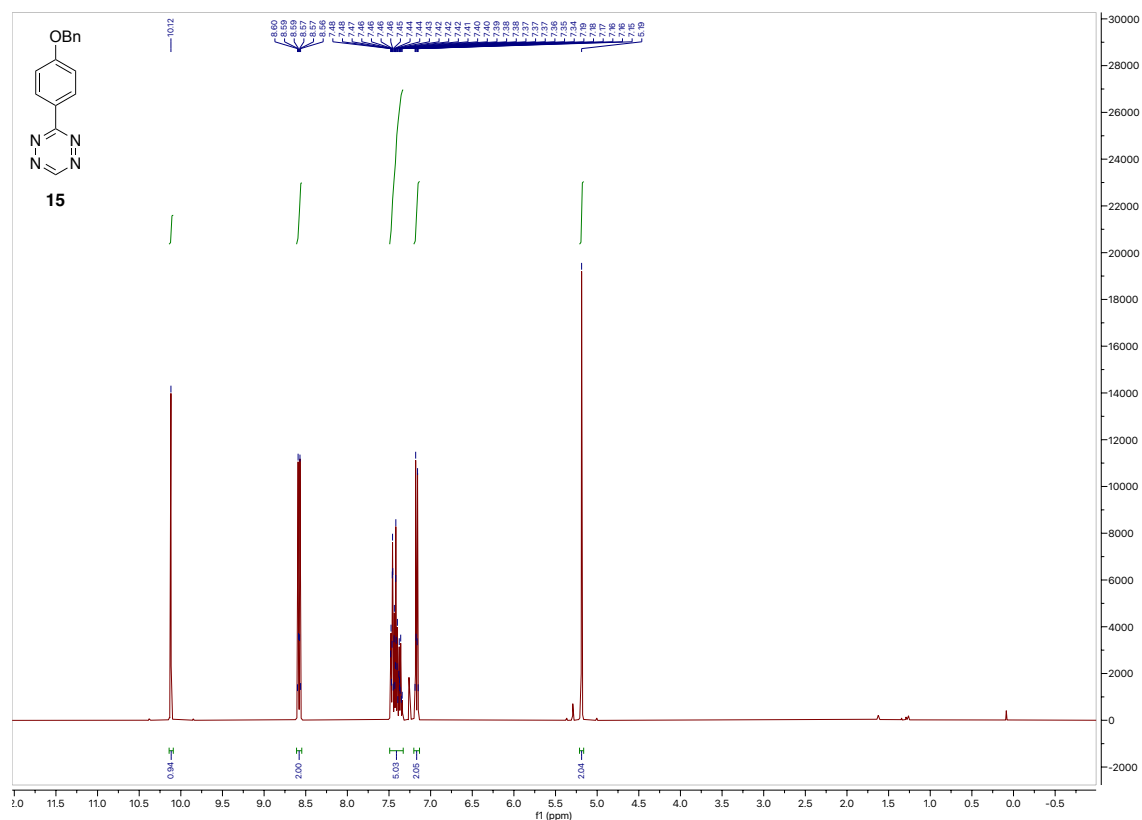
¹³C NMR of 15
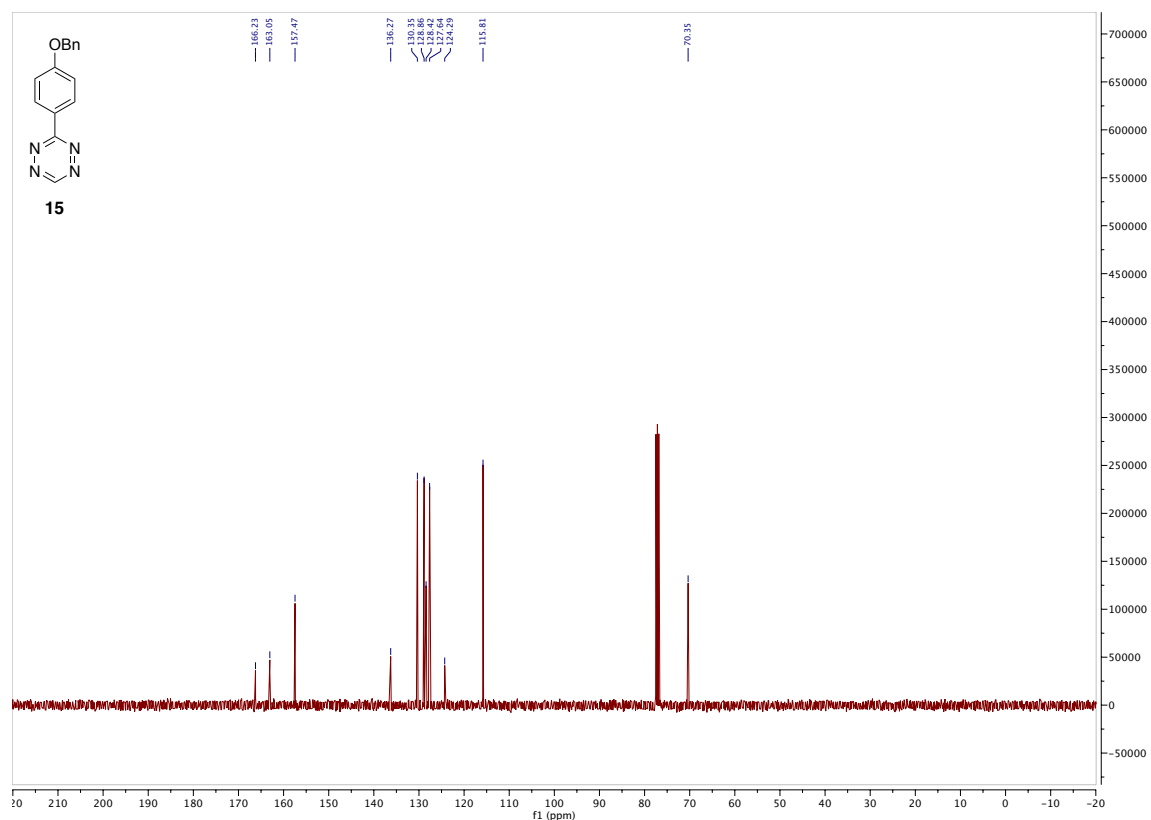
¹H NMR of 16
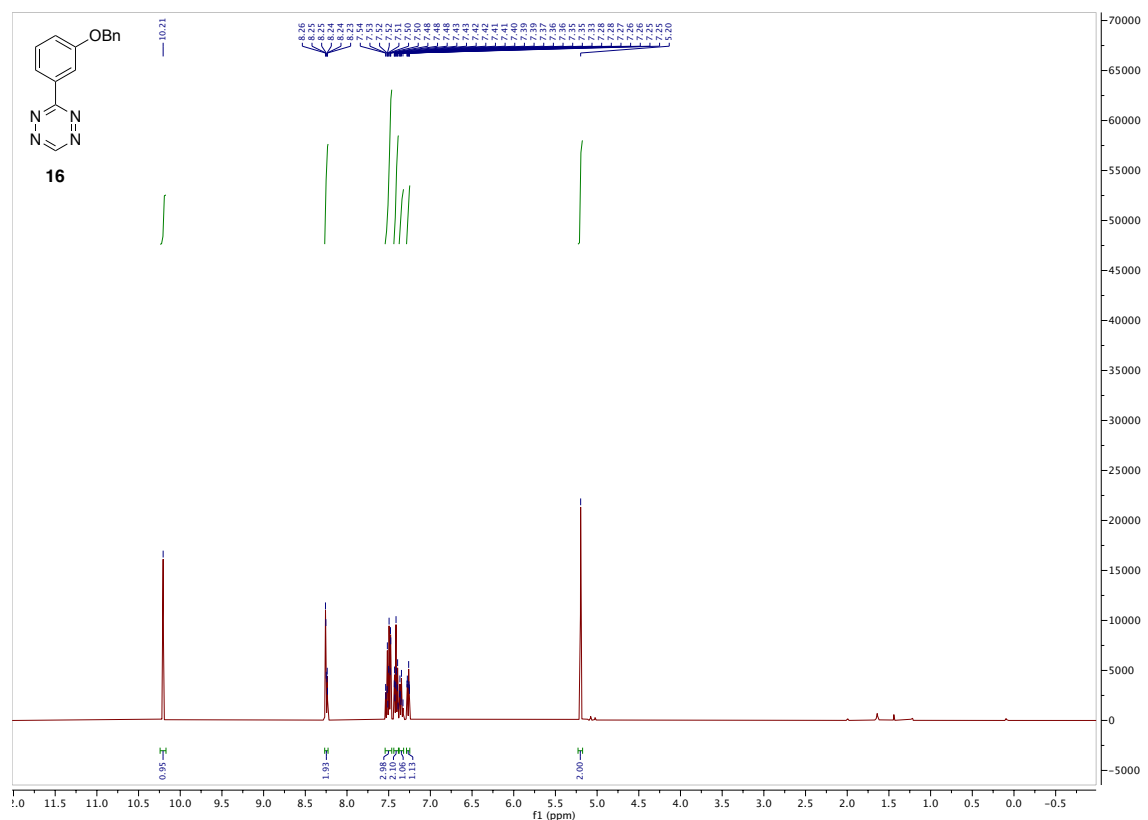
¹³C NMR of 16
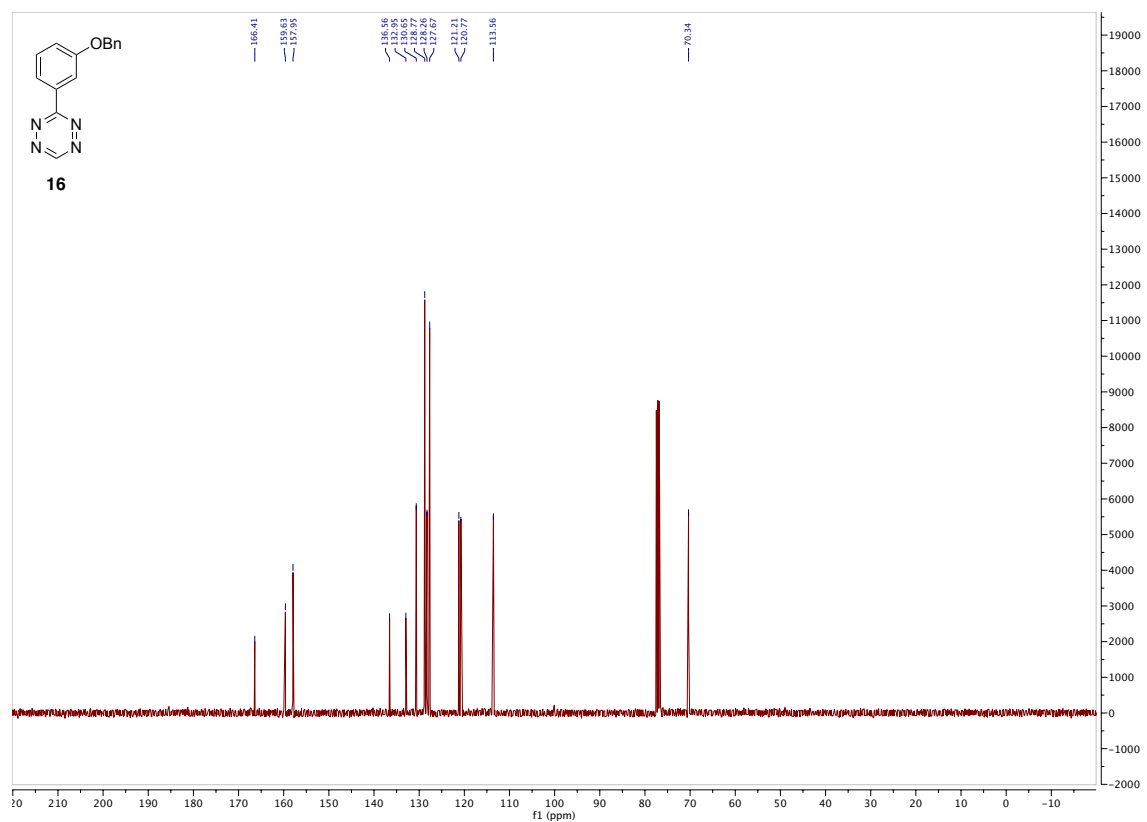
¹H NMR of 17
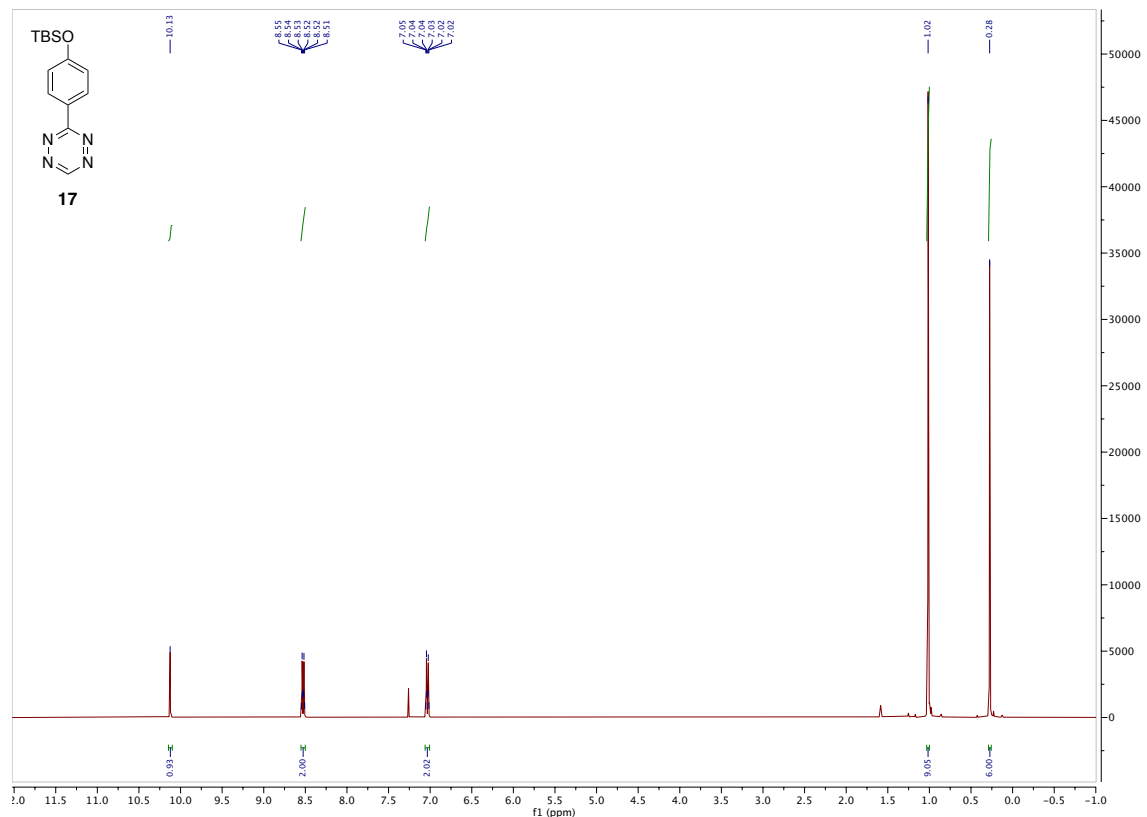
^{13}C NMR of **17**
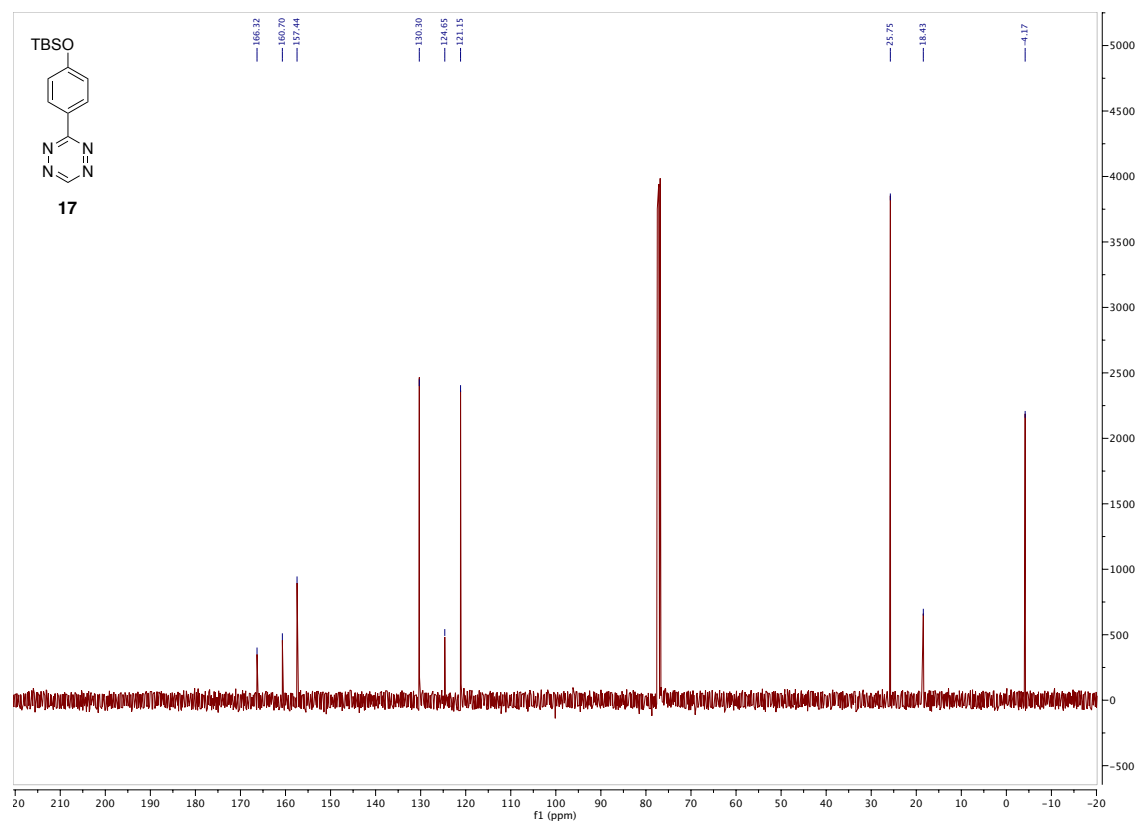
^{1}H NMR of **18**
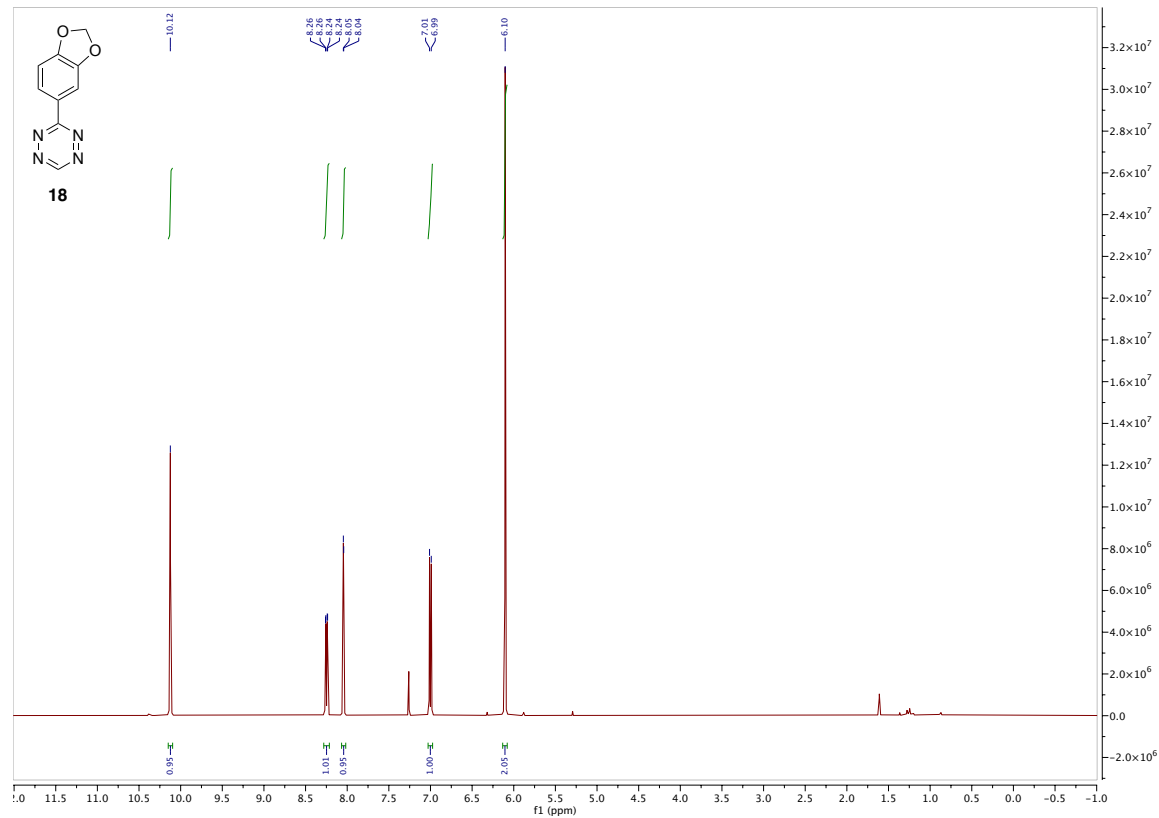
^{13}C NMR of **18**
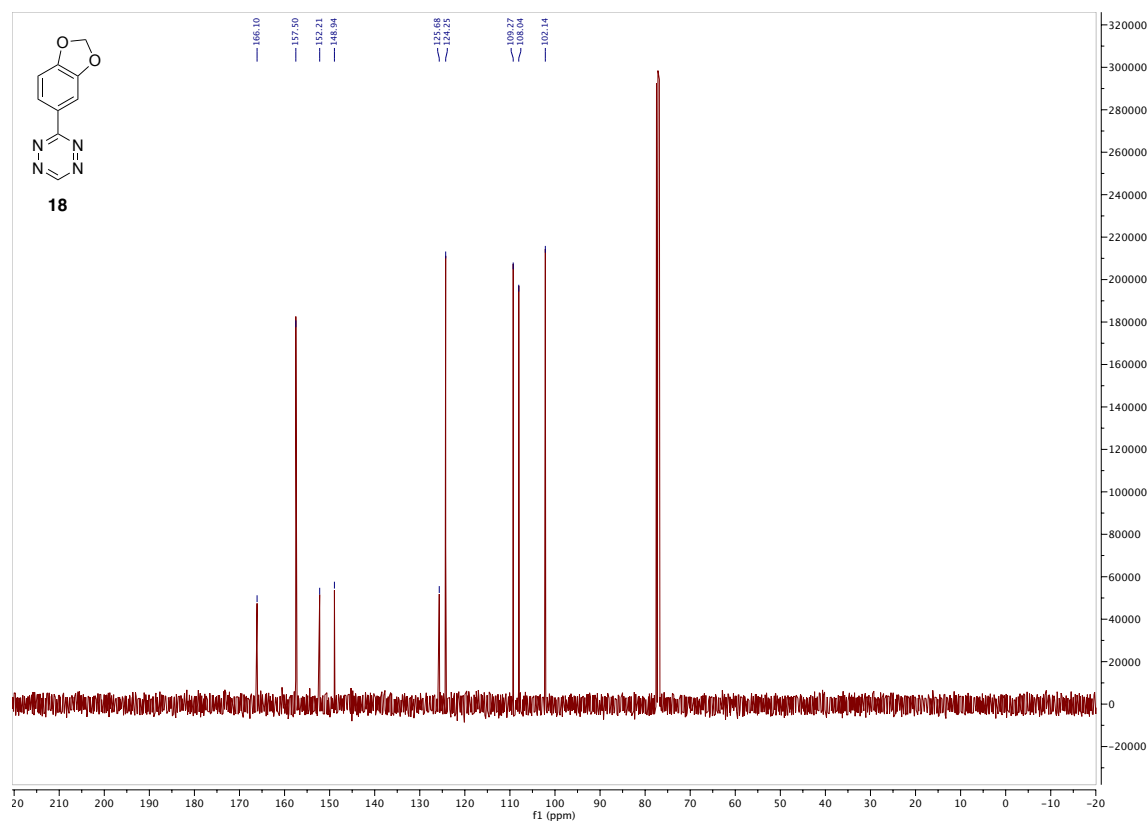
^{1}H NMR of **19**
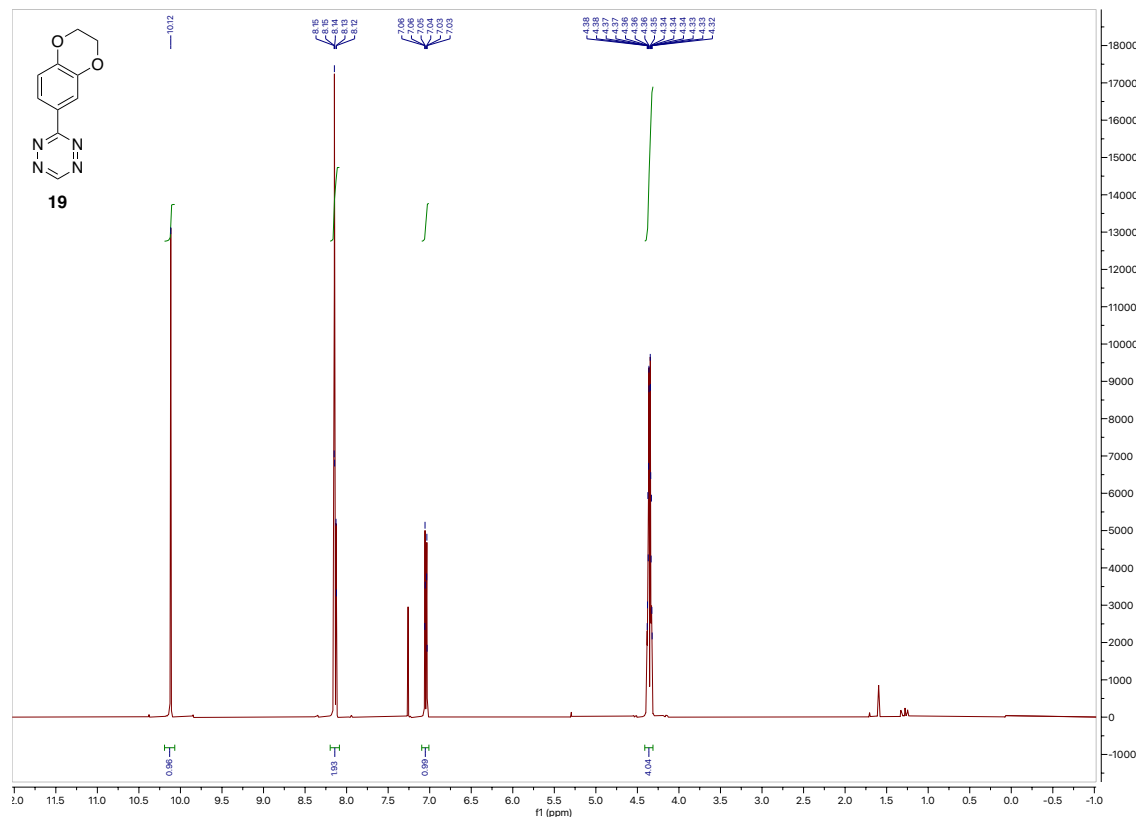
^{13}C NMR of 19

^{1}H NMR of 20

^{13}C NMR of 20

NHAc

20

169.02, 165.08, 157.78, 143.57, 128.73, 125.89, 119.17, 24.22

^{1}H NMR of 21

NH$_2$

21

10.04, 8.45, 8.45, 8.43, 8.43, 6.82, 6.82, 6.80, 4.10

0.93, 2.02, 2.10, 1.98
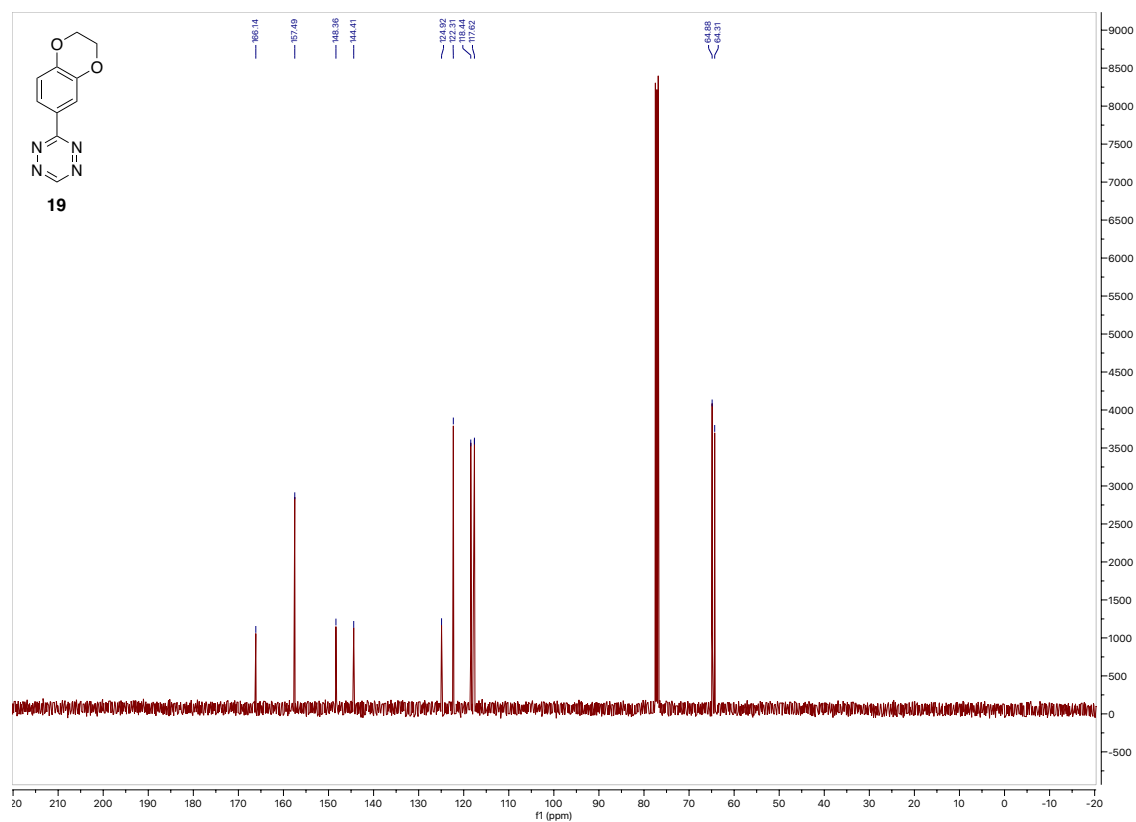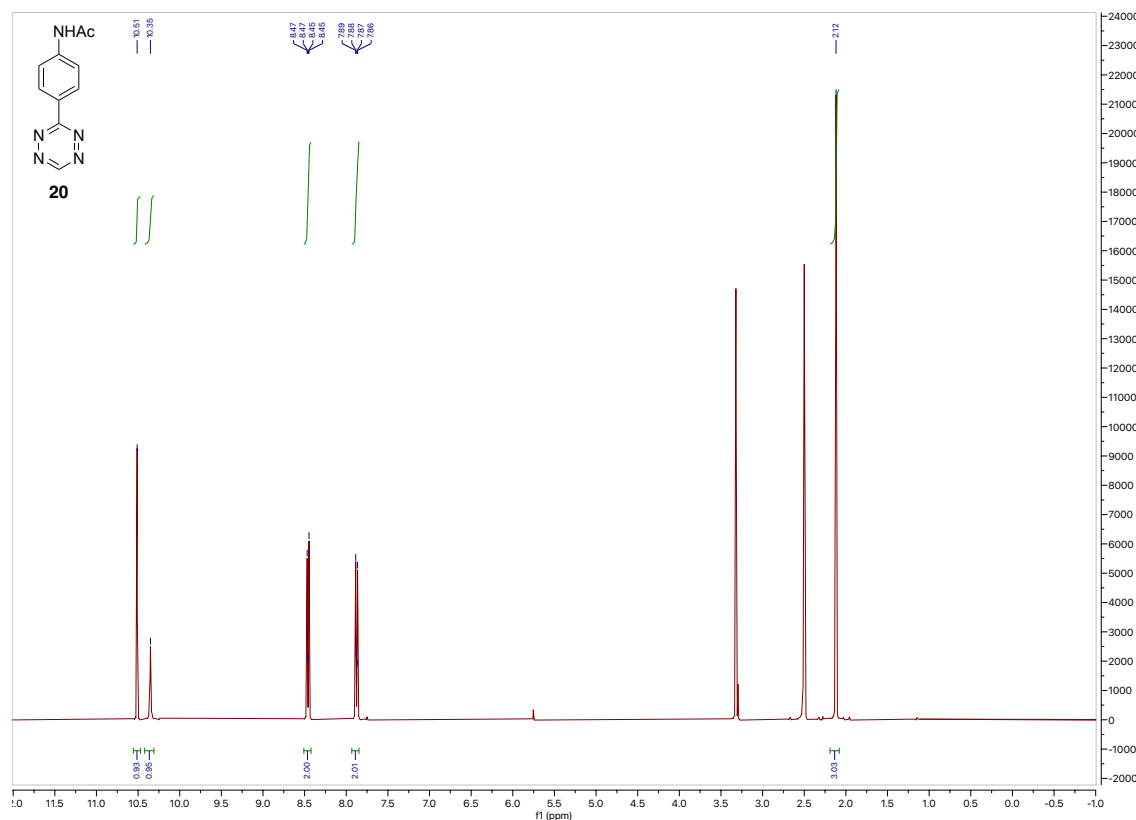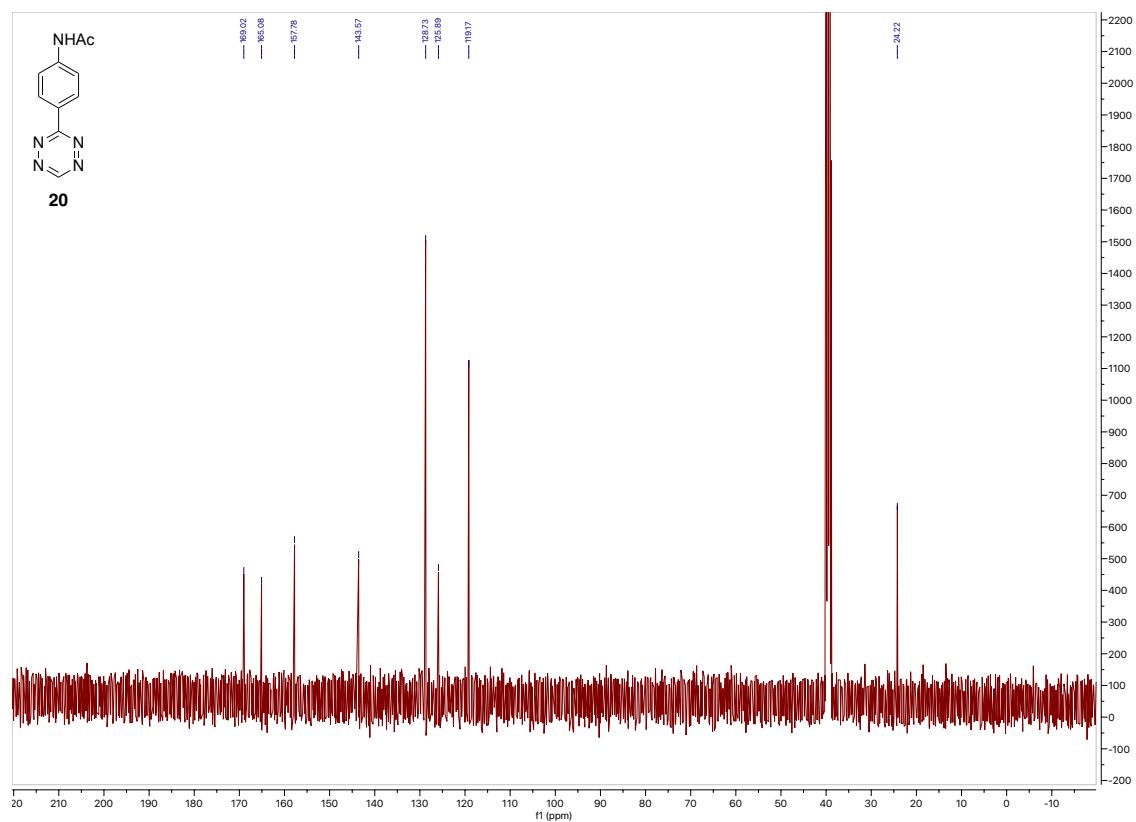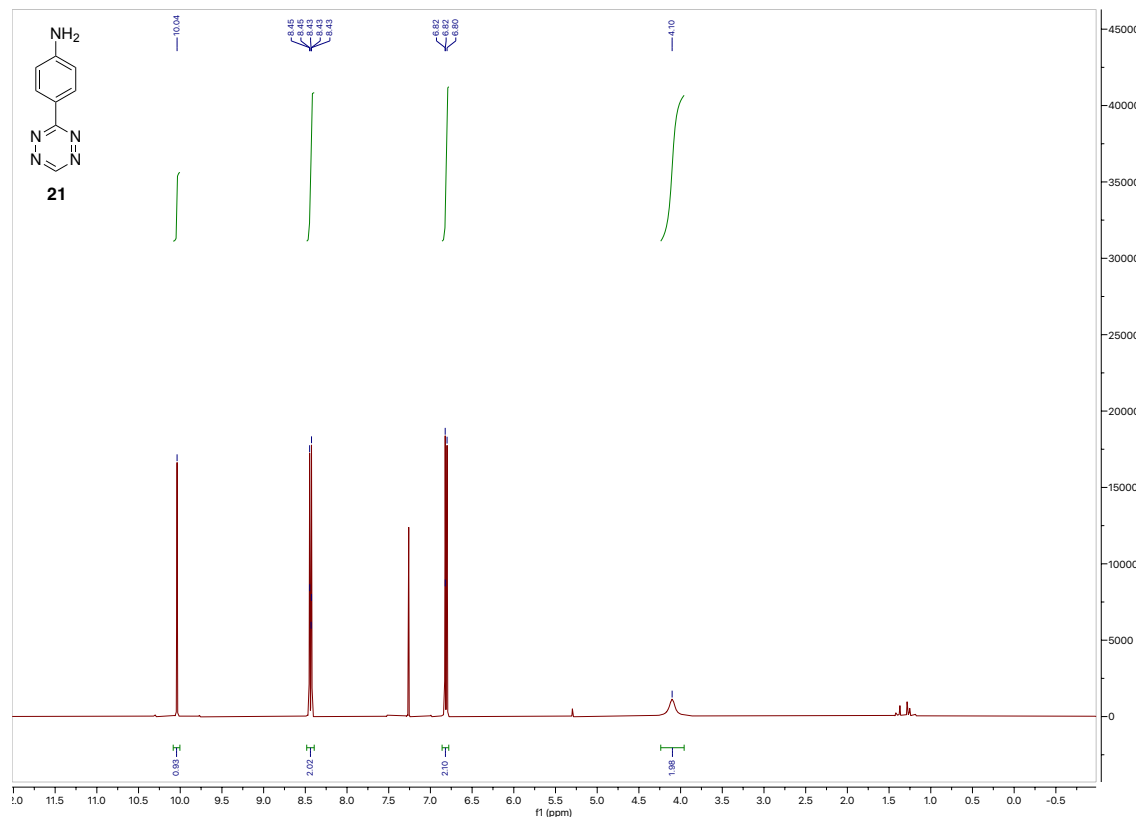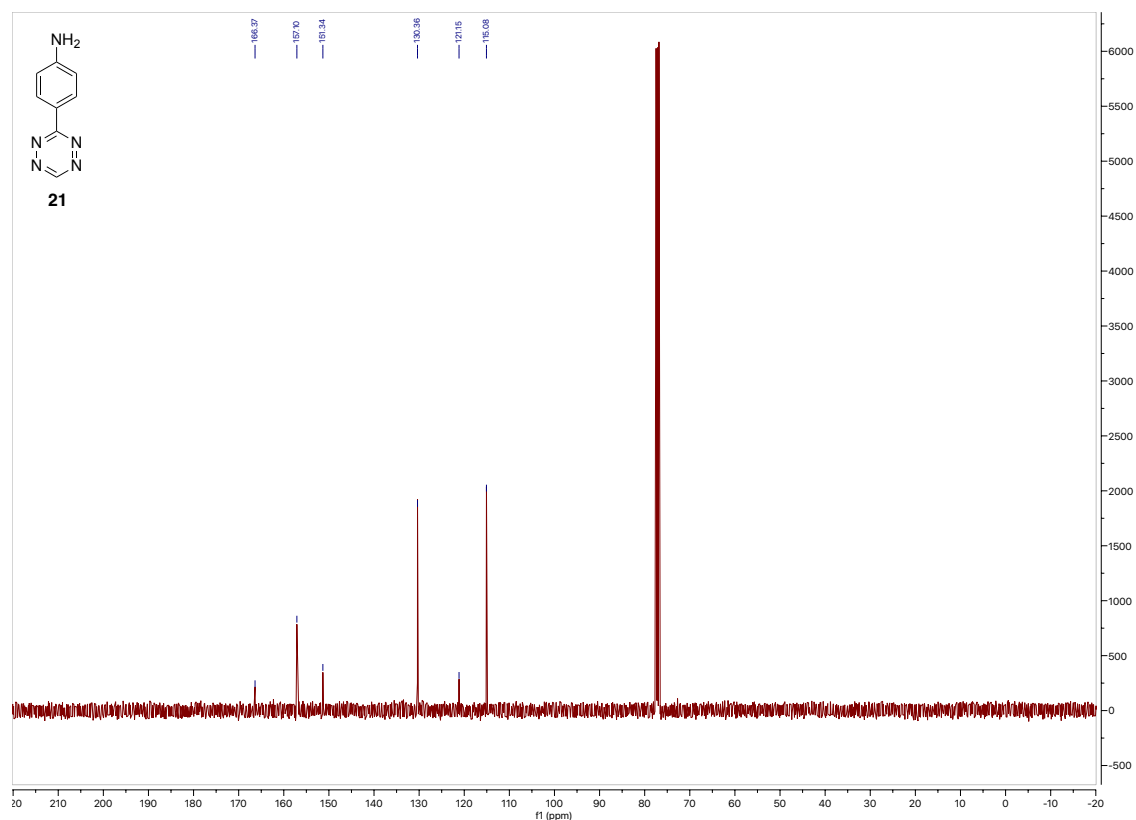
^{13}C NMR of 21
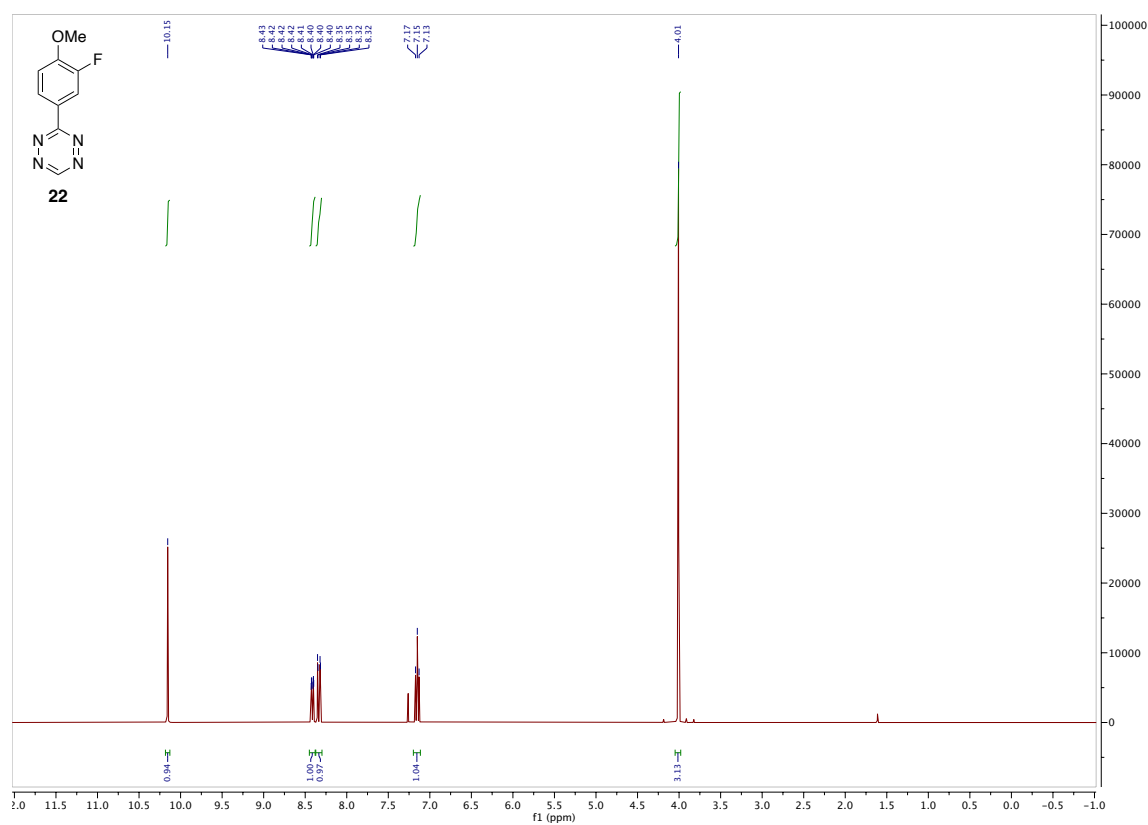
^{1}H NMR of 22

^{13}C NMR of 22
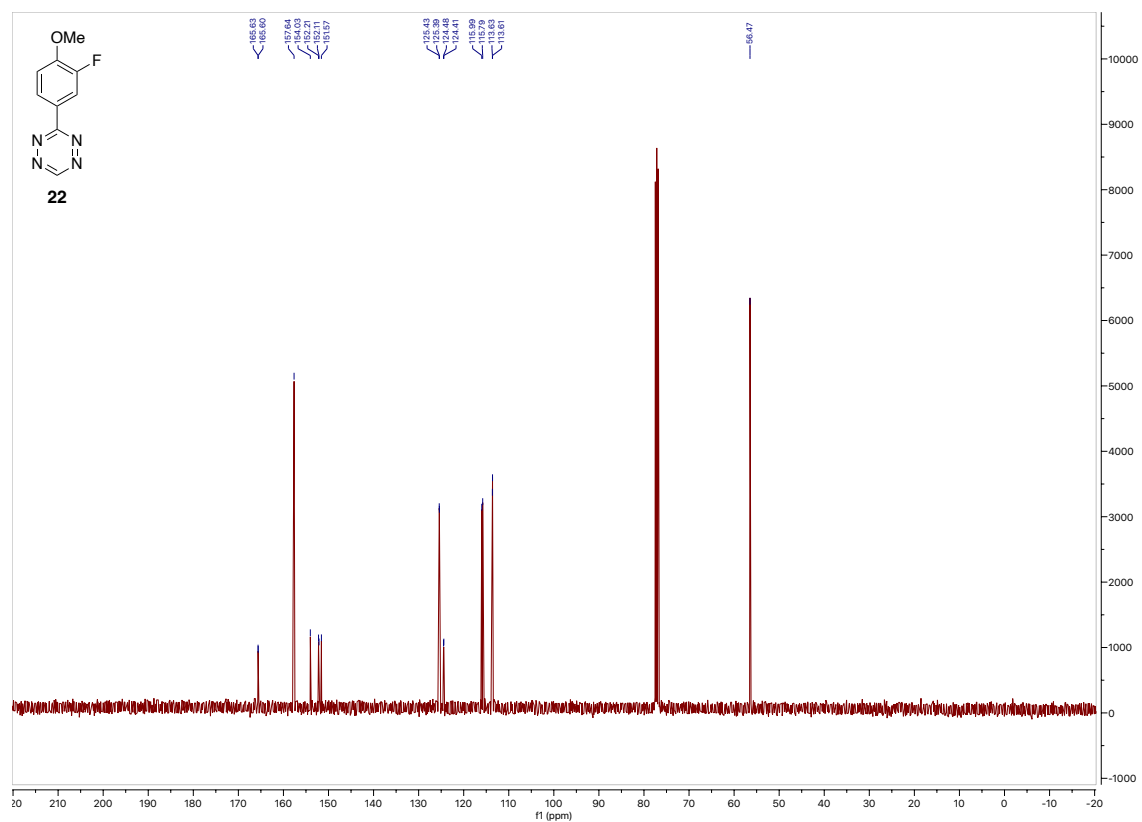
^{19}F NMR of 22
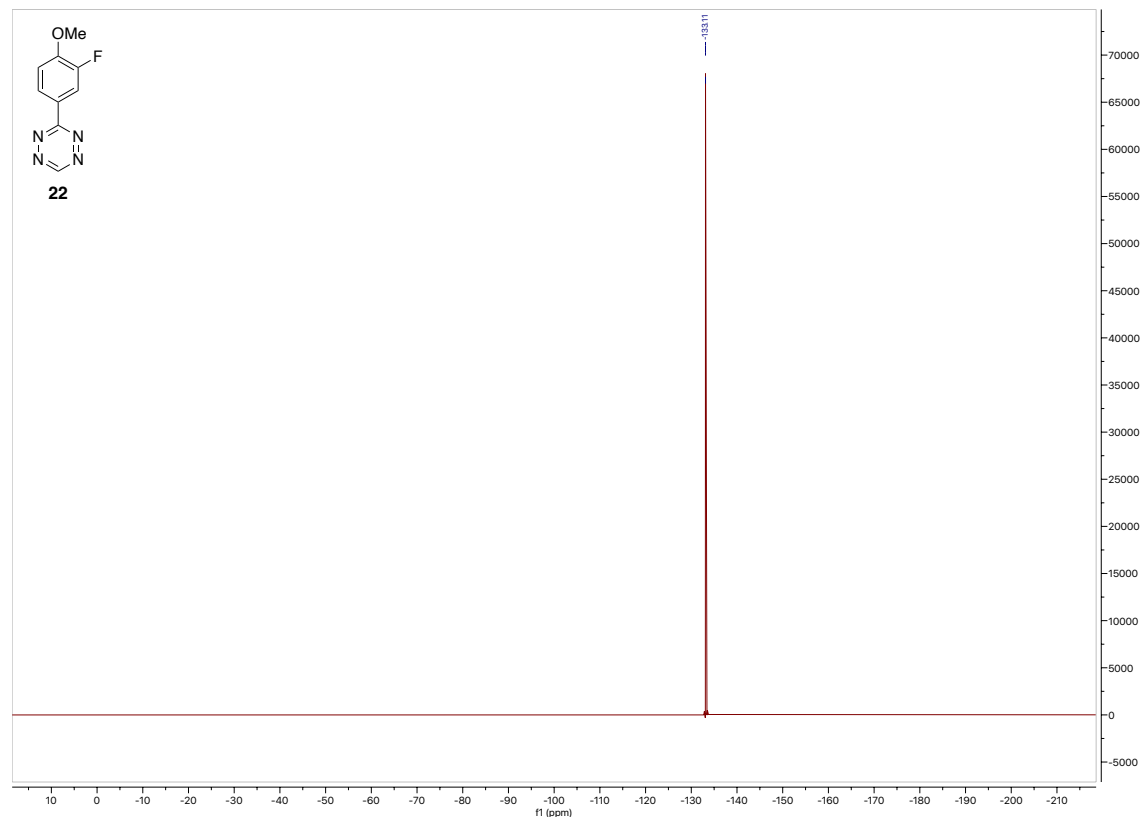
¹H NMR of **23**
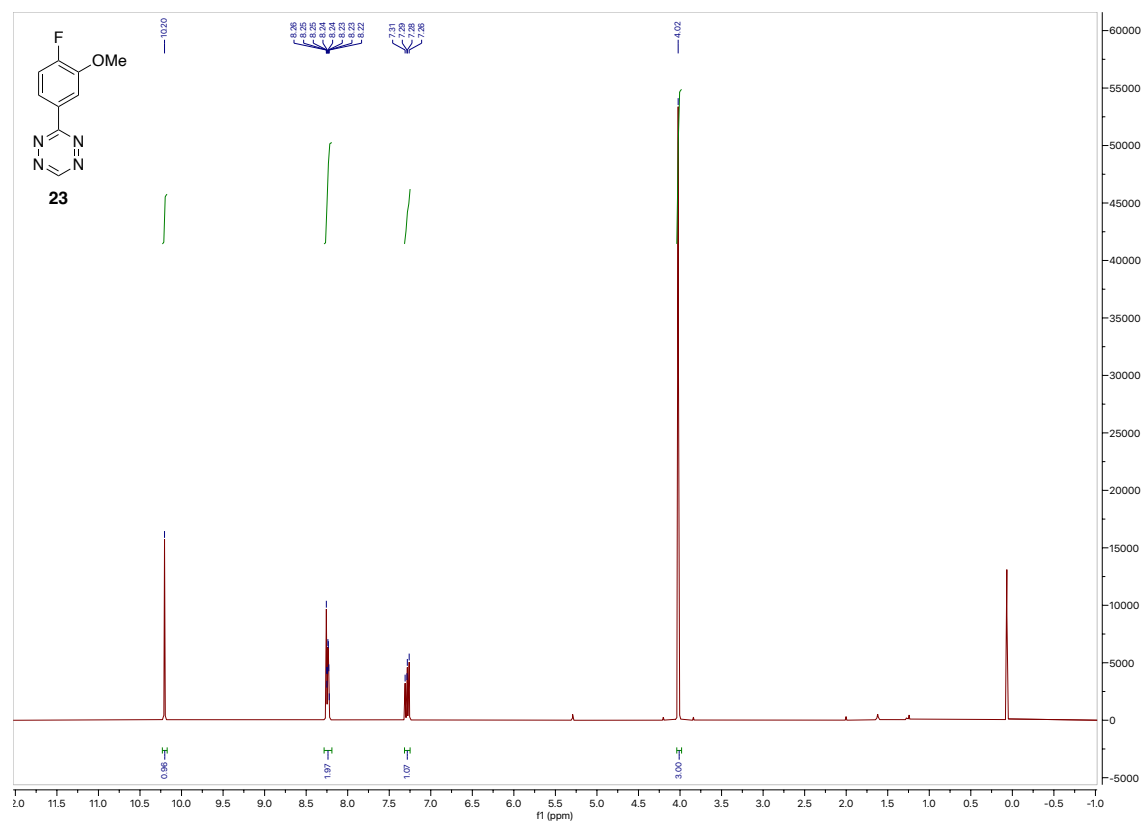
¹³C NMR of **23**
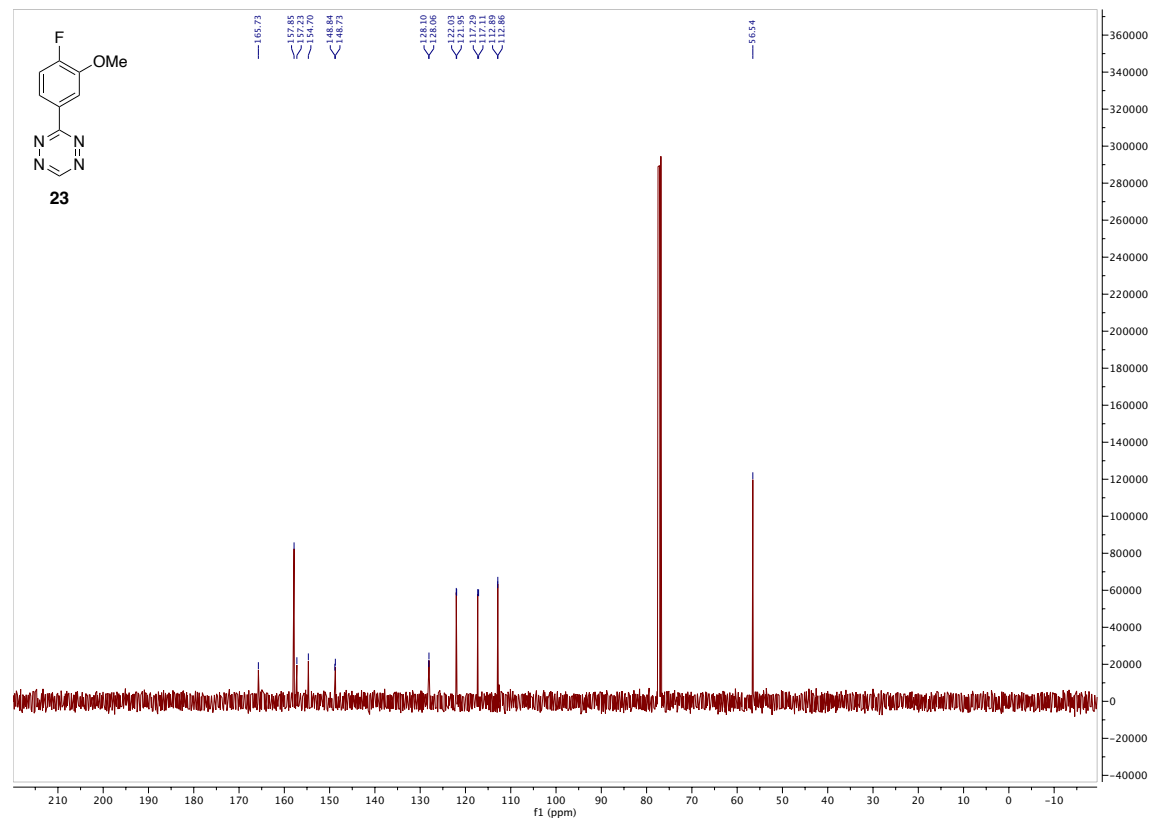
¹⁹F NMR of 23
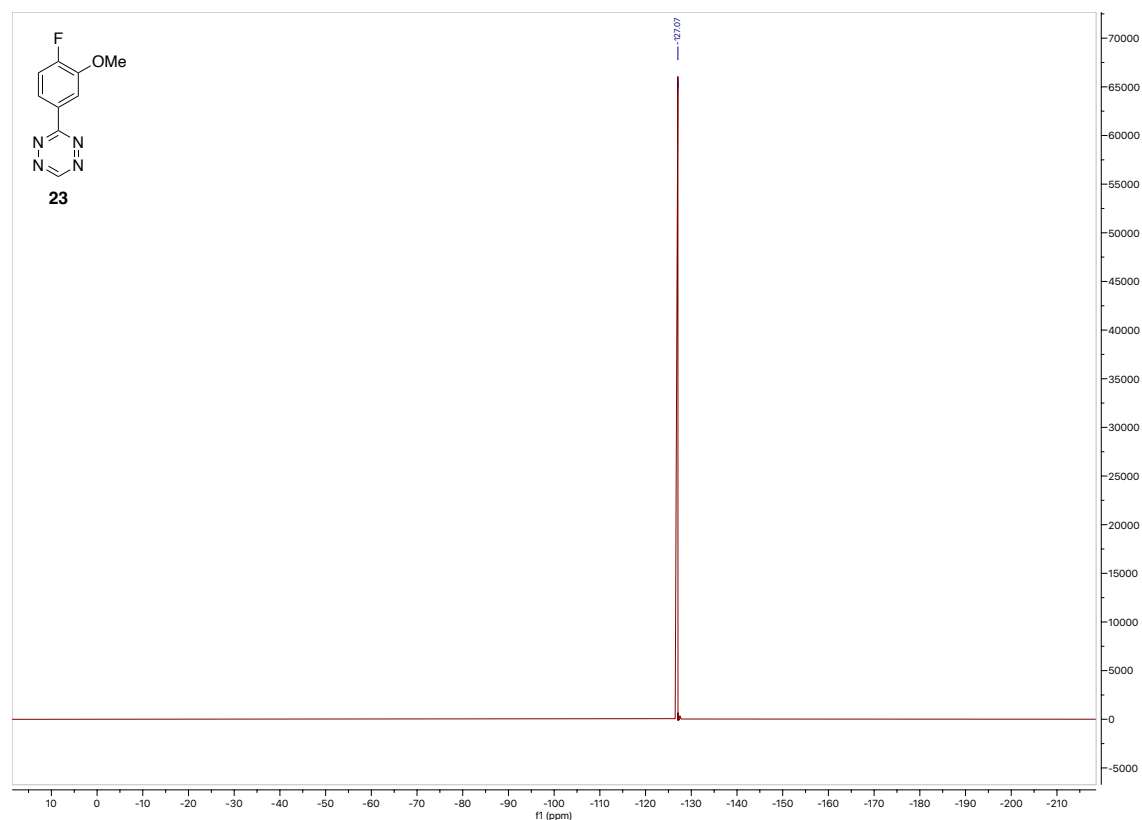
¹H NMR of 24
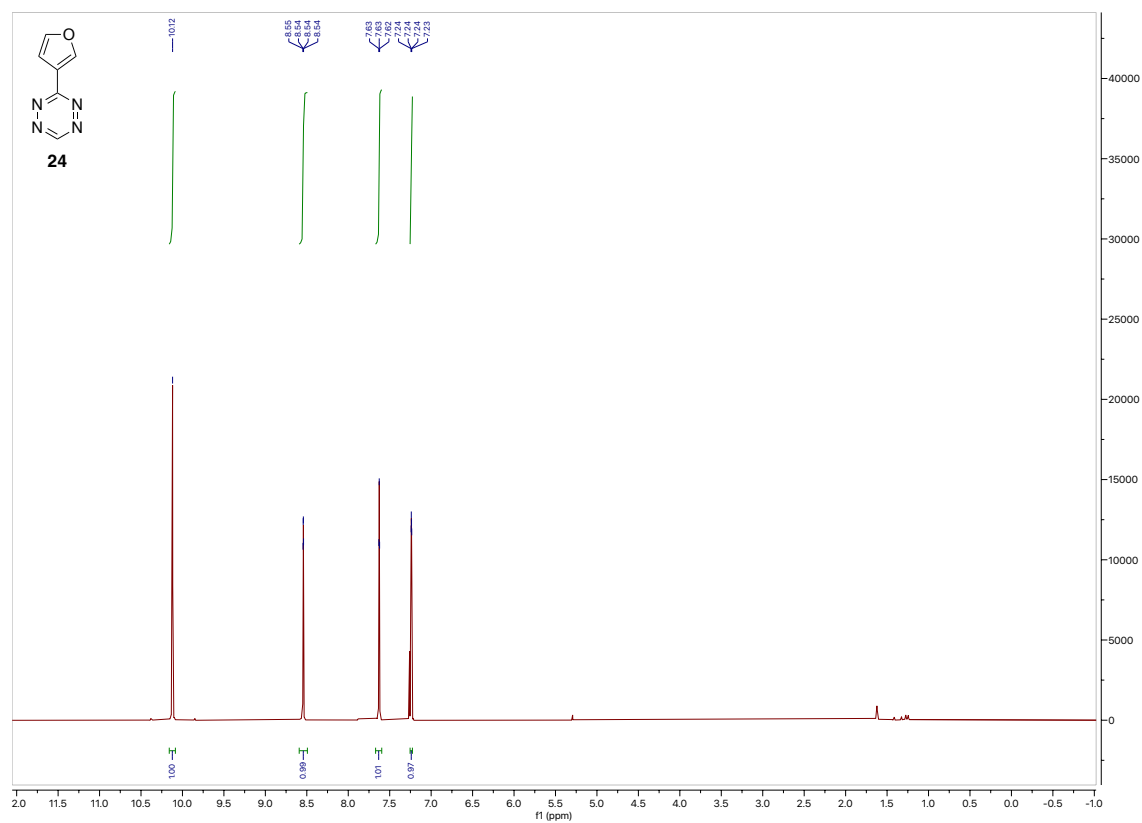
¹³C NMR of **24**

¹H NMR of **25**

SI-52
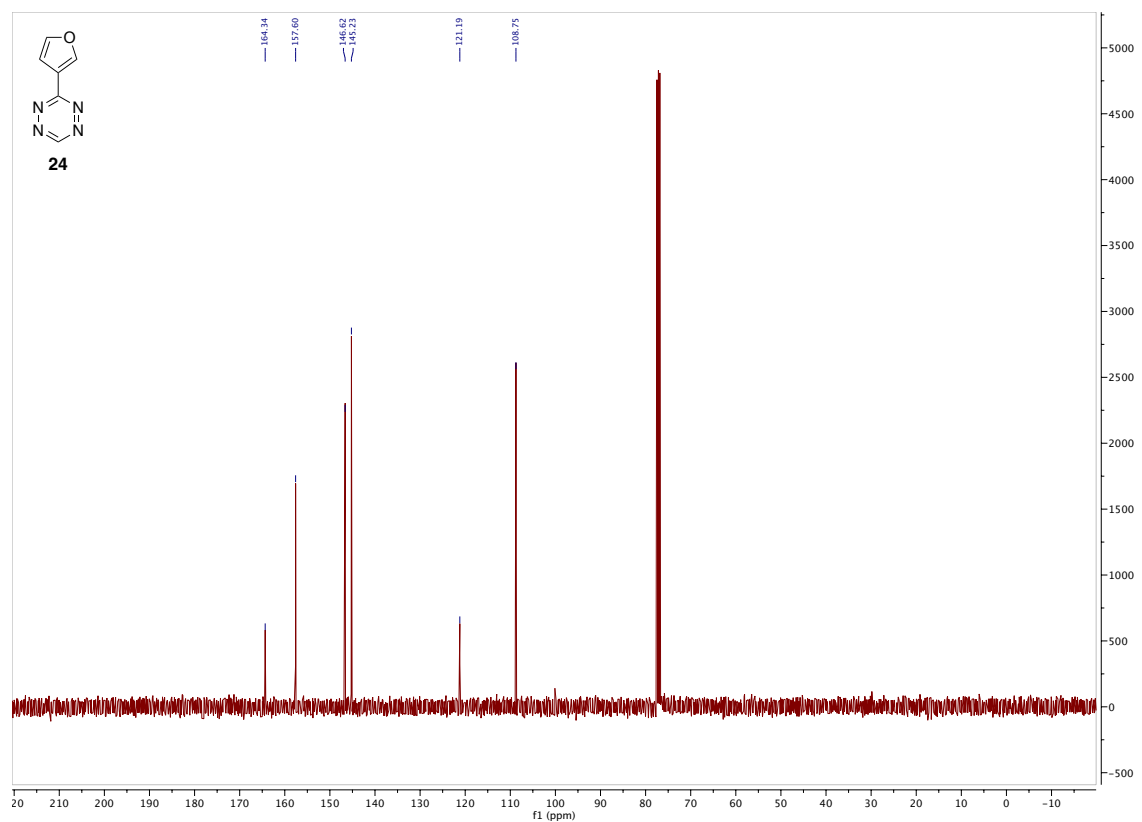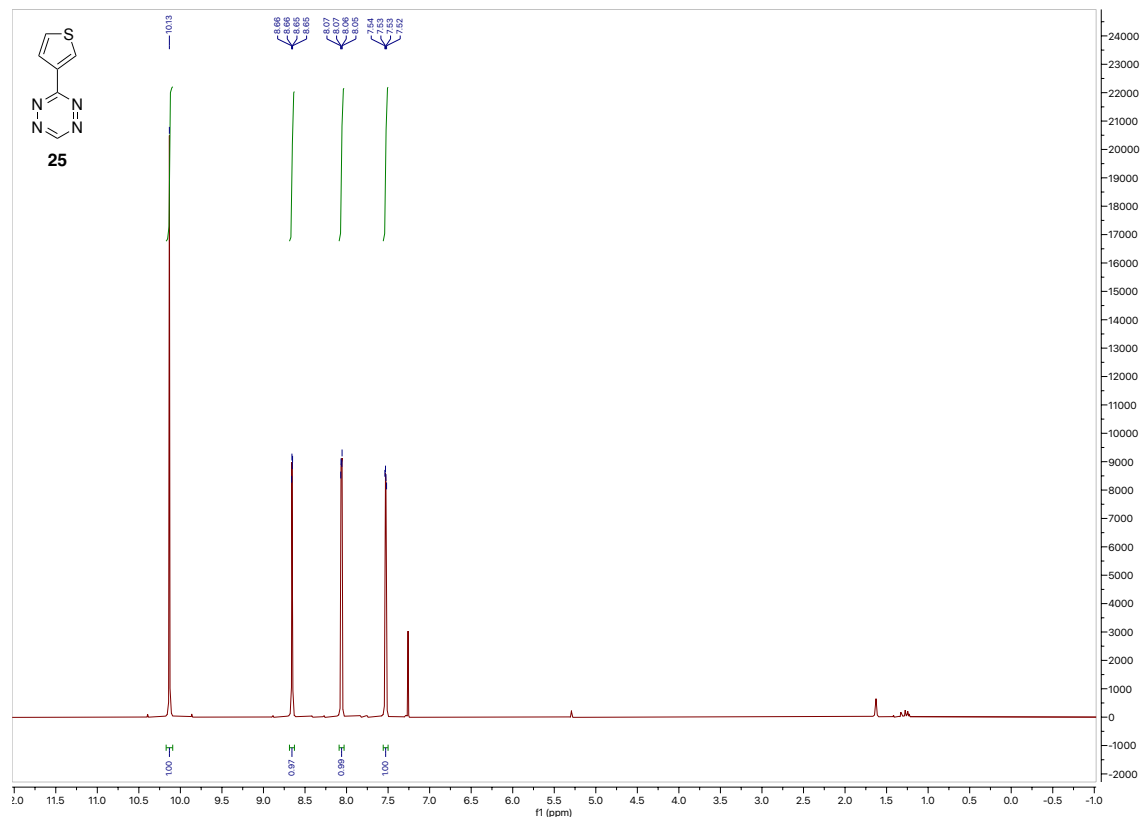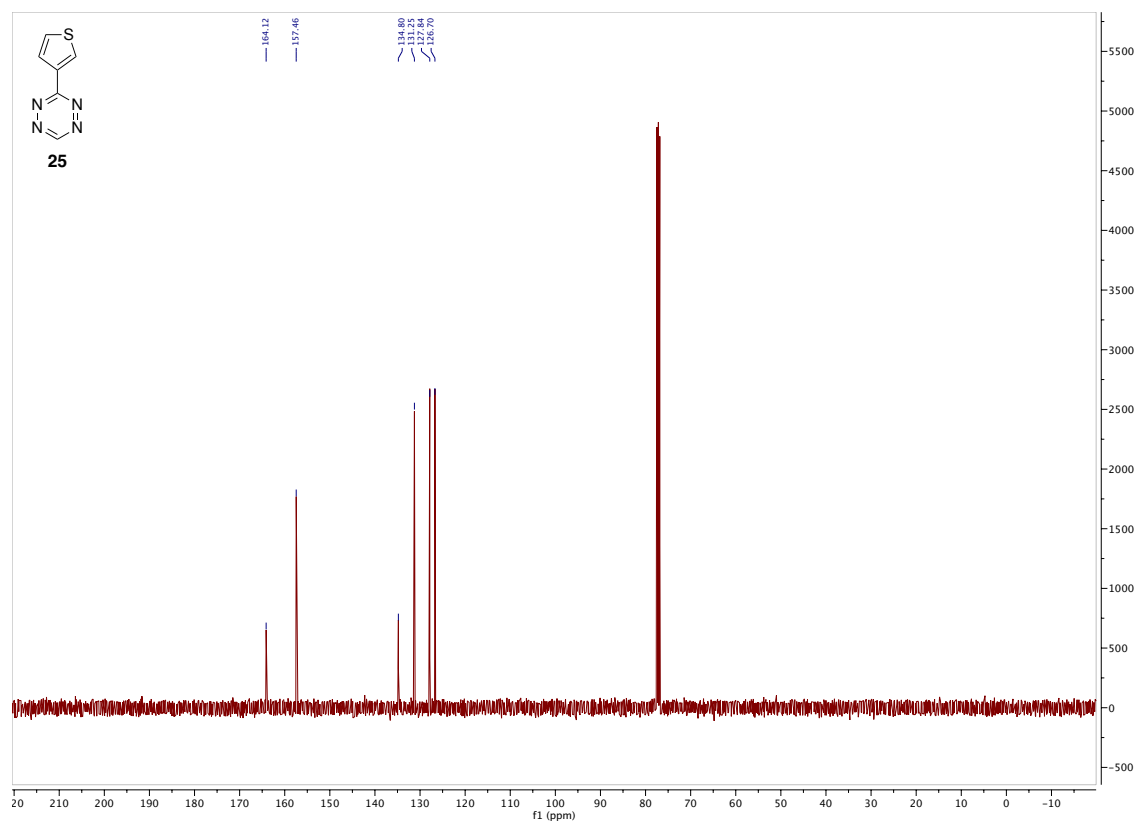
13C NMR of **25**

1H NMR of **26**
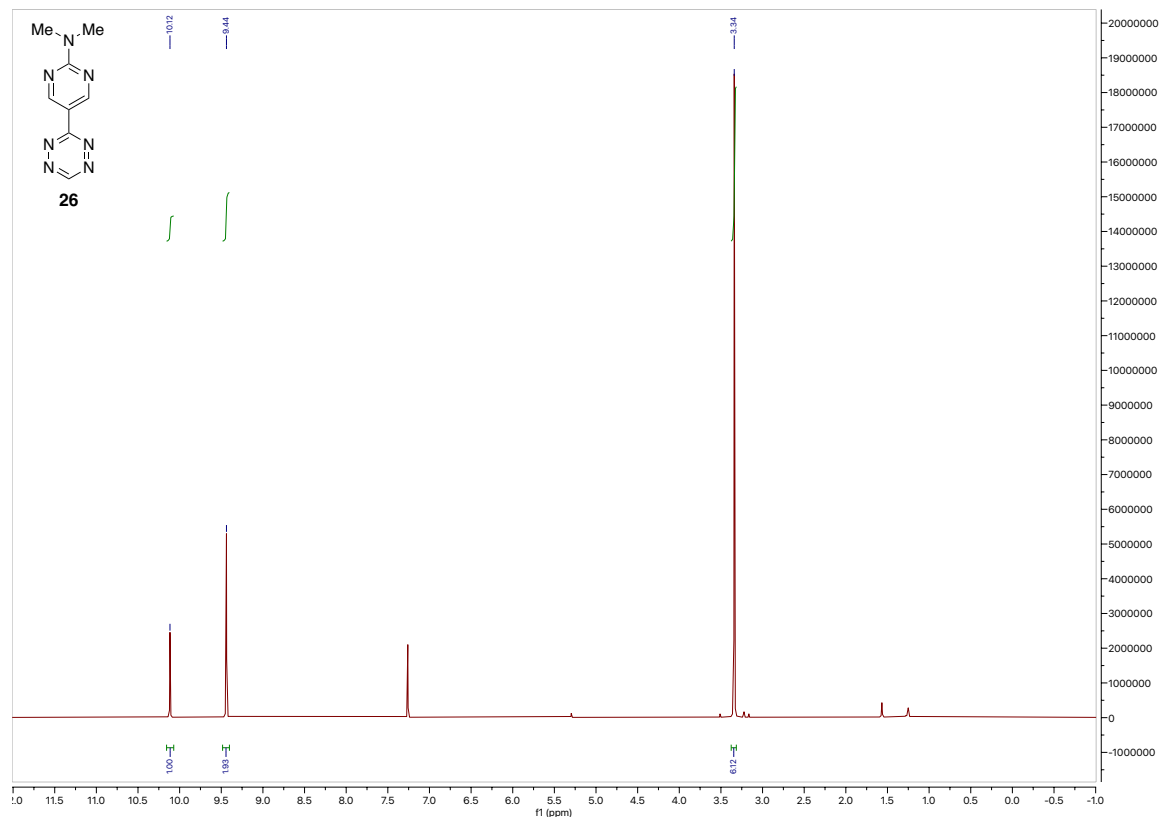
^{13}C NMR of **26**
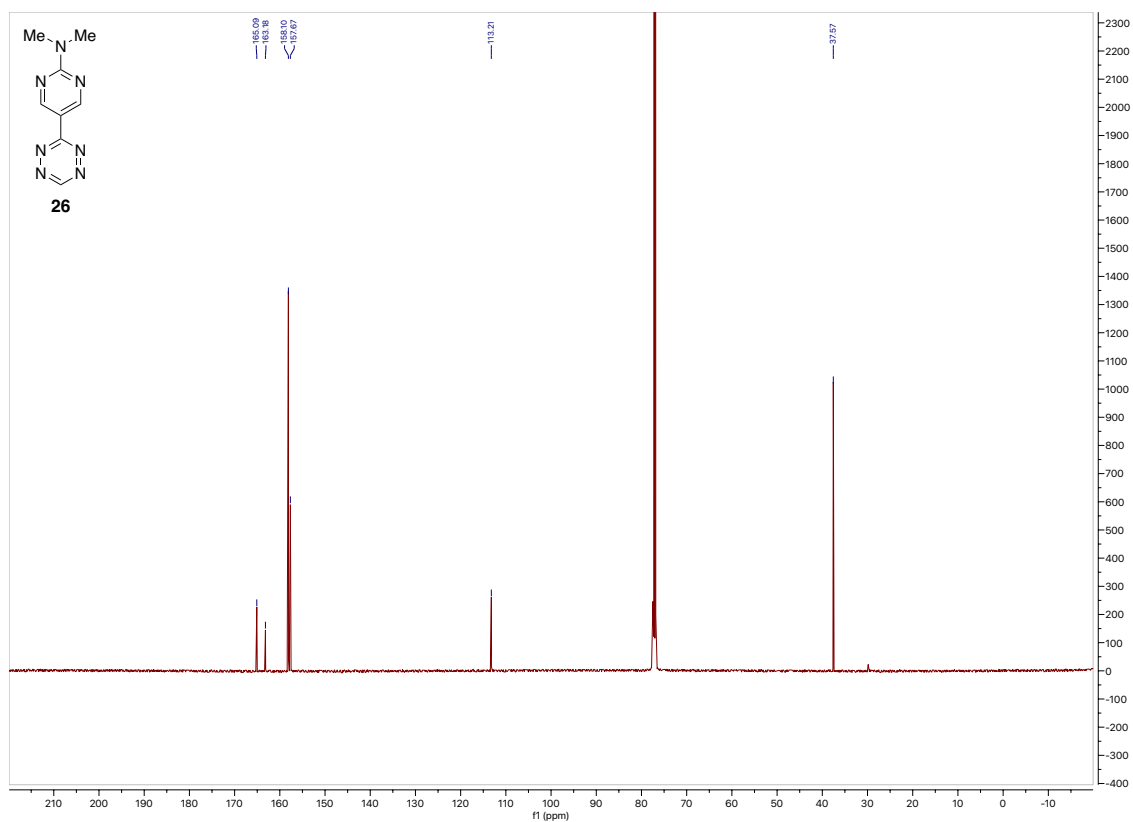
^{1}H NMR of **27**
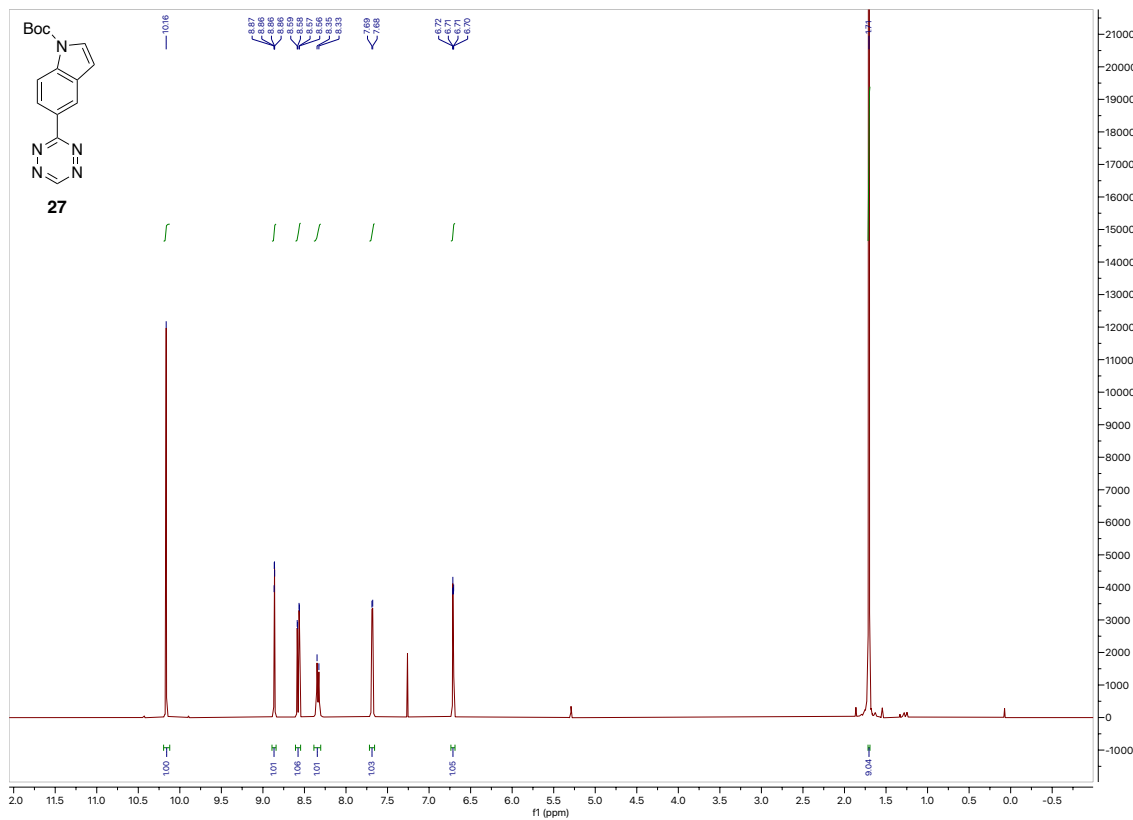
^{13}C NMR of **27**
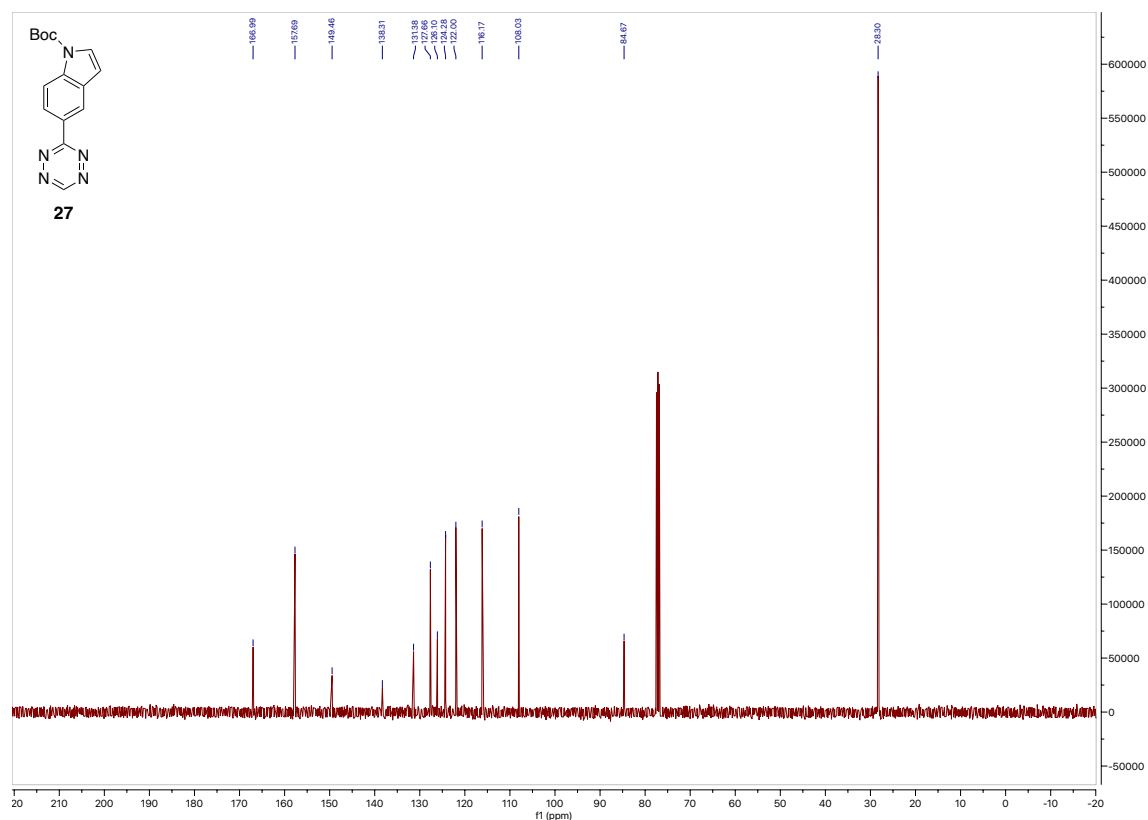
^{1}H NMR of **28**
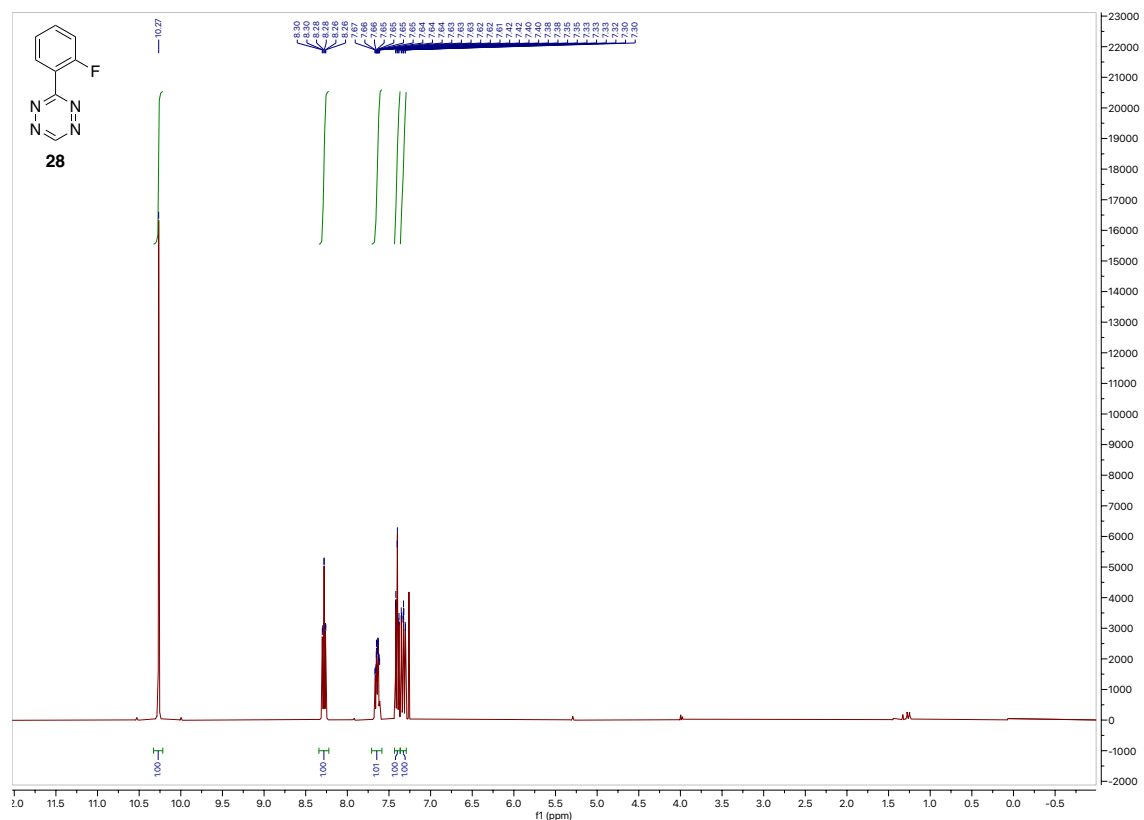
^{13}C NMR of 28
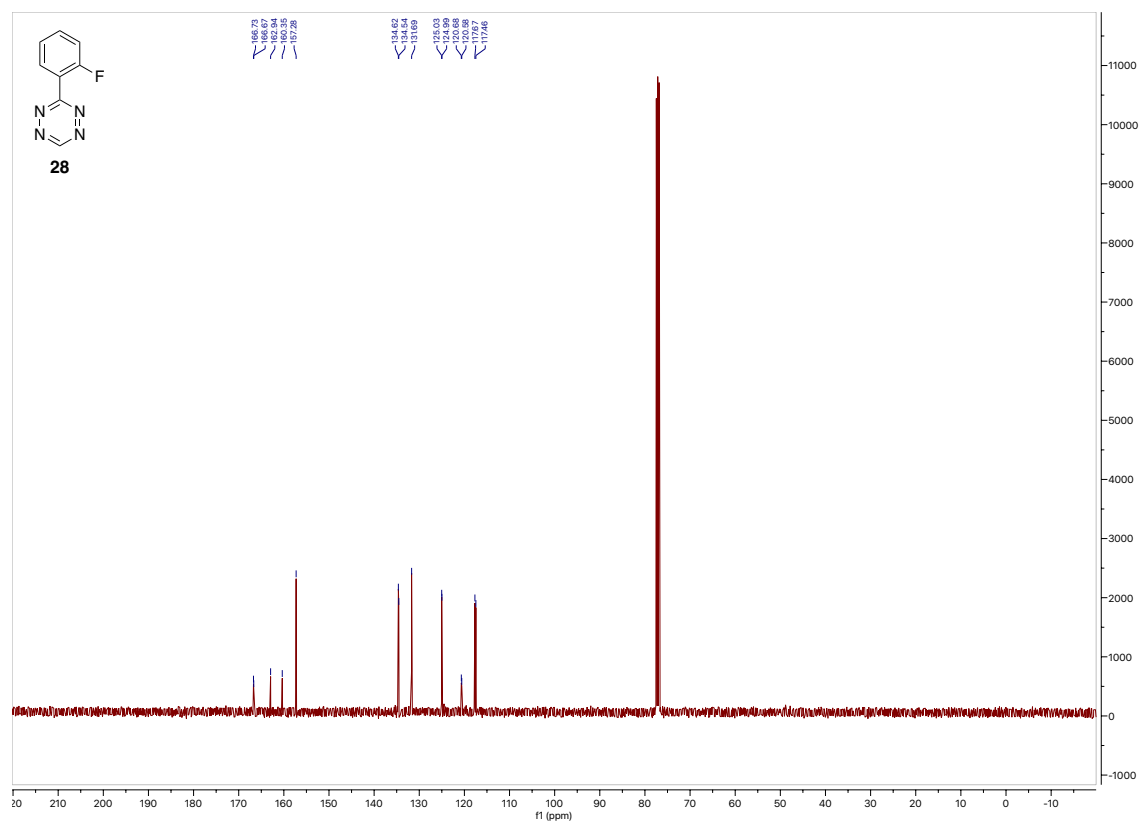
^{19}F NMR of 28
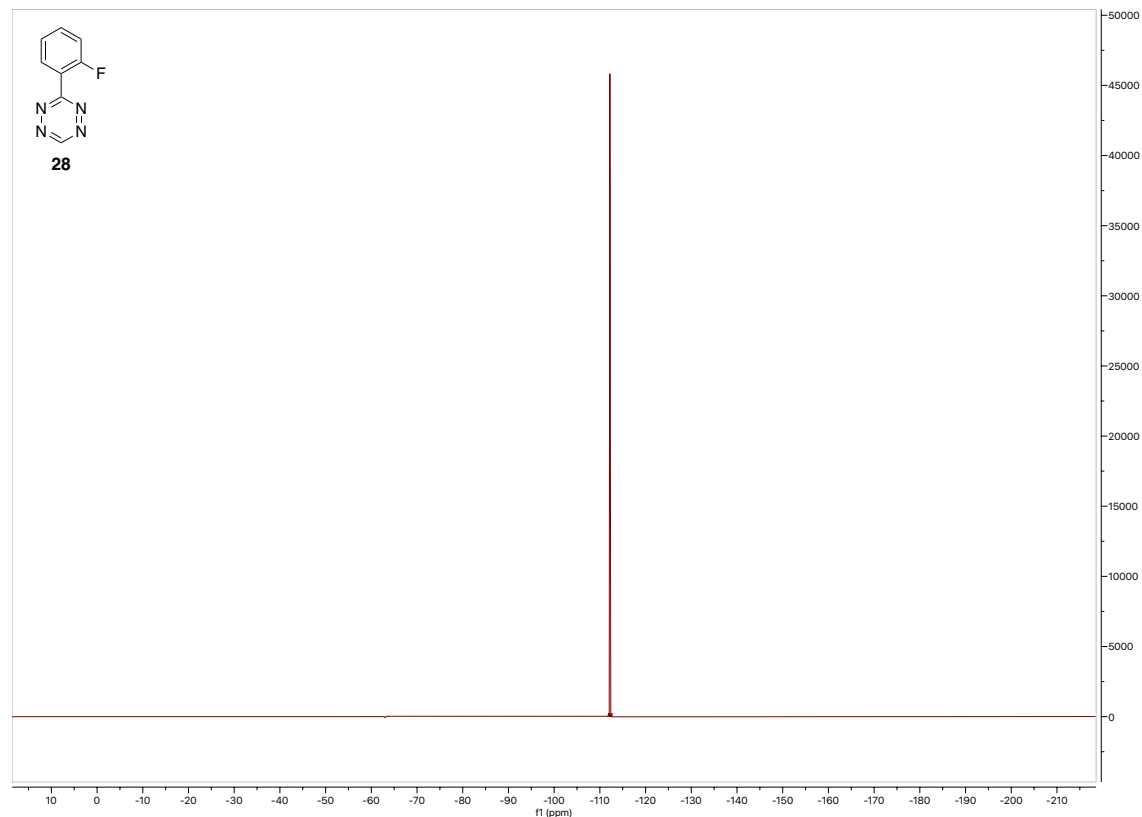
¹H NMR of **29**
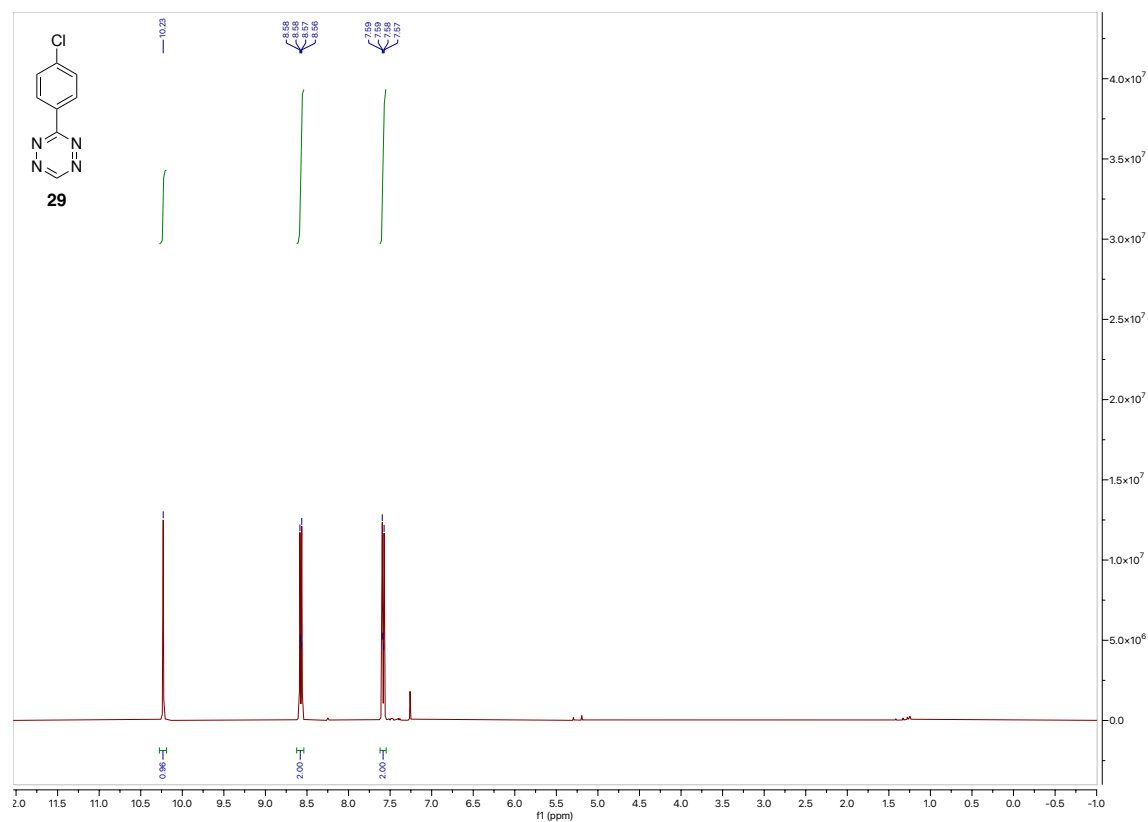
¹³C NMR of **29**
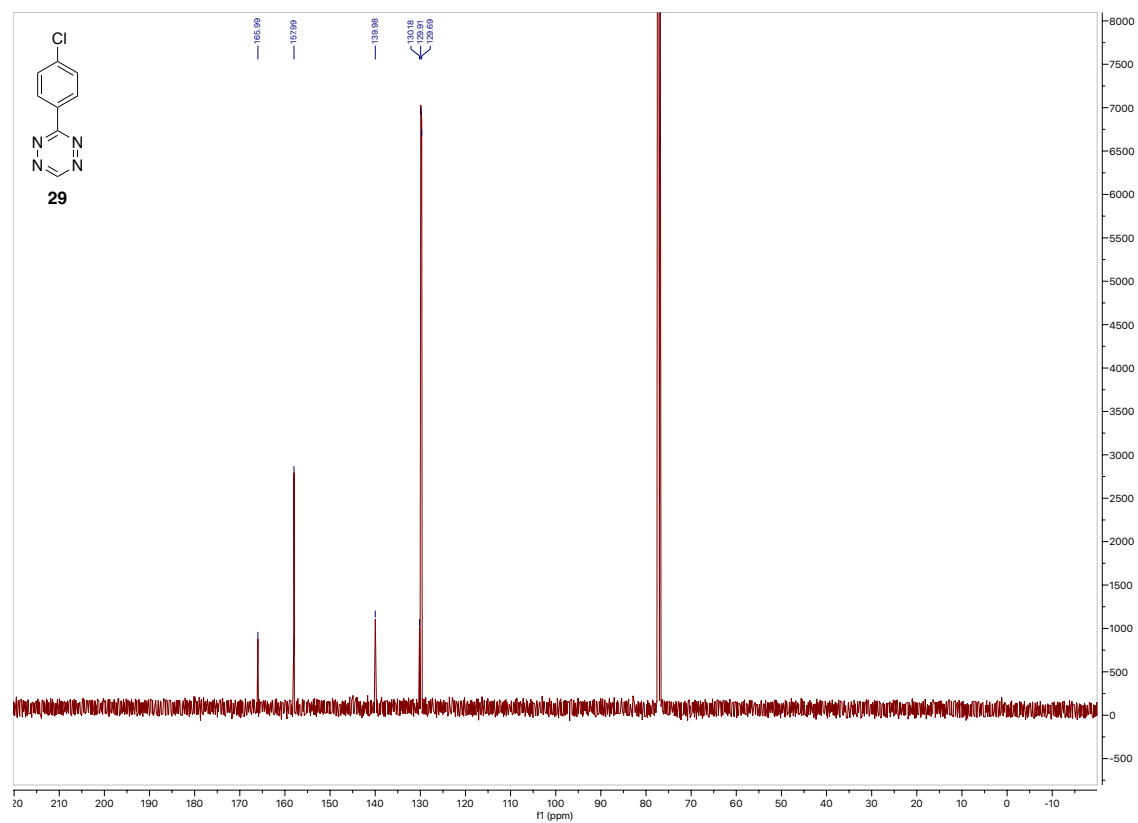
¹H NMR of **30**
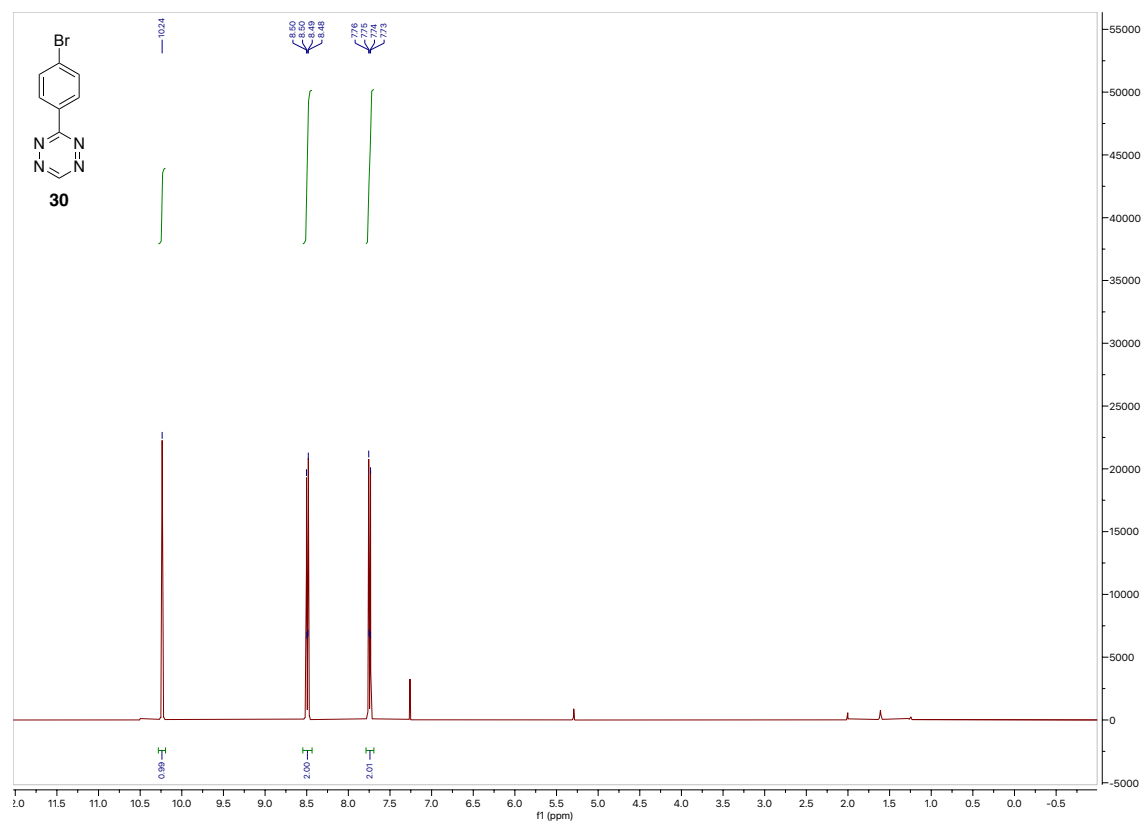
¹³C NMR of **30**
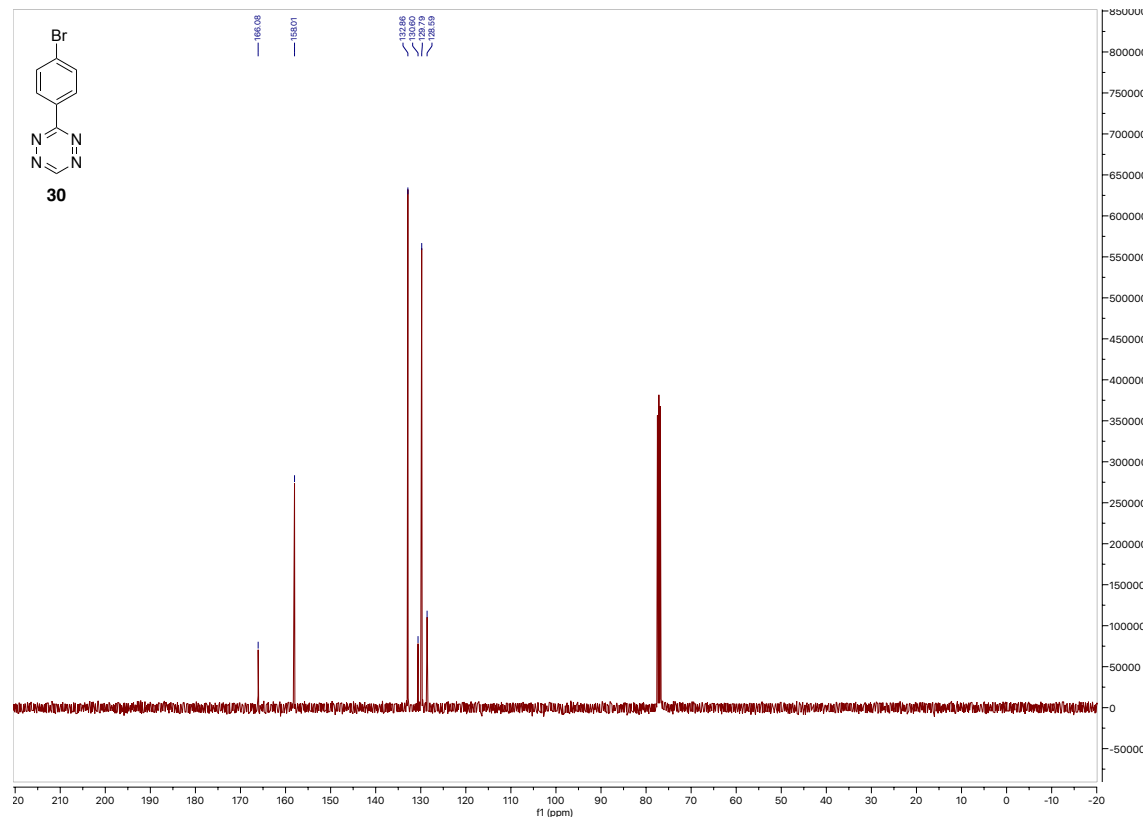
^{1}H NMR of SI1
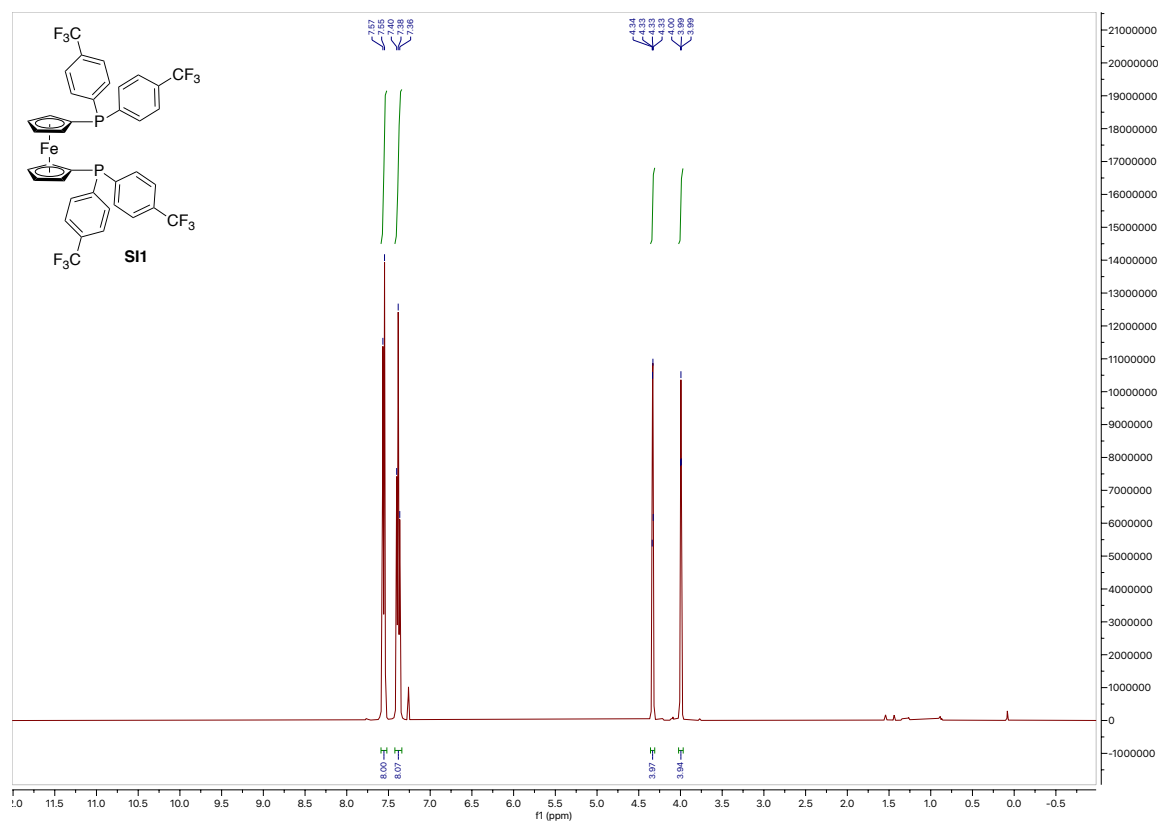
^{13}C NMR of SI1
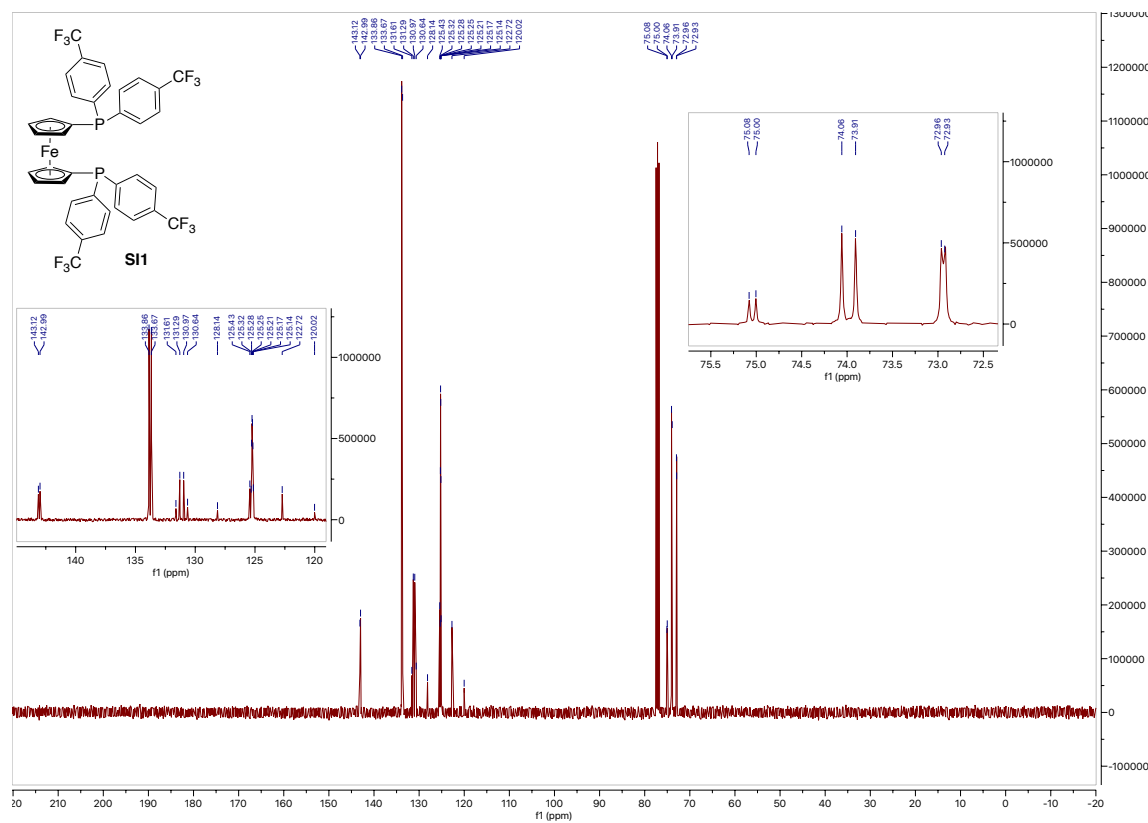
¹⁹F NMR of **SI1**
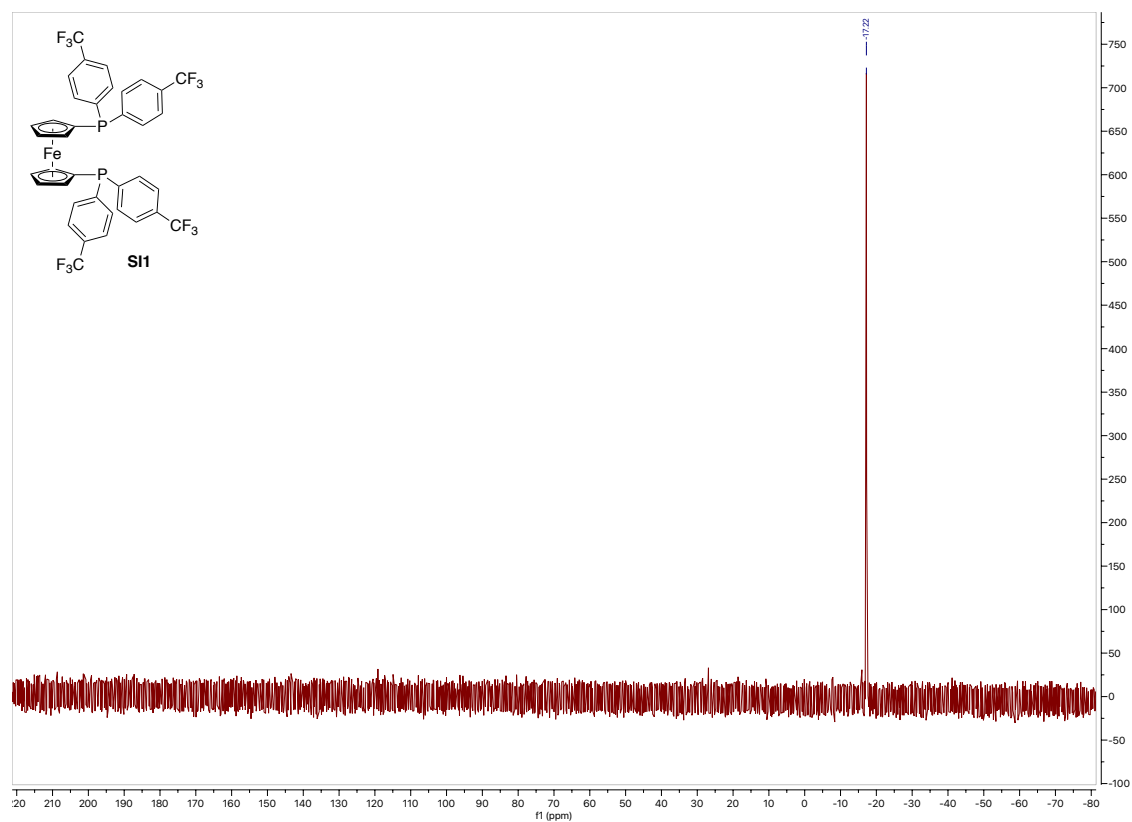
³¹P NMR of **SI1**
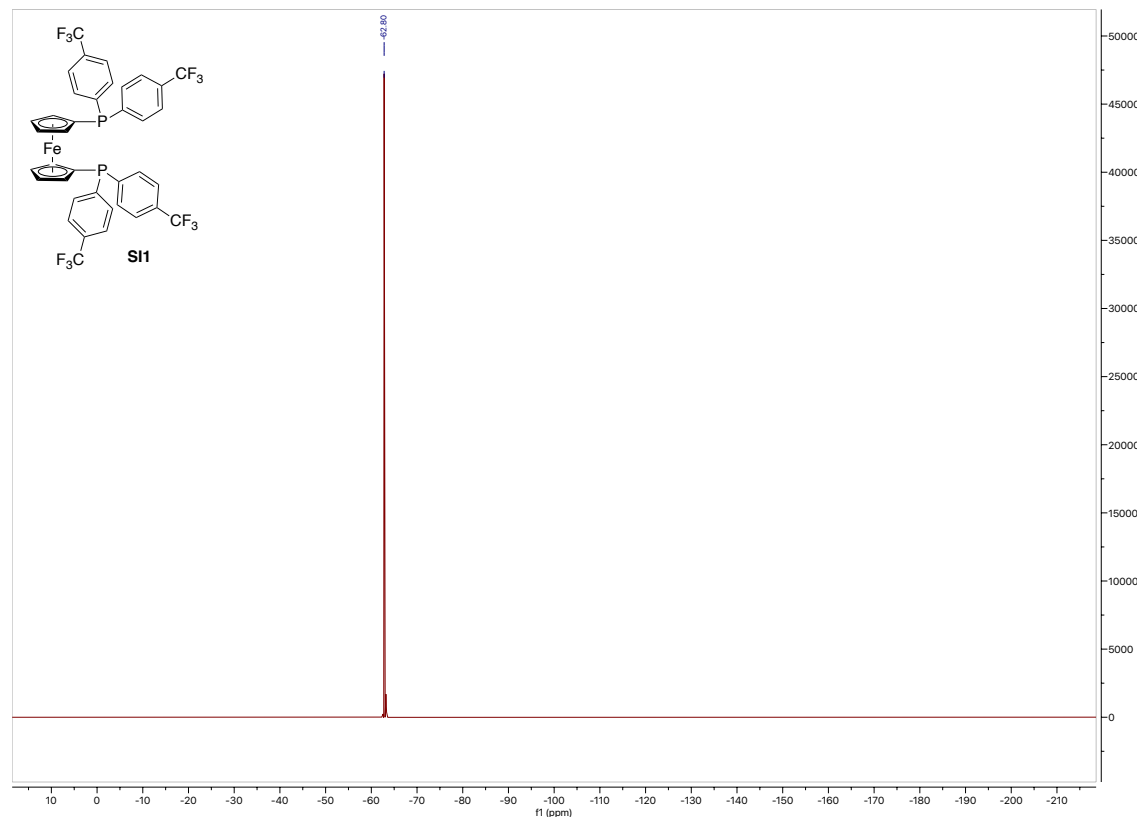
¹H NMR of **SI2**
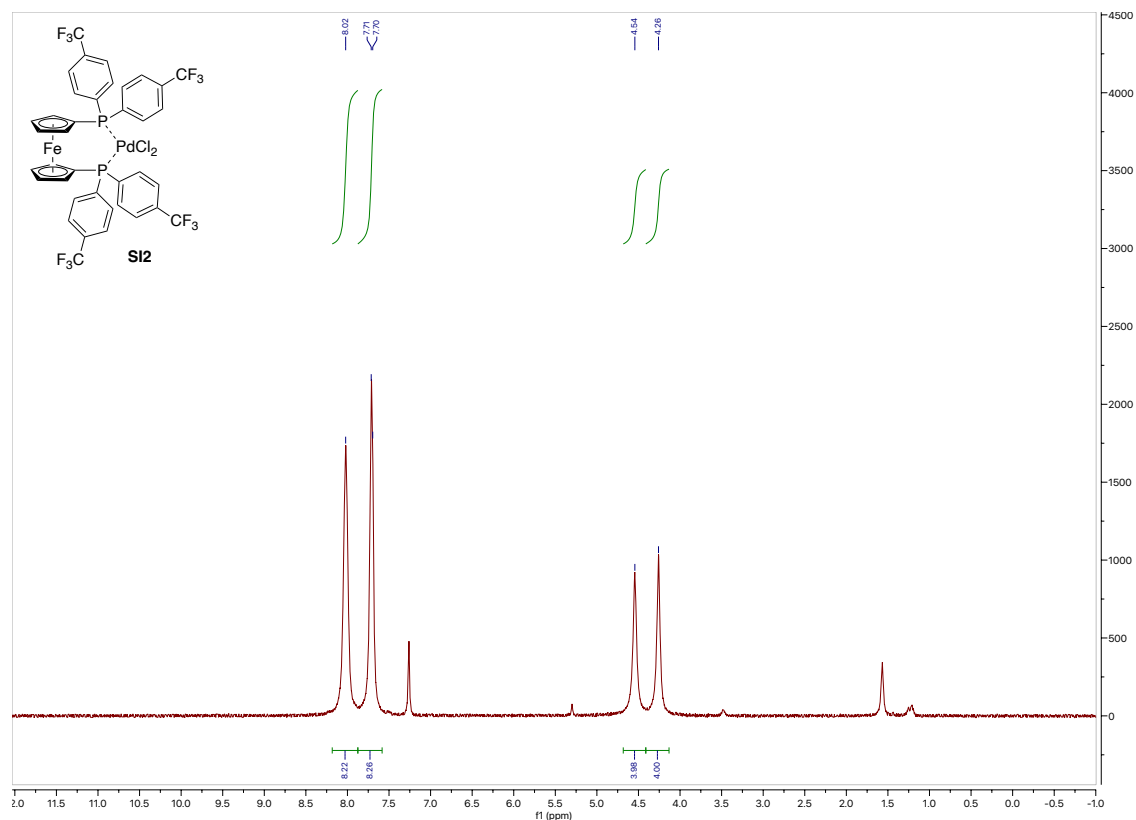
¹³C NMR of **SI2**
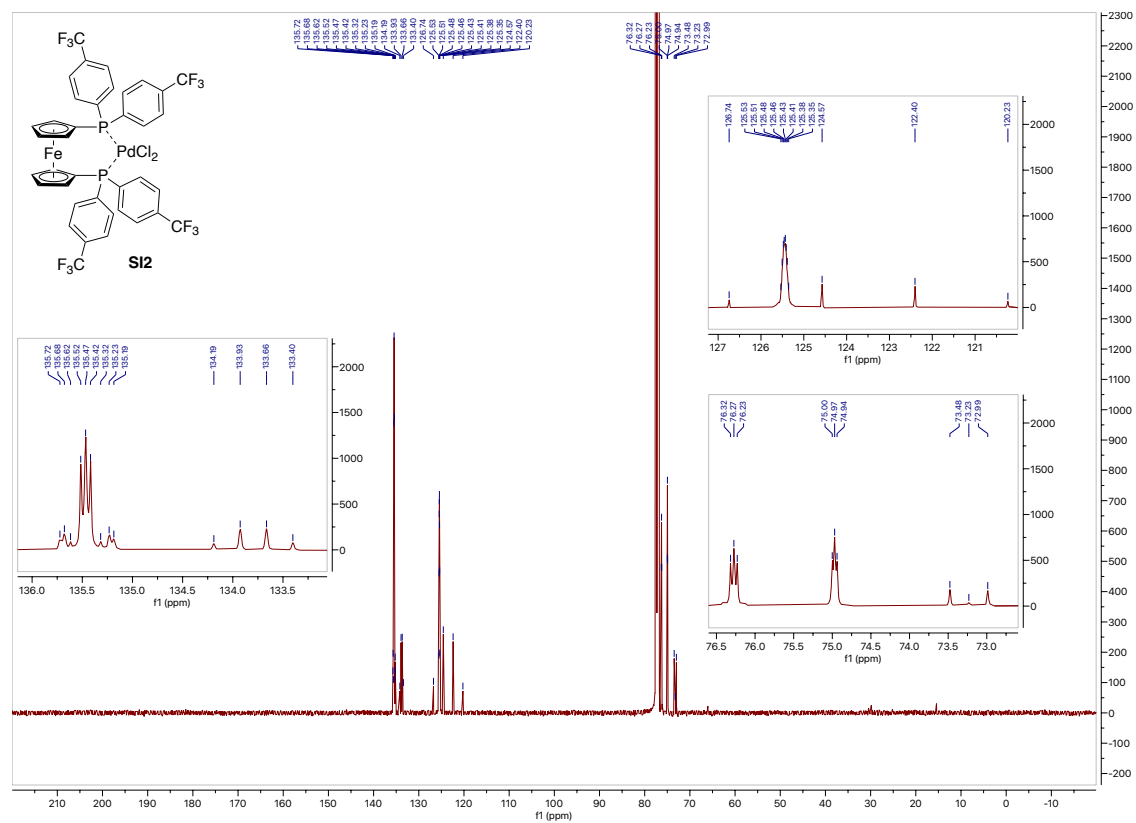
¹⁹F NMR of SI2

³¹P NMR of SI2

SI-62